Non-destructive Technology for evaluation of fruit and vegetable quality

By

Anupun Terdwongworakul

Department of Agricultural Engineering
Faculty of Engineering at Kamphaengsaen
Kasetsart Universtiy

Overview

- Fluorescence
- Visible light
- Ultrasonic measurement
- **Acoustic response***
- **Near infrared spectroscopy (NIRS)***
- Nuclear magnetic resonance (NMR)

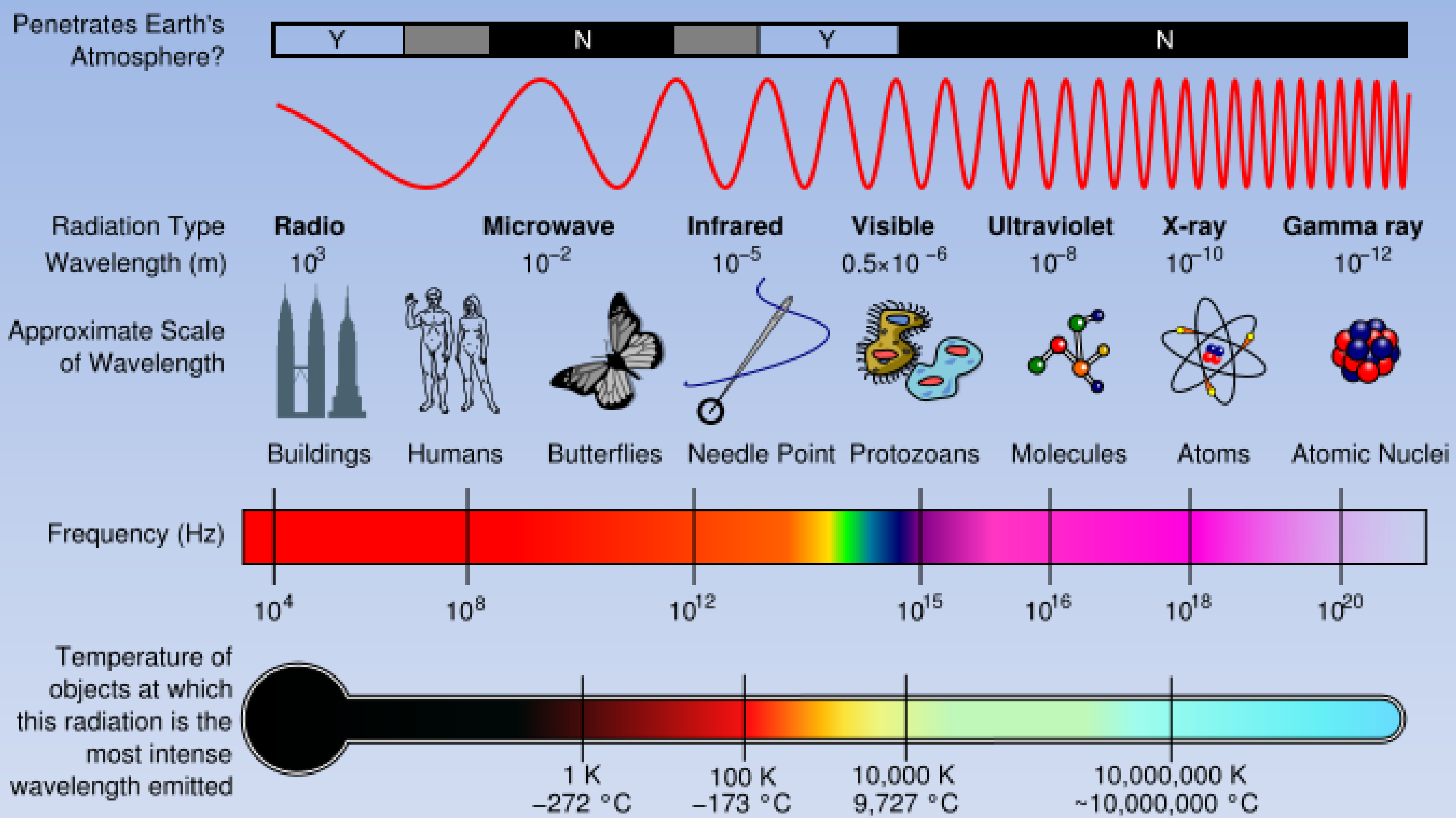

http://chemwiki.ucdavis.edu/Physical_Chemistry/Spectroscopy/Fundamentals/Electromagnetic_Radiation

1. Fluorescence

- Some molecules can re-release absorbed optical energy as a lower energy photon (longer wavelength).

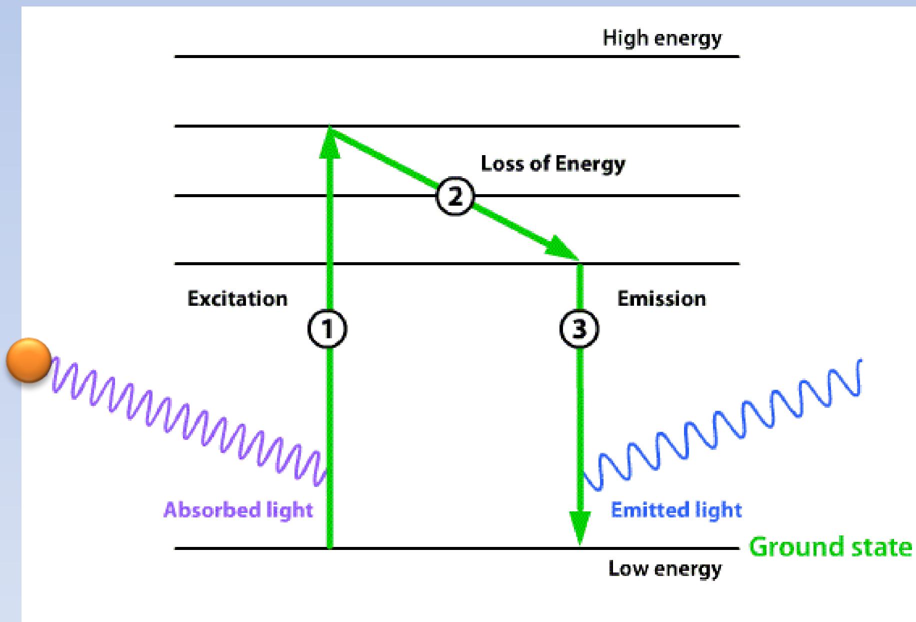

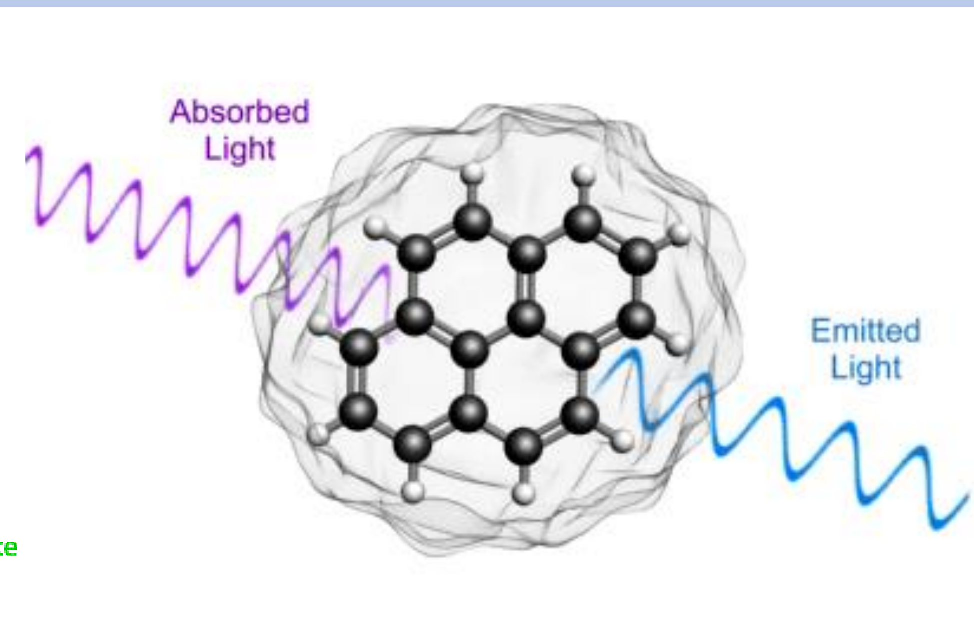

http://www.lifetechnologies.com/th/en/home/references/molecular-probes-the-handbook/introduction-to-fluorescence-techniques.html

Fluorescence

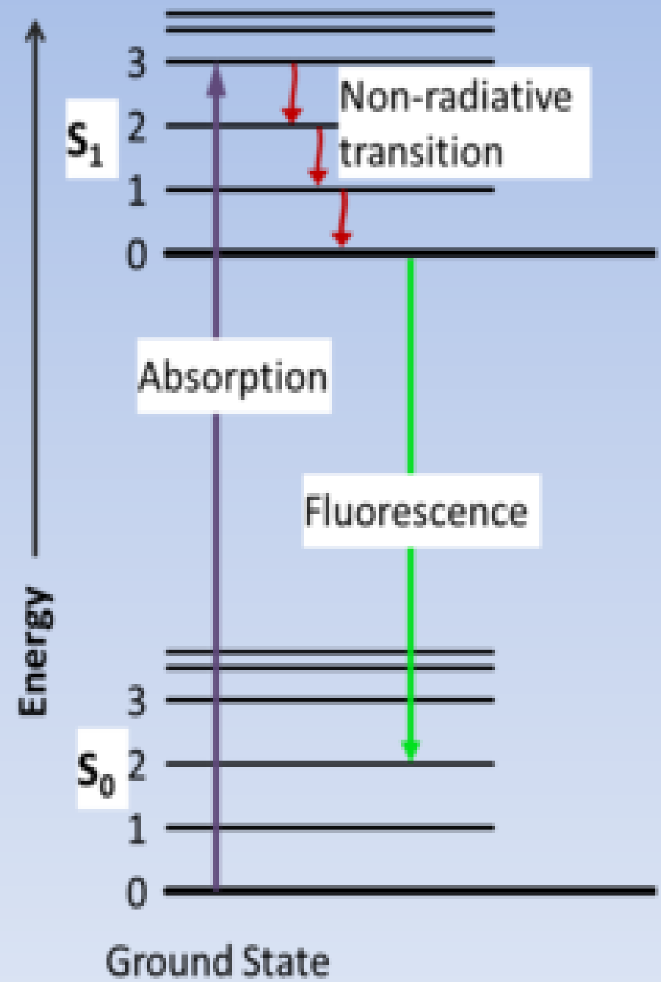

http://en.wikipedia.org/wiki/Florescence

Principle of fluorescence

http://www.youtube.com/watch?v=SGFlr1jFNBM

Applications:
Fluorescence and ultra violet photos

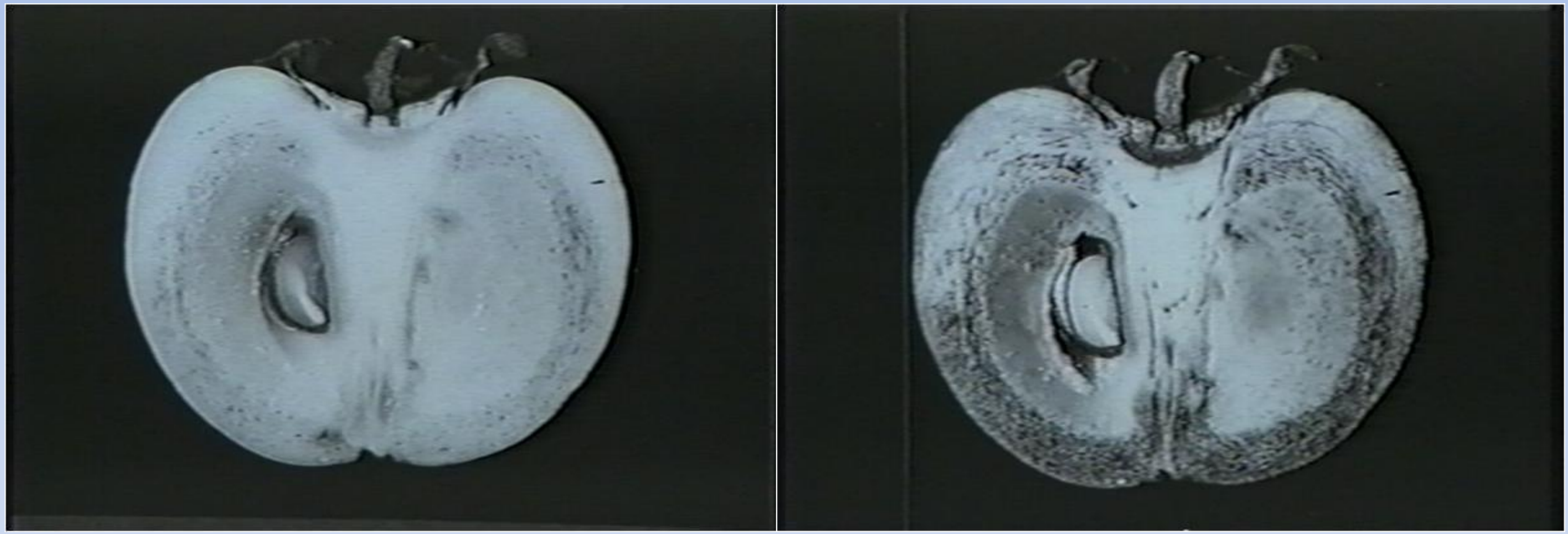

Visible UV

The most striking examples:
Material is excited in ultraviolet region and light is emitted in the visible region

From Prof. Sumio Kawano, Kagoshima University, Japan

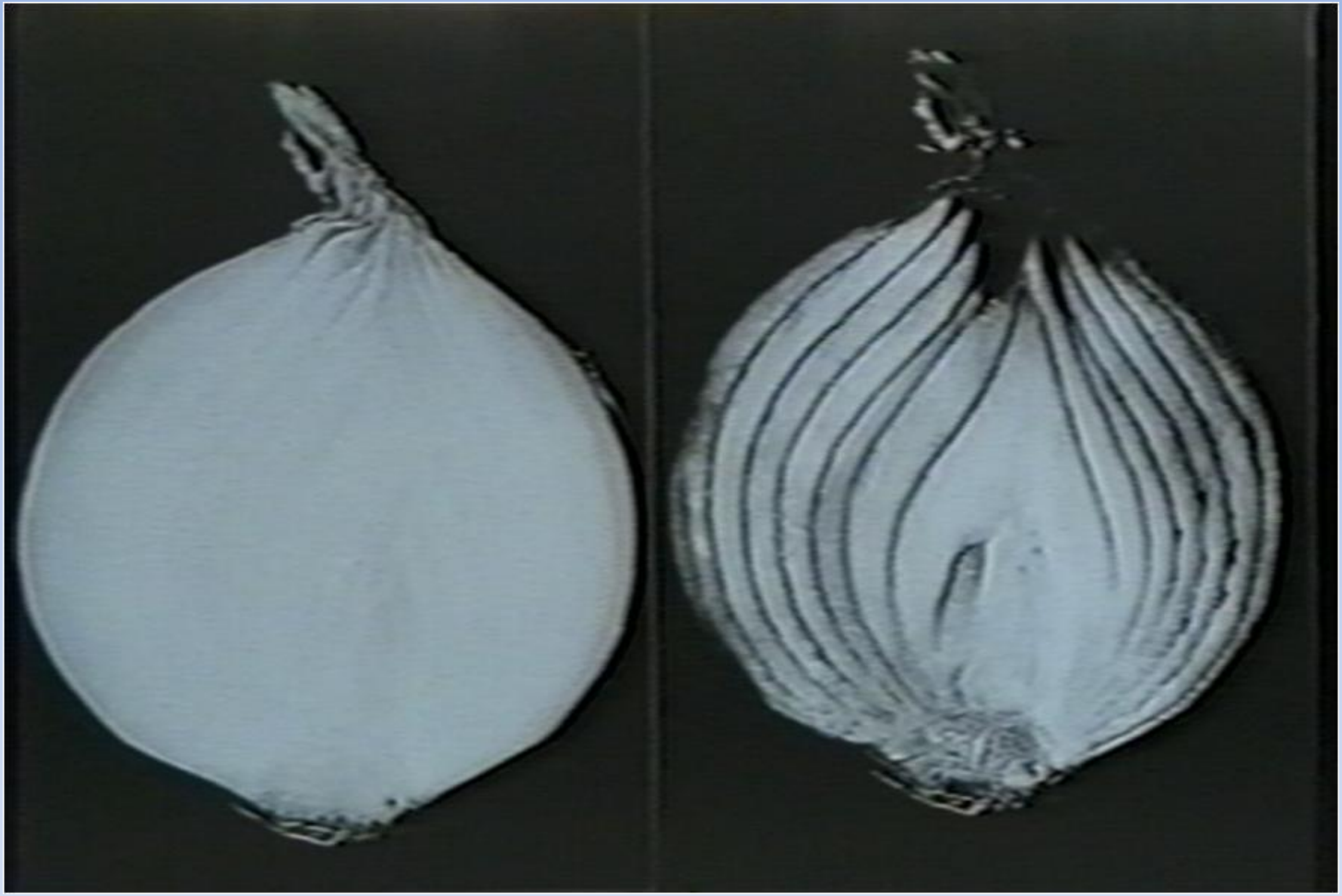

Visible UV

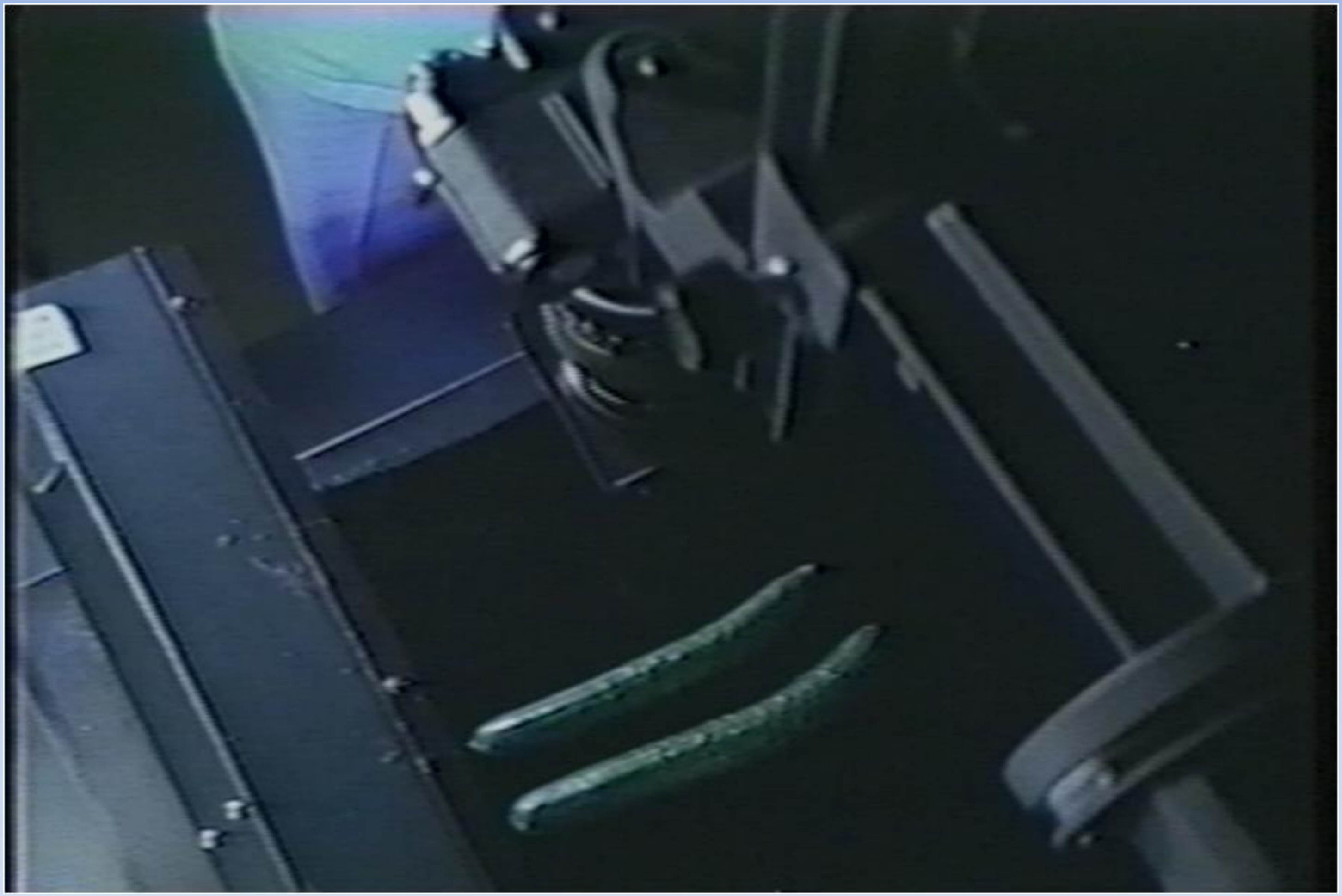

Fluorescence Photo of Cucumber showing difference in freshness

Fluorescence Photo of Eggs

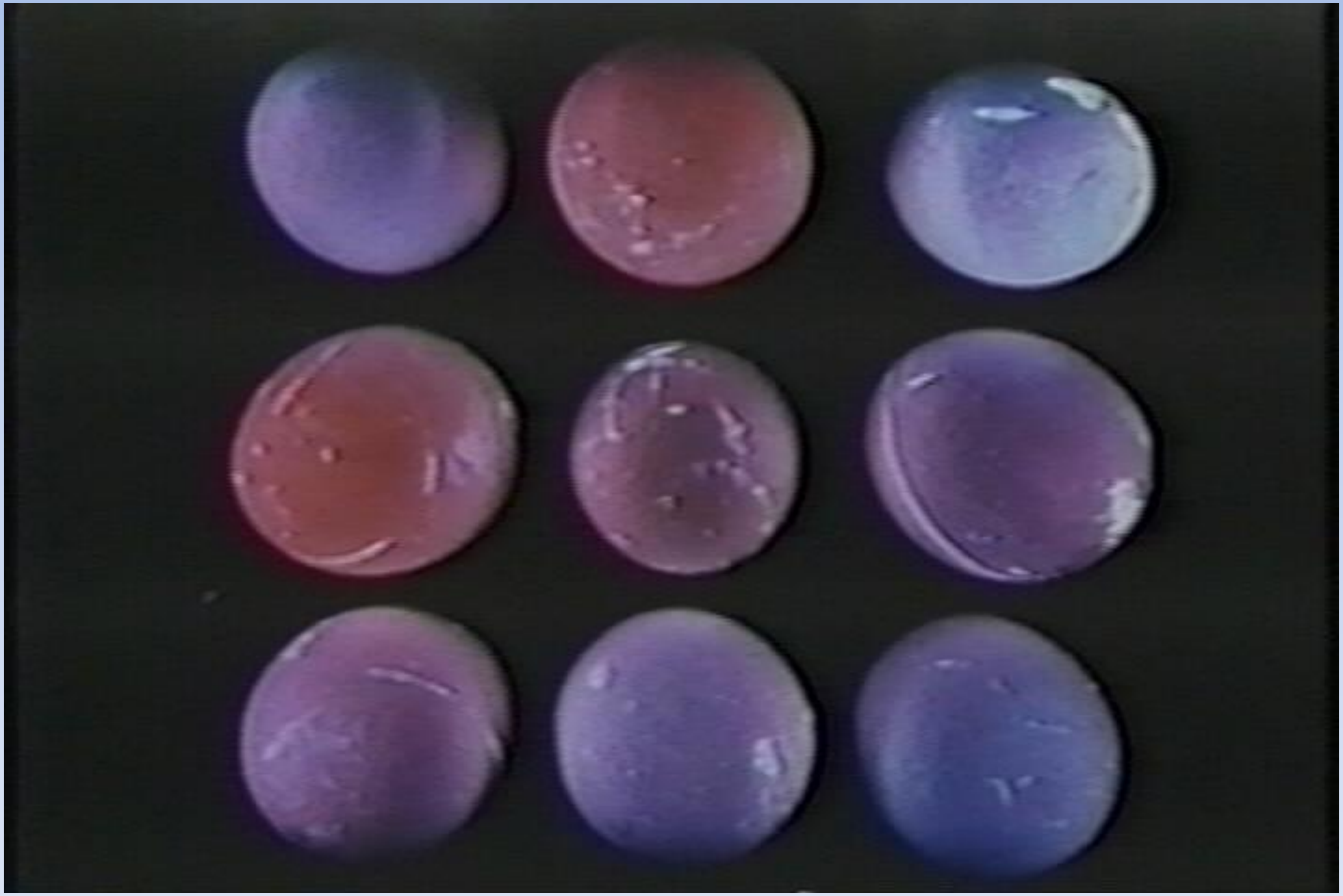

Fluorescence Photo of Egg (Fresh)

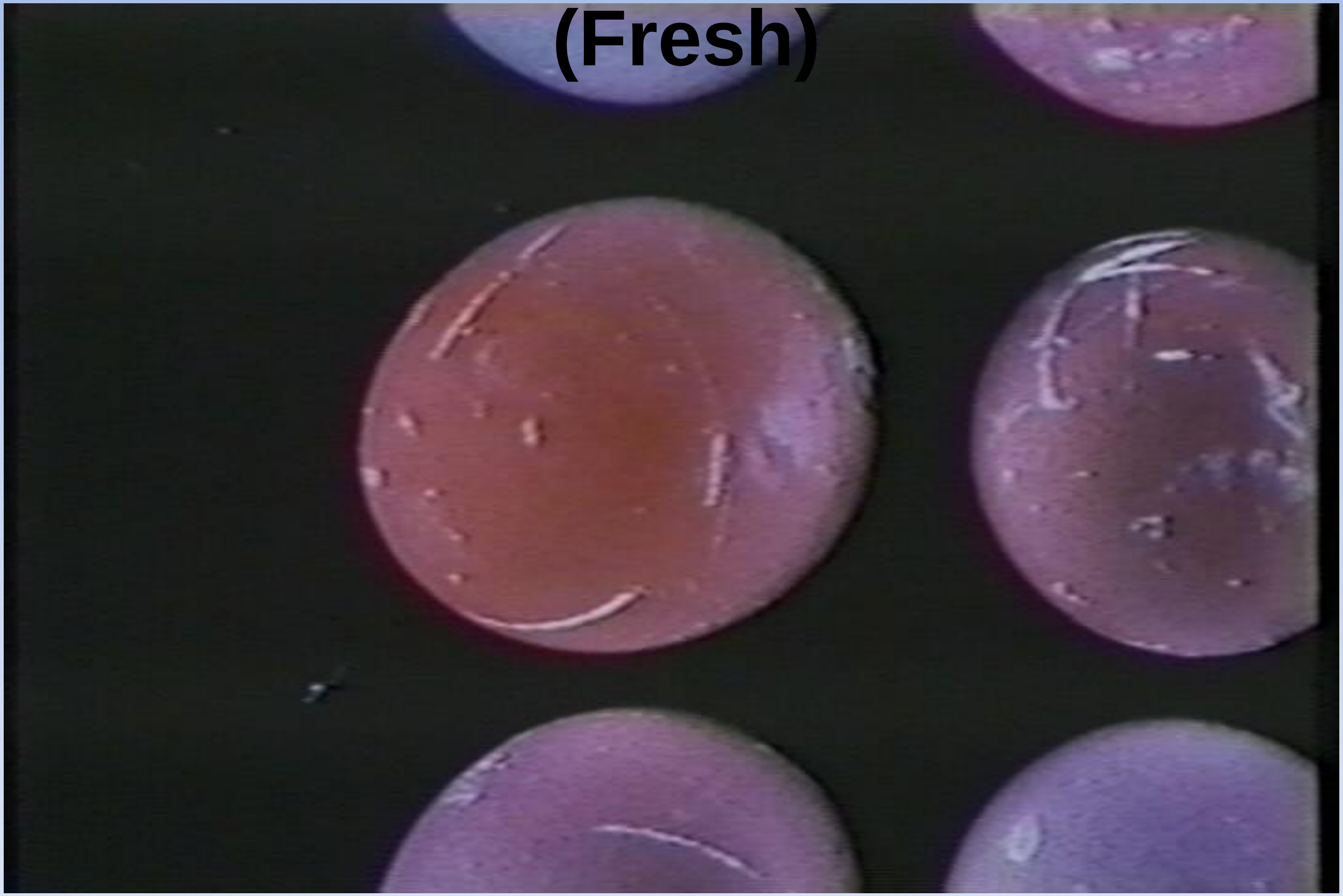

2. Visible light

Astringency detection of persimmons

- Persimmons produce astringent taste because they contain soluble tannin.
- If the astringent persimmon is treated with carbon dioxide to change the tannin from soluble to insoluble, the persimmon becomes sweet.
- For some varieties, the flesh of the sweet persimmon changes its color with black specks of insoluble tannin cells.

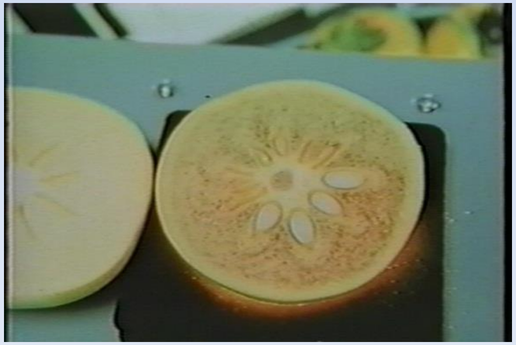

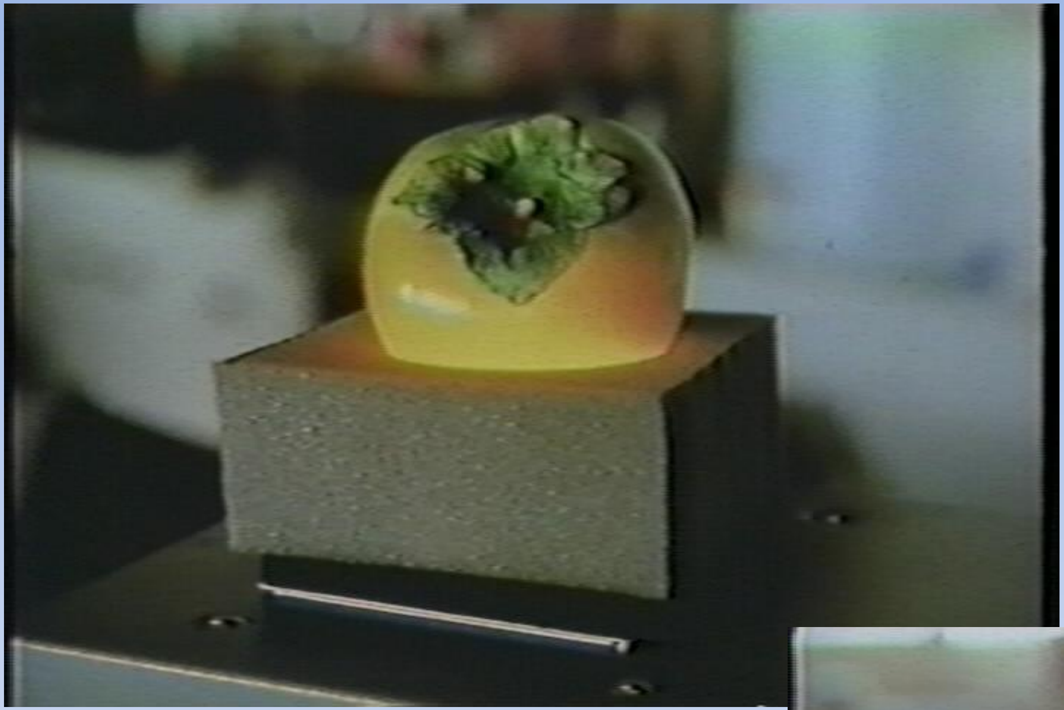

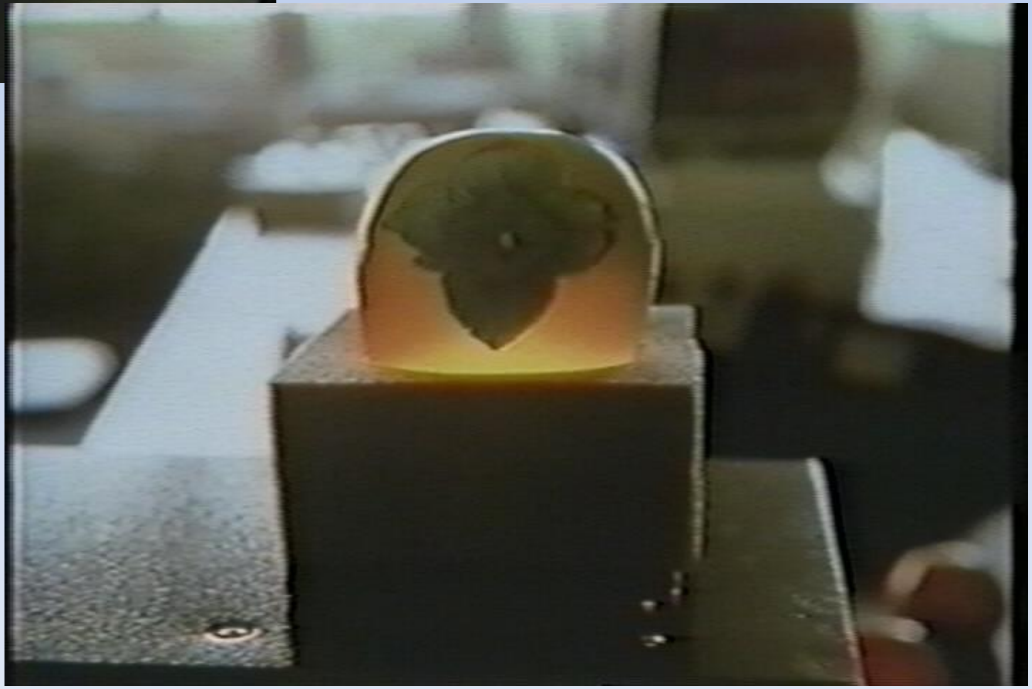

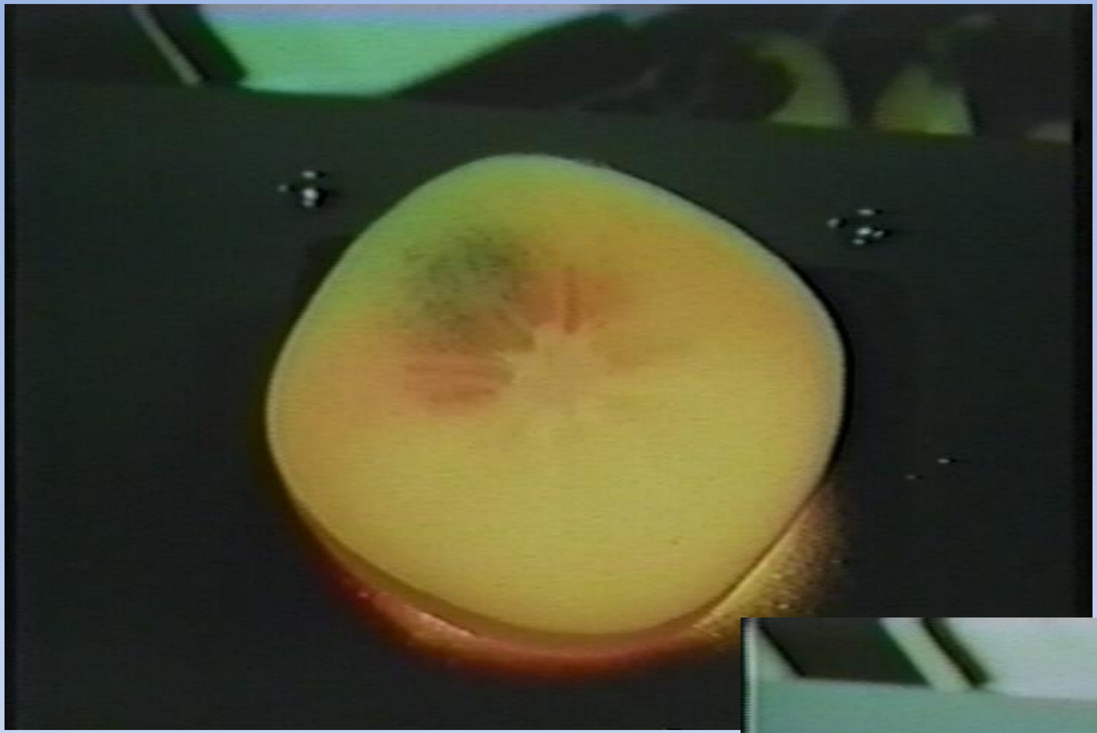

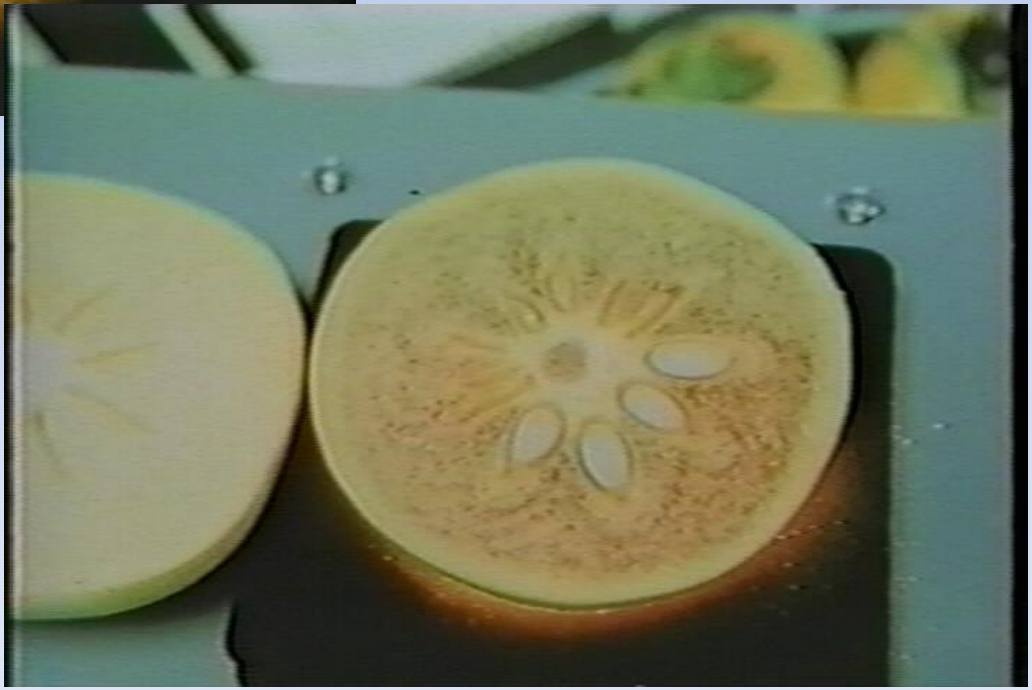

Application:
Detection of maturity and internal physiological disorder of pineapple using visible light

- Pineapple is a fruit of which the internal quality is hard to evaluate using the external appearances.
- This is because the surface color is not directly correlated to the internal quality.

Maturity detector of pineapples has been developed, which consists of a 100 W halogen tungsten lamp as a light source, a photo multiplier and a sensitive CCD camera.

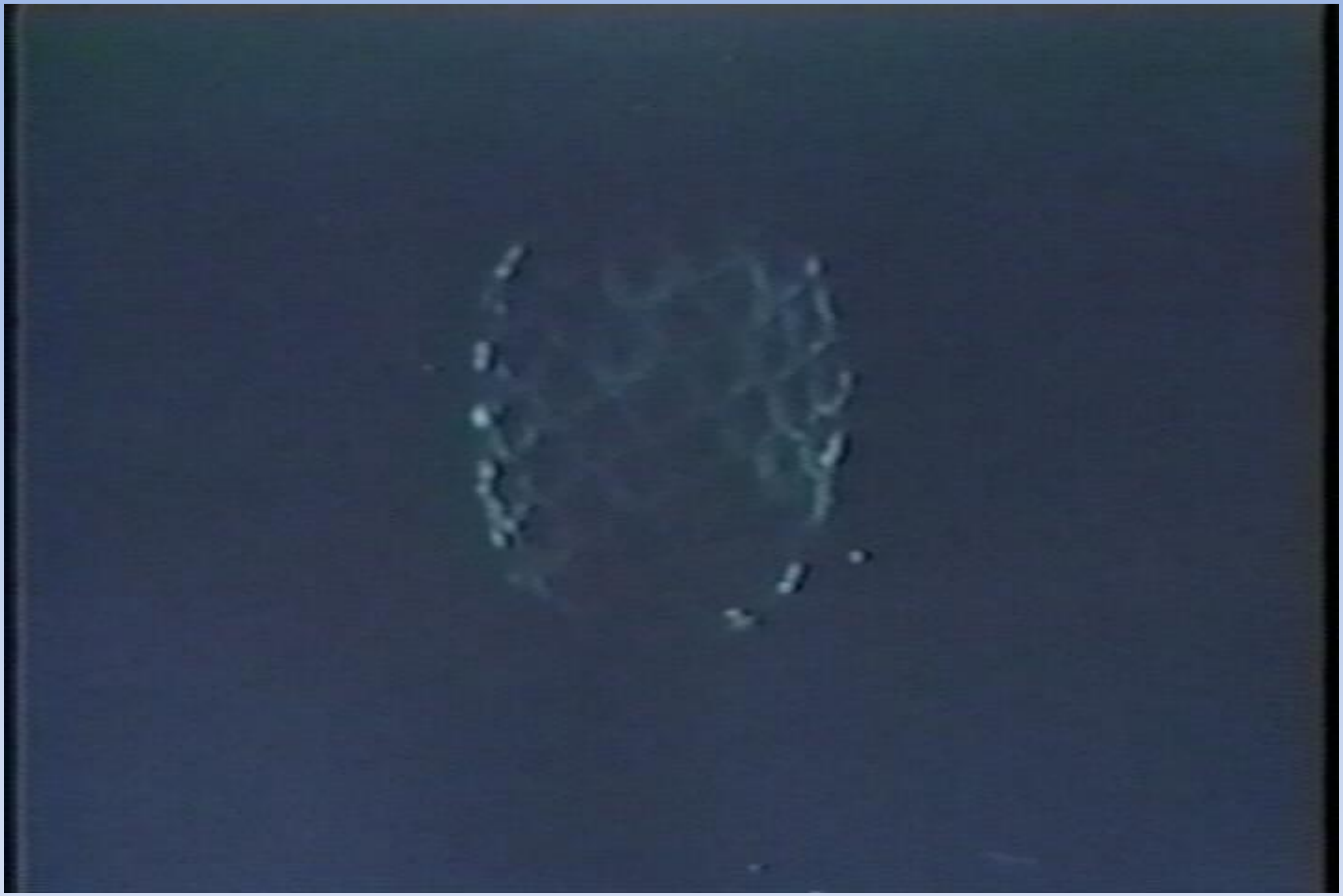

The transmitted light intensity is very low when the fruit has internal browning or when the fruit is immature.

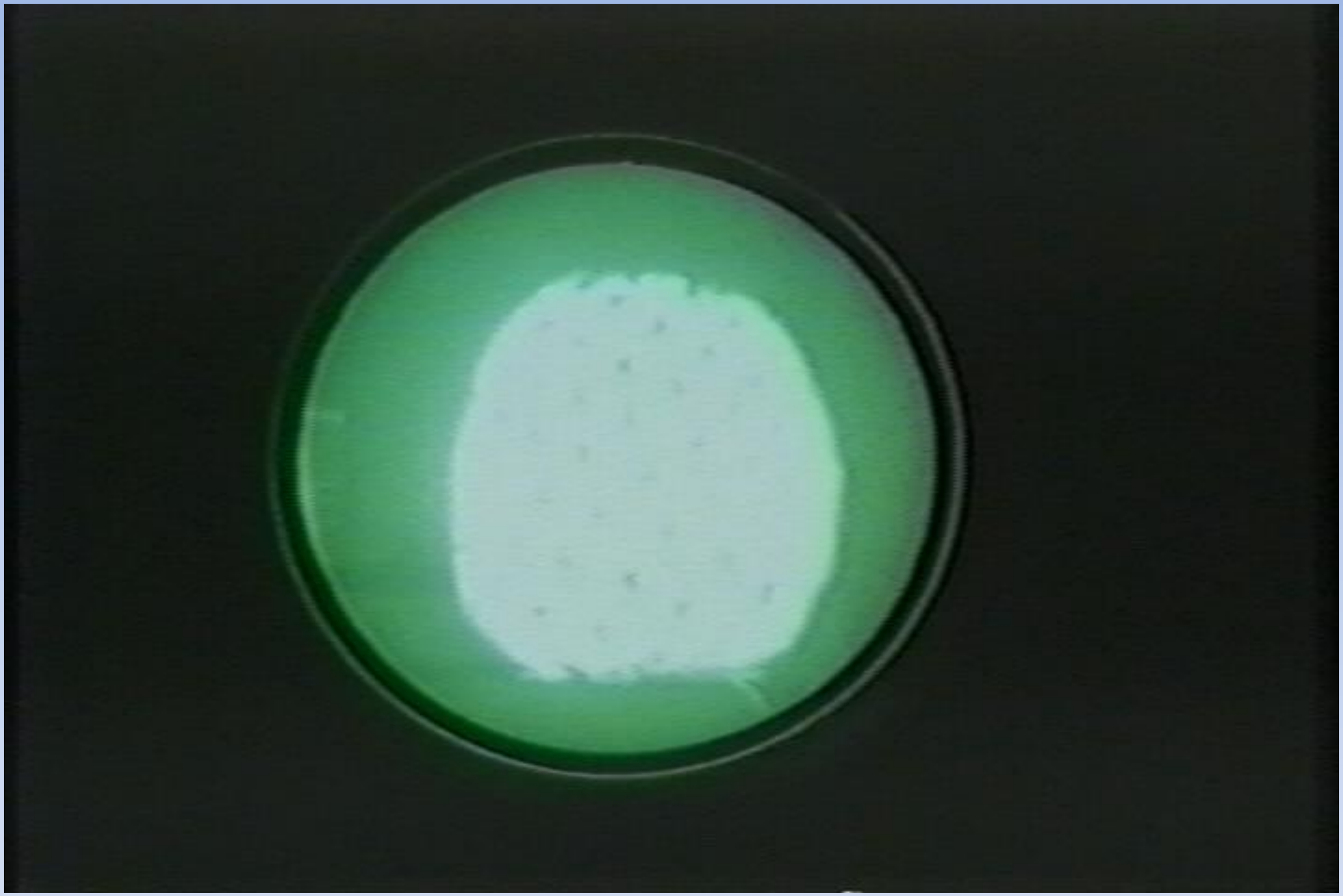

The intensity is very high when the fruit has water core or when the fruit is overripe.

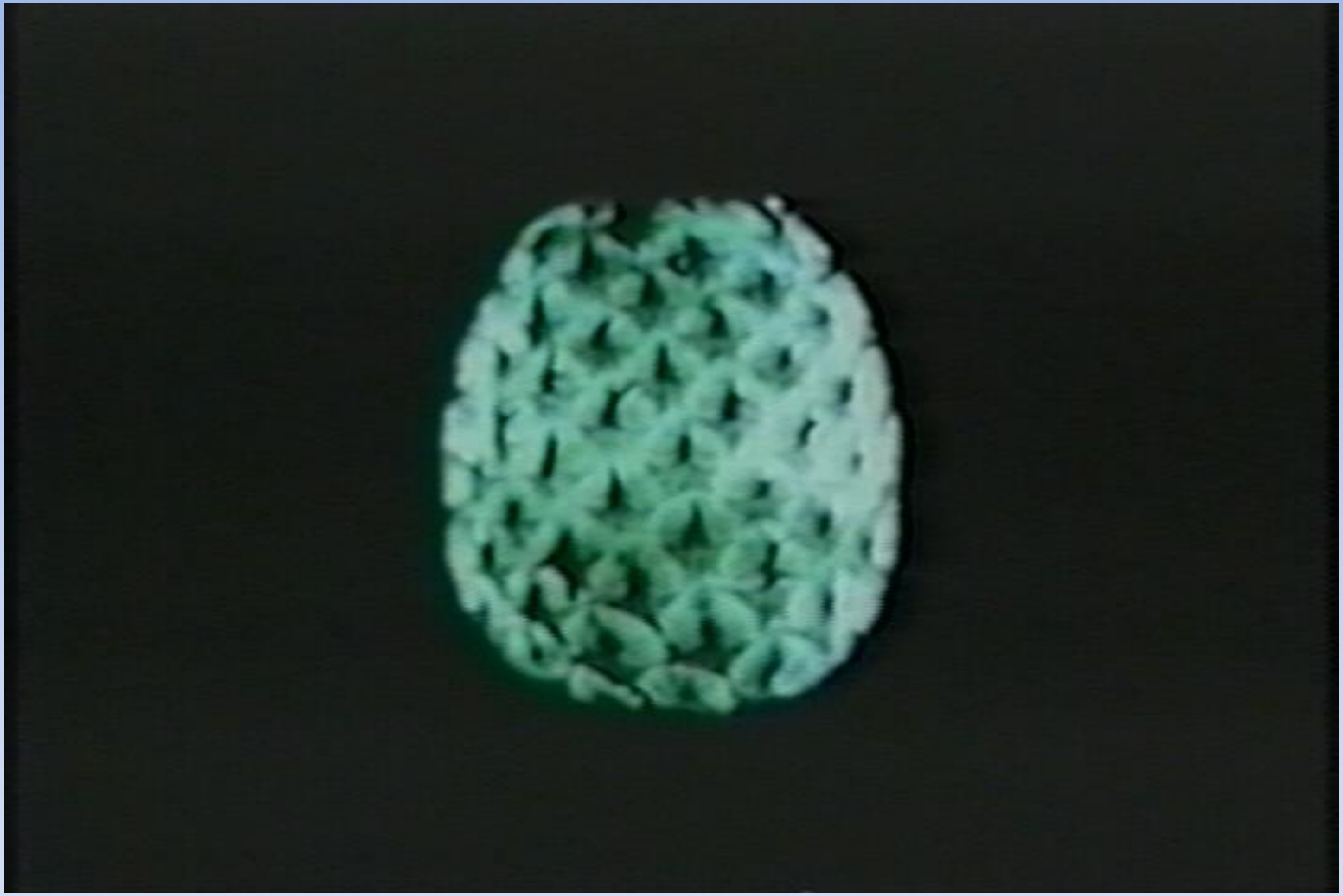

The image of the fruit is very good when the fruit is mature one.

3. Ultrasonic measurement

"Ultrasound is an oscillating sound pressure wave with a frequency greater than the upper limit of the human hearing range."

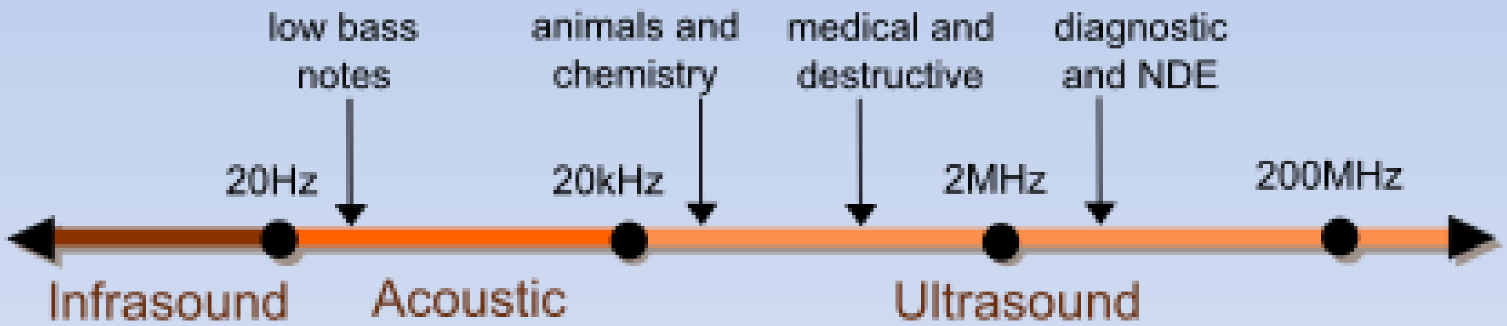

Ultrasound devices operate with frequencies from 20 kHz up to several gigahertz.

http://en.wikipedia.org/wiki/Ultrasound

Ultrasonic measurement

- Ultrasonic is an established technique for:
  - Detection of flaws in terms of size and position in material
  - Measurement of thickness of material

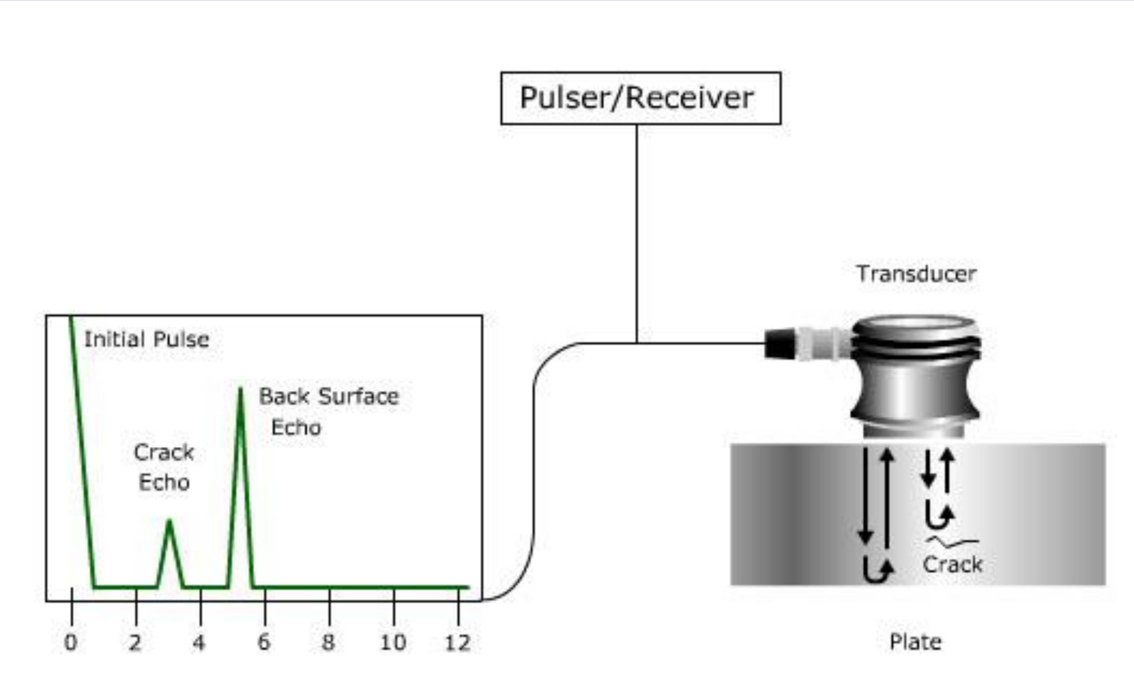

Ultrasonic measurement

Principle:

- Input vibration energy at ultrasonic frequency
- Measure output vibration which is different from the input energy due to sample characteristic
- Extract features in the output vibration which is used to represent quality of the sample

Ultrasonic measurement

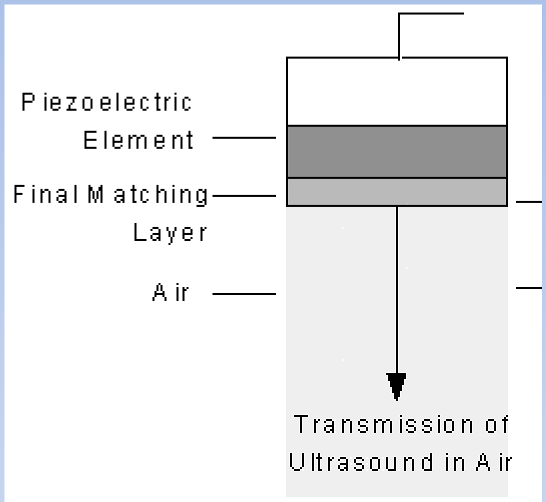

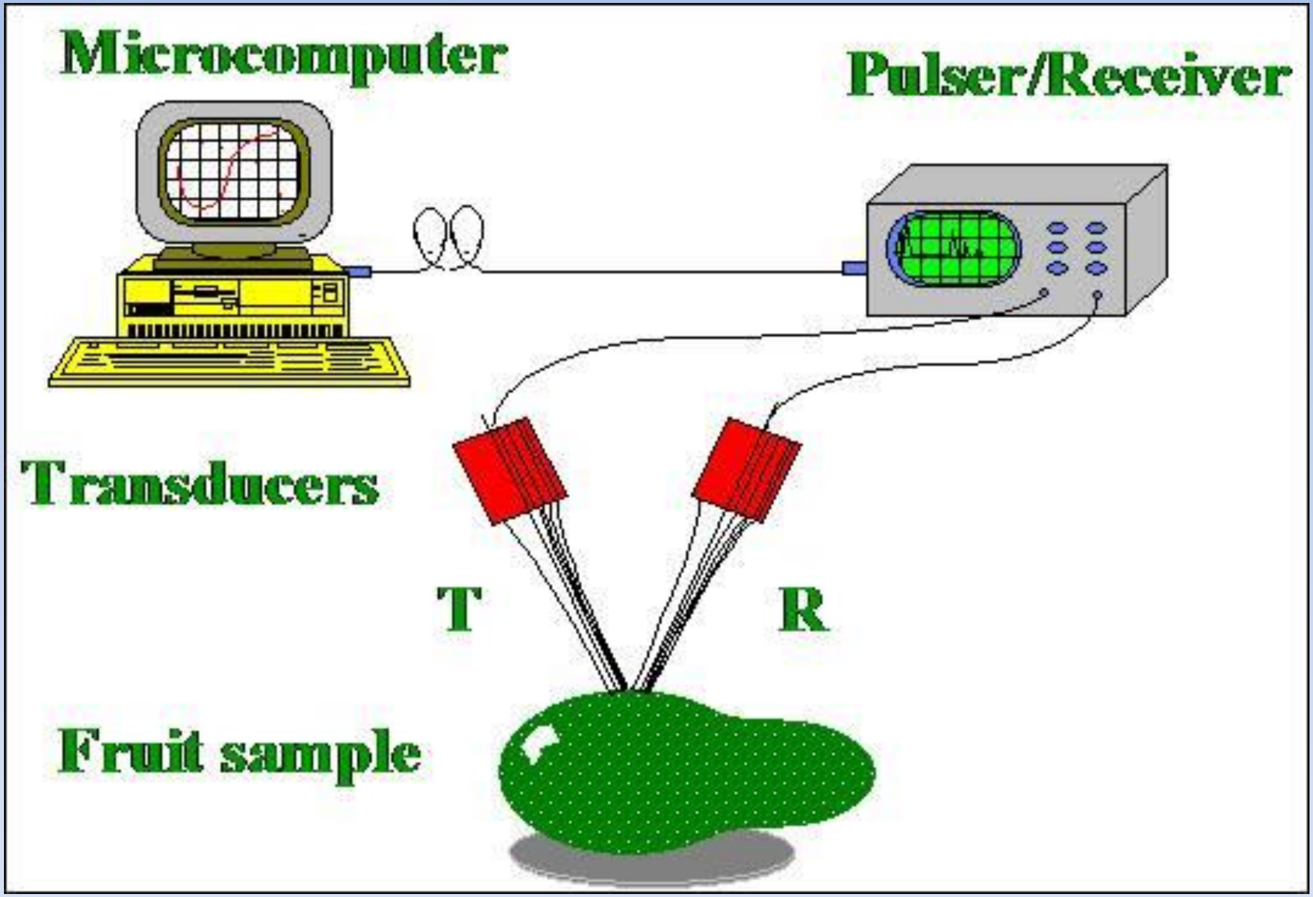

www.ndt.net

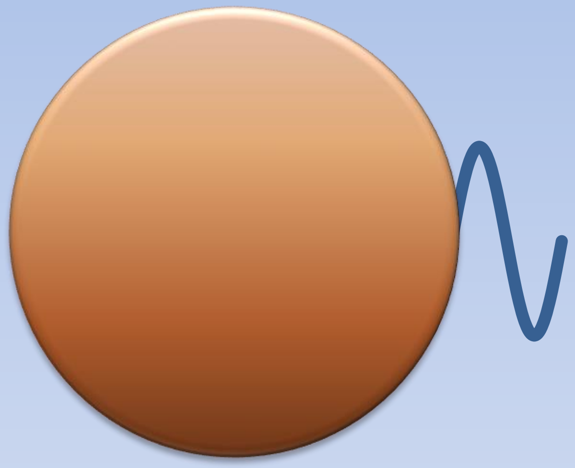

The input and output share the same frequency with difference in amplitude as affected by a sample characteristic

Ultrasonic measurement

- Low frequency ultrasonics has been proposed as an objective analytical technique for non-destructive evaluation of maturity and quality, such as textural properties and dry matter content, in fruit or vegetable.
- The technique measures the changes in ultrasonic waves passing through the peel and flesh.

Ultrasonic measurement

- The parameters commonly measured are velocity (υ) and attenuation (α), which are characteristic for the material and can be related to its physical properties e.g.

    elastic constants,

    density,

    composition, and microstructure

  (McClemments, 1991).

Application

Available online at www.sciencedirect.com

ScienceDirect

Postharvest Biology and Technology 46 (2007) 271–274

Postharvest Biology and Technology

www.elsevier.com/locate/postharvbio

Research Note

Nondestructive ultrasonic monitoring of tomato quality during shelf-life storage

Amos Mizrach *

Institute of Agricultural Engineering, ARO, Volcani Center, P.O. Box 6, Bet Dagan 50250, Israel

- A nondestructive ultrasonic method was used to monitor the firmness of greenhouse tomatoes during their shelf-life.

- This method is based on measurement of acoustic wave attenuation in the fruit tissue, by means of ultrasonic probes in contact with the fruit peel.
- The tomatoes were picked at stage 7 (light red), (1: green to 12: full red) Agrexco Q4-VG-22 color card (Carmel Produce, Israel), and placed in an air-conditioned laboratory at 20 ◦C and about 85% relative humidity (RH).

- The ultrasonic measurement system comprised
  1. a Model USL33 low-frequency ultrasonic pulser-receiver with high penetration power,
  2. a pair of 50-kHz ultrasonic transducers and
  3. a microcomputer system for data acquisition and analysis (Mizrach et al., 1997).
- The transducers were mounted with an angle of about 120◦ between their axes and were held in contact with the fruit by application of a fixed load.

- The penetration tests were applied to unpeeled fruit, with a Chatillon Durometer fitted with a 6.35mm diameter conical head with a 60◦ cone angle.
- Each fruit was subjected to a penetration test at each of the two marked points, which were near the location of the ultrasonic transducer contact points, and the tests were applied in the radial direction.

- The maximum penetration force (firmness) was recorded at a penetration rate of 3 mm/s, and the maximum penetration depth was about 7 mm.

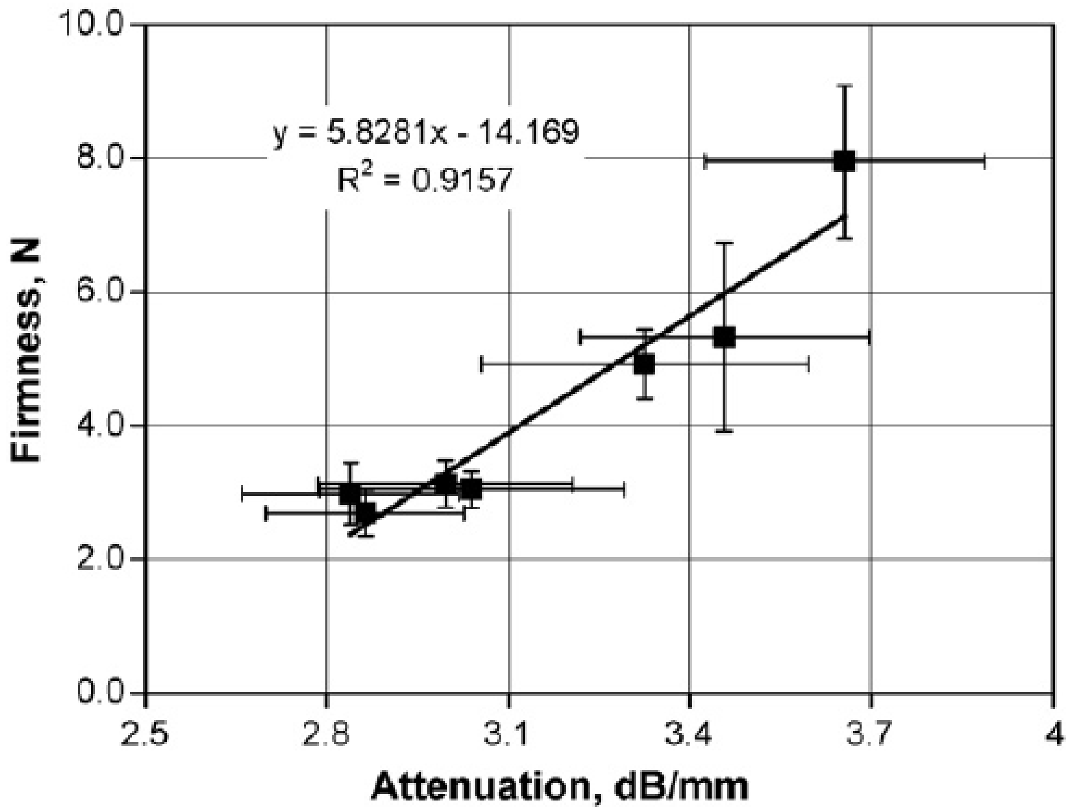

Fig. 3. Attenuation vs. firmness of tomatoes during the course of shelf-life. Vertical and horizontal lines represent confidence limits of the mean ($\alpha = 0.05$).

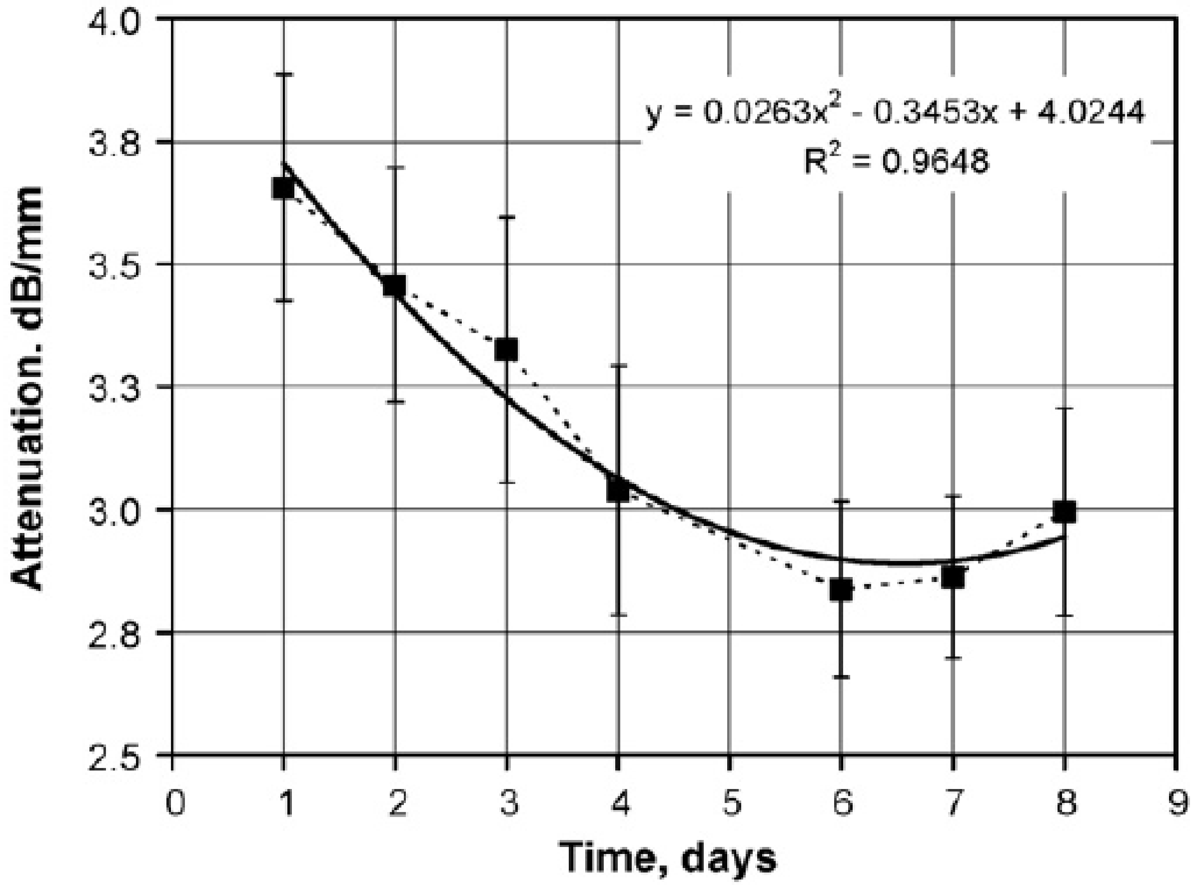

Fig. 1. Variation of the mean values of wave attenuation with storage time in fruit group N1–N10. Vertical lines represent confidence limits of the mean ($\alpha = 0.05$).

$$\text{attenuation} = \left(\frac{10}{L}\right)\log_{10}\left(\frac{P_i}{P_o}\right)$$

Pi = input power, Po = output power and L = pathlength

4. Acoustic response

- Quality of some agricultural produces are related to the sound generated after tapping
- Based on resonant characteristic
- Two methods:
  1. Forced vibration
  2. Free vibration
  (Different duration of input)

Resonance

"a phenomenon that occurs when a given system is driven by another vibrating system or external force to oscillate with greater amplitude at a specific preferential frequency"

- Examples of resonance phenomena
  - Tahoma bridge
  - Vibrating wine glass
  - Pendulum

https://en.wikipedia.org/wiki/Resonance

Resonance phenomena

(Failure of Tacoma bridge)

http://www.youtube.com/watch?v=lXyG68_caV4

Resonance phenomena
(Wine glass breaking)

http://www.youtube.com/watch?v=BE827gwnnk4

Resonance phenomena

(Maximum vibration at the resonant frequency)

http://www.youtube.com/watch?v=iyw4AcZuj5k

Forced vibration

- Object responses most to the vibration corresponding to its resonant frequency.
- How to determine the resonant frequency:

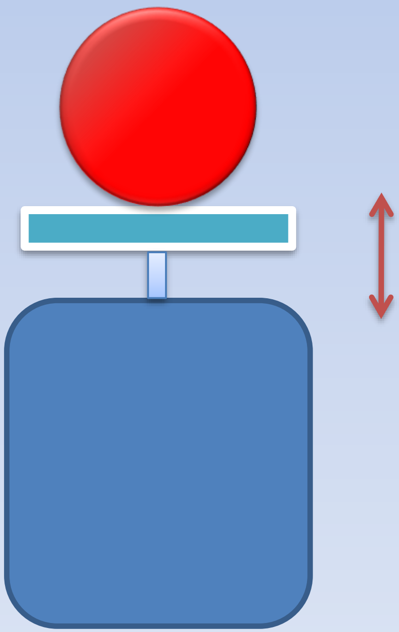

1. Subject object to a range of vibration covering the resonant frequency.
2. Record the frequency and the corresponding amplitude.
3. The frequency at the maximum peak being the resonant frequency.

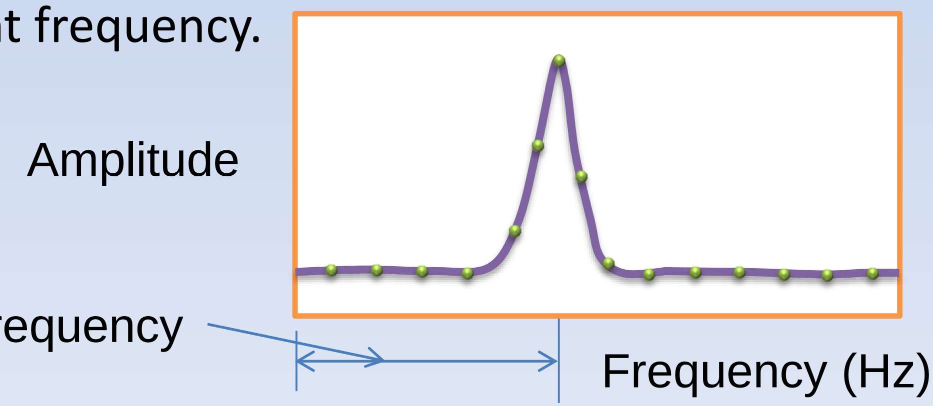

Experiment to determine the acoustic related parameter

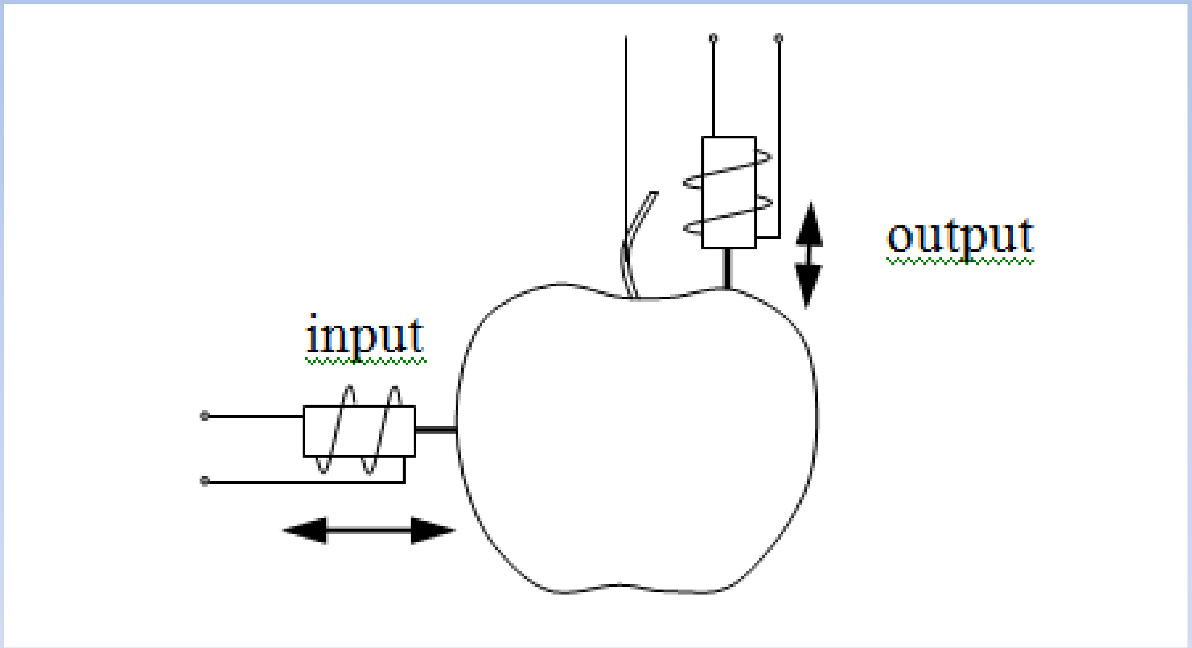

Experiment to determine the acoustic related parameter

Determination of resonant frequency of apple (results)

- The greater the weight the lower the frequency
- The greater the ripeness the lower the frequency

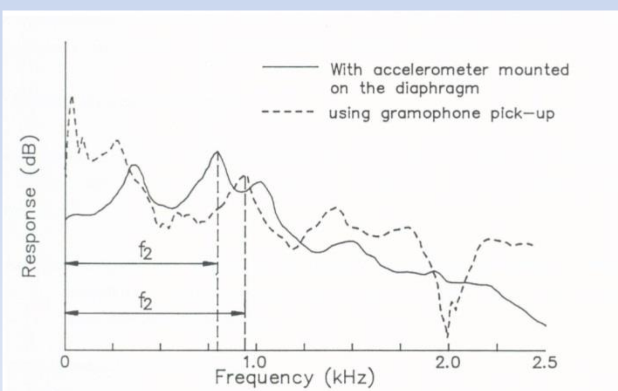

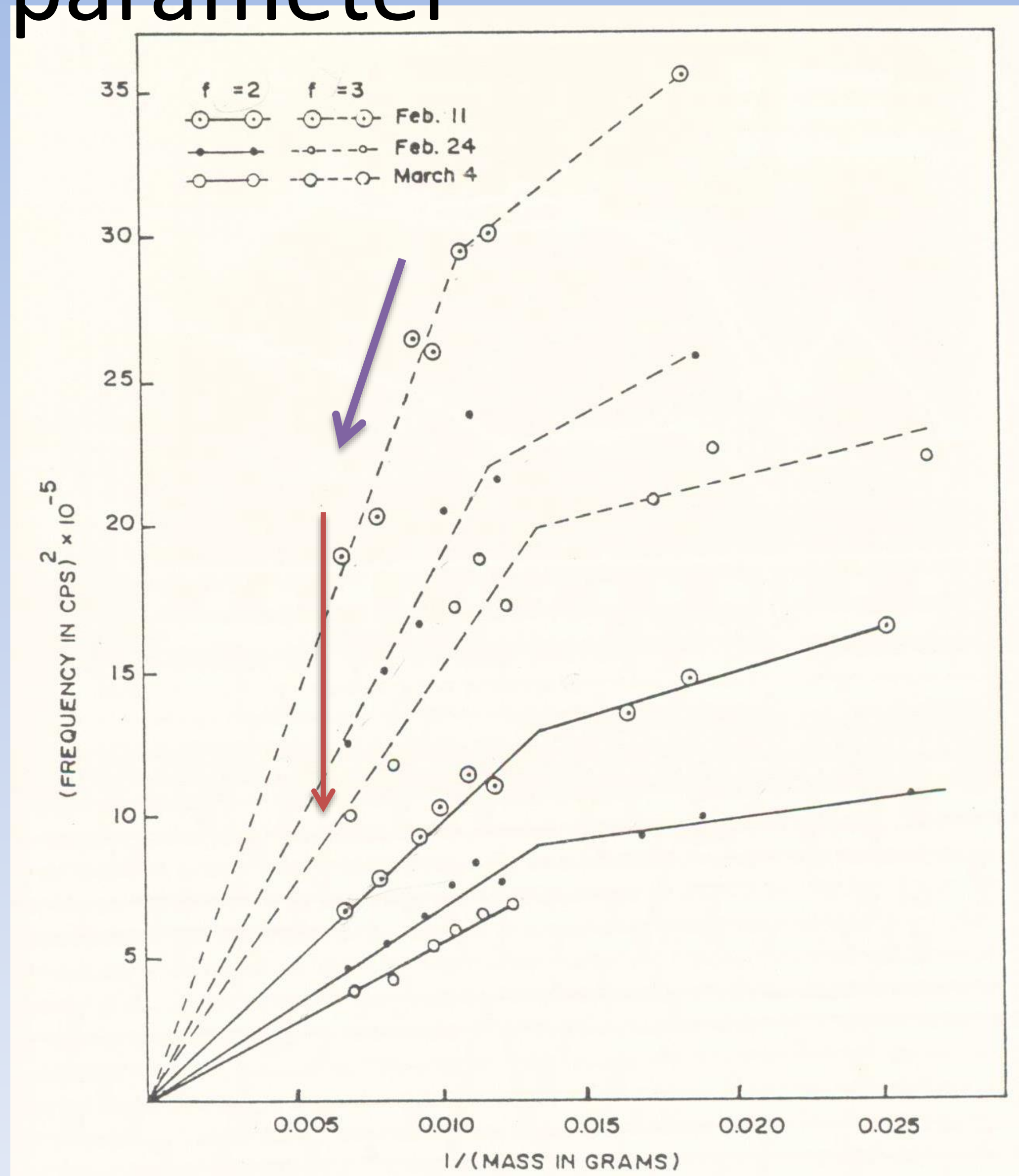

(Abbott et al., 1968)

Experiment to determine the acoustic related parameter

Determination of resonant frequency of apple (results)

$$\text{stiffness coefficient} = f_2^2 m$$

f_2 = second resonant frequency
m = weight

So the slope of this graph represents the firmness of apple

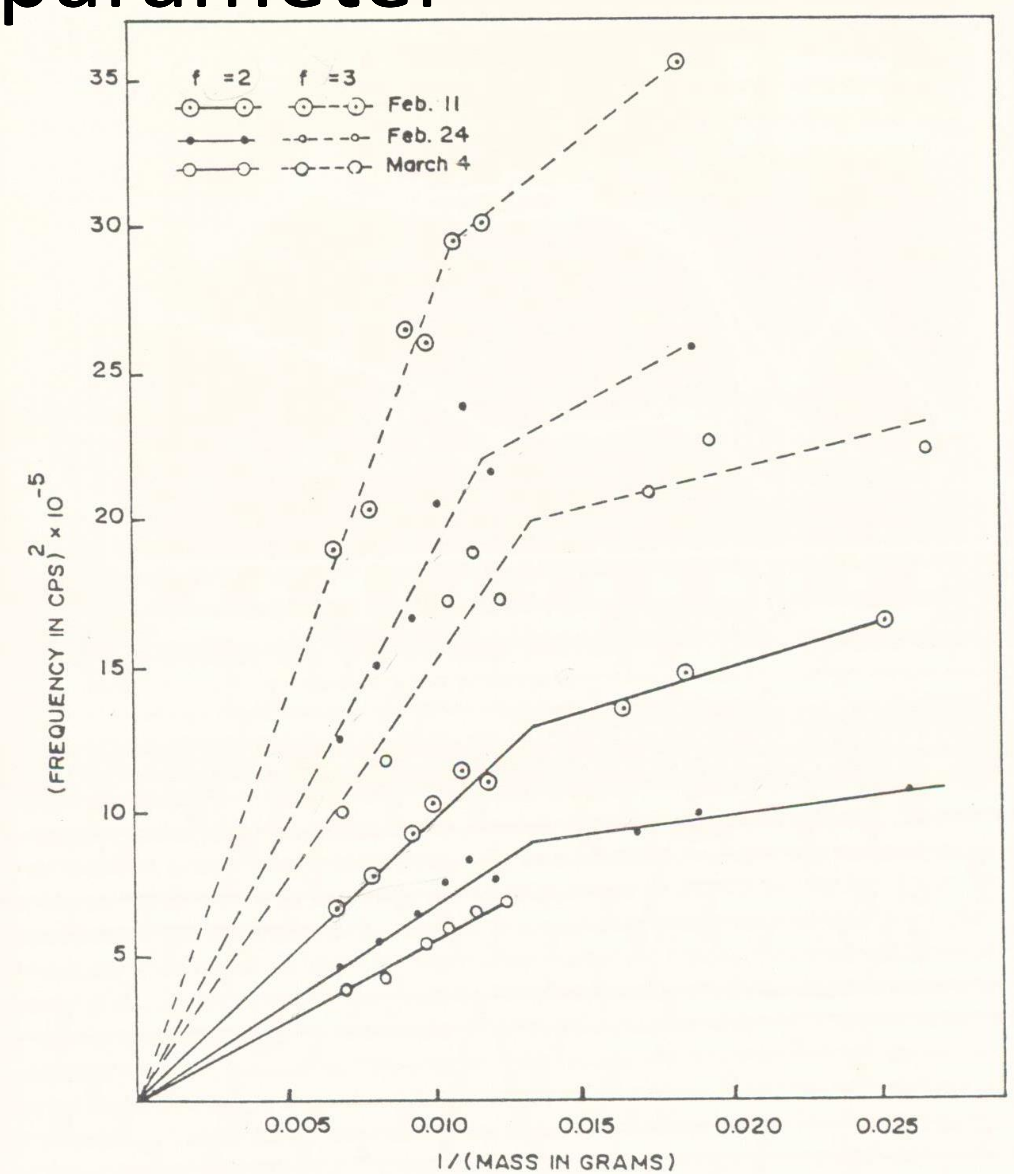

(Abbott et al., 1968)

Maness-Taylor penetrometer

$f_2^2 m$ α Magness-Taylor firmness

www.ipt.us.com

msue.anr.msu.edu

Experiment to determine the acoustic related parameter

Determination of resonant frequency of apple

- Input vibration through vibrator
- Pick up output through accelerometer
- Repeat by increasing frequency in step to cover the given range

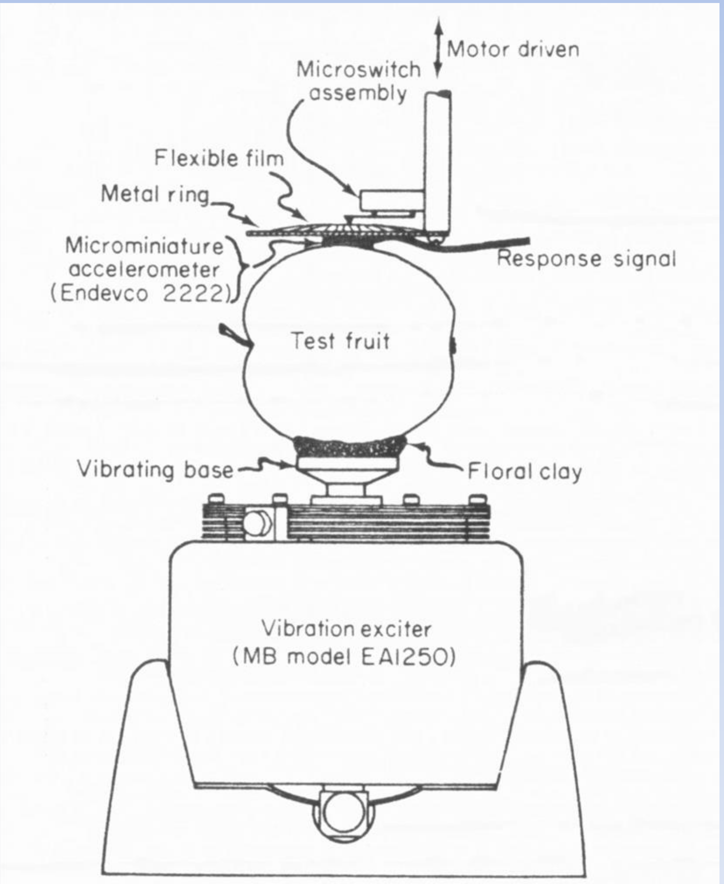

(Finney, 1970)

Forced vibration

Tomato sorter (Qualitative sorting)

- The system utilizes an elongate sorting zone incorporating a surface which oscillates at a predetermined frequency and amplitude which varies from a minimum at the input of the zone to a maximum value at the output.

United States Patent [19]

Holmes

[54] **SORTING SYSTEM AND APPARATUS**

[75] Inventor: **Robert G. Holmes,** Columbus, Ohio

[73] Assignee: **Ohio Agricultural Research & Development Center,** Wooster, Ohio

[21] Appl. No.: **156,600**

[22] Filed: **Jun. 5, 1980**

Forced vibration

Tomato sorter

- Conveyor belts transport the objects to be sorted along the zone for a coding interval promoting their dynamic reaction with the oscillatory surface.
- Objects with higher resilience characteristic are rejected from the zone, while those exhibiting a lesser resilience are transported therethrough.

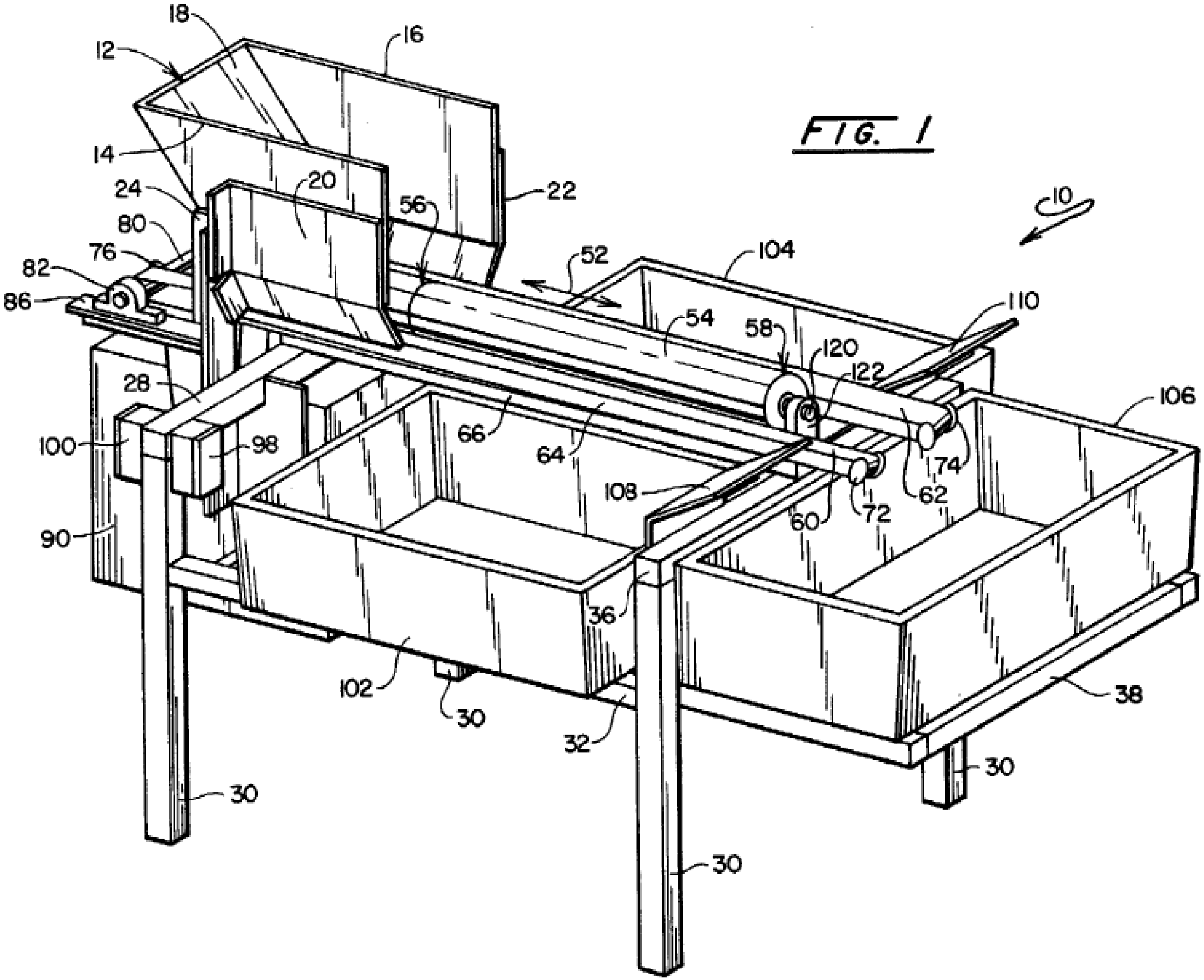
18
16
12
14
24
20
22
80
56
76
52
104
82
86
54
58
110
120
122
28
106
100
98
66
64
74
108
62
72
60
90
36
102
30
32
38
30
30
30

FIG. 1

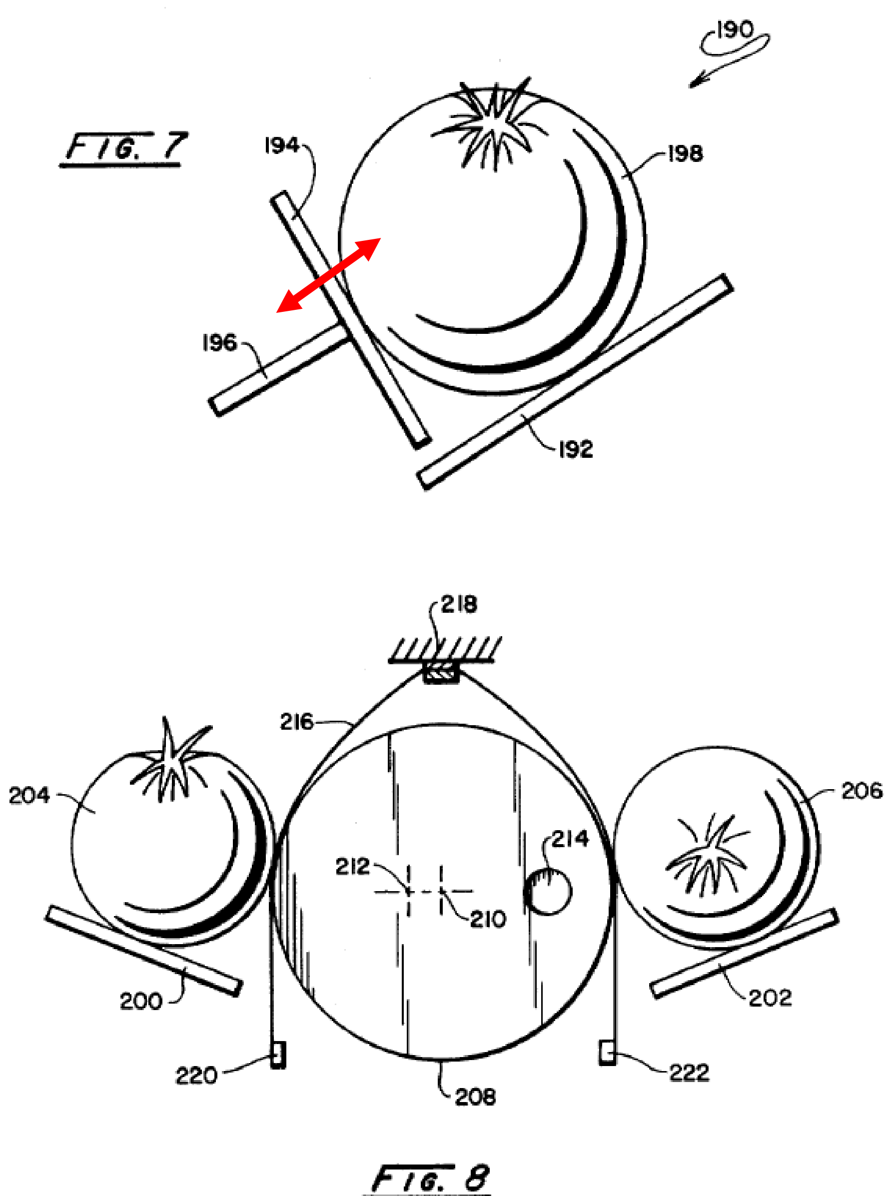
FIG. 7
190
194
198
196
192
218
216
204
206
214
212
210
200
202
220
208
222
FIG. 8

Firmness sorting machine

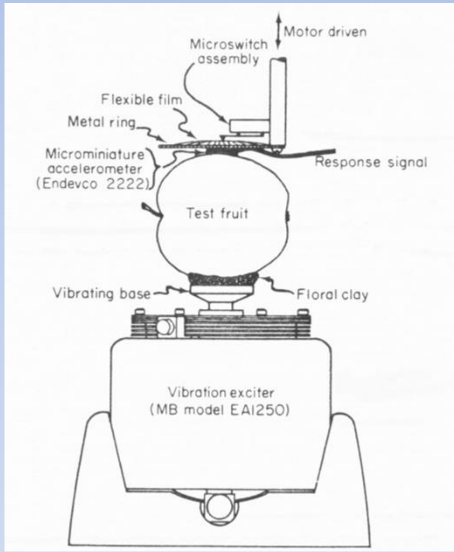

http://peleg.com/pfs/index.html

Free vibration

The duration of input is short.

Free vibration

Determination of resonant frequency of water melon

- Set fruit into vibration with pendulum
- Record the sound by a microphone
- FFT to create acoustic spectrum and determine the resonant frequency

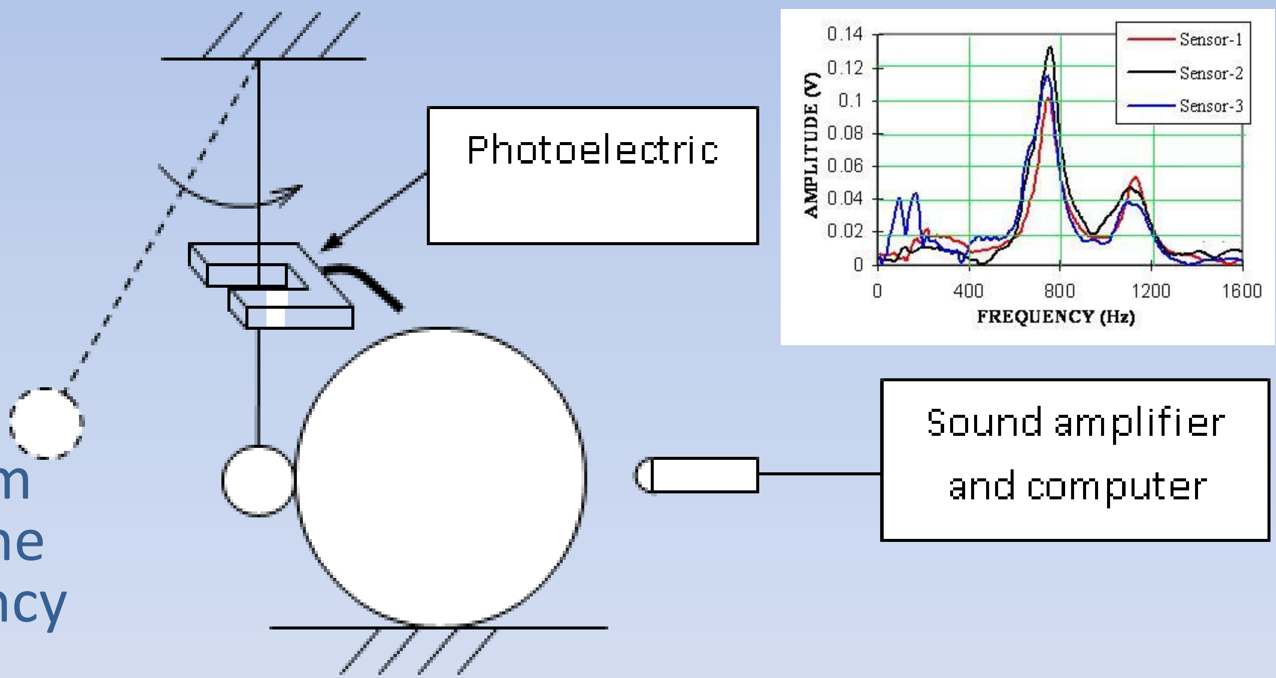

- (FFT = Fast Fourier Transform: used to transform time domain signal into frequency domain signal)

(Yamamoto et al., 1980)

Acoustic Watermelon Ripeness Sensor

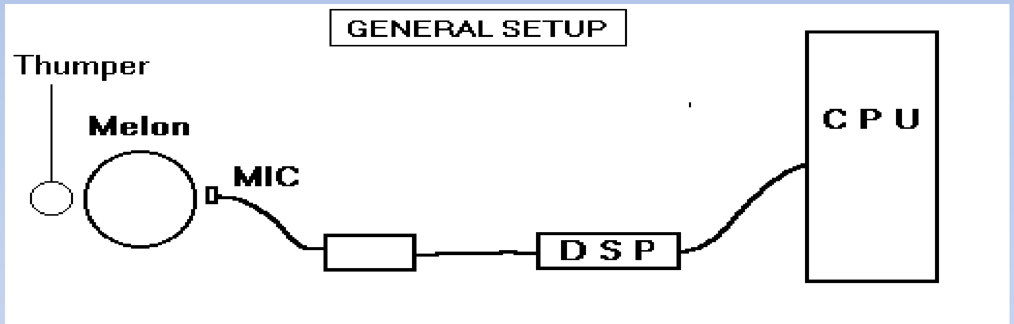

Resonant frequency is not affected by the hitting strength

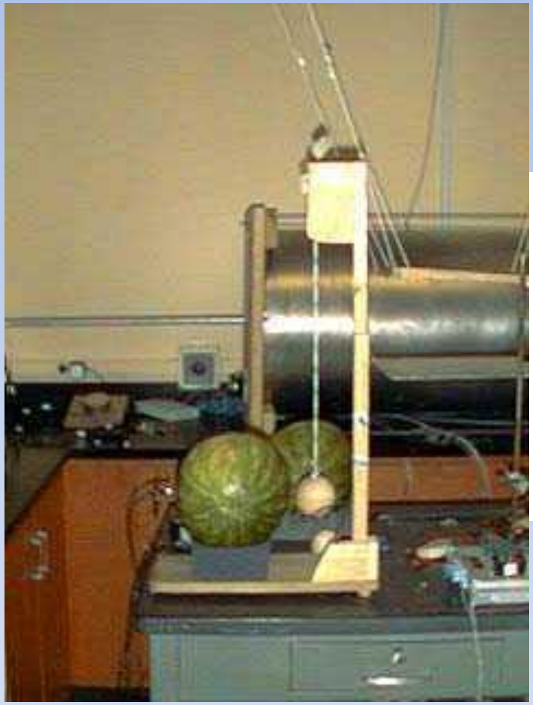

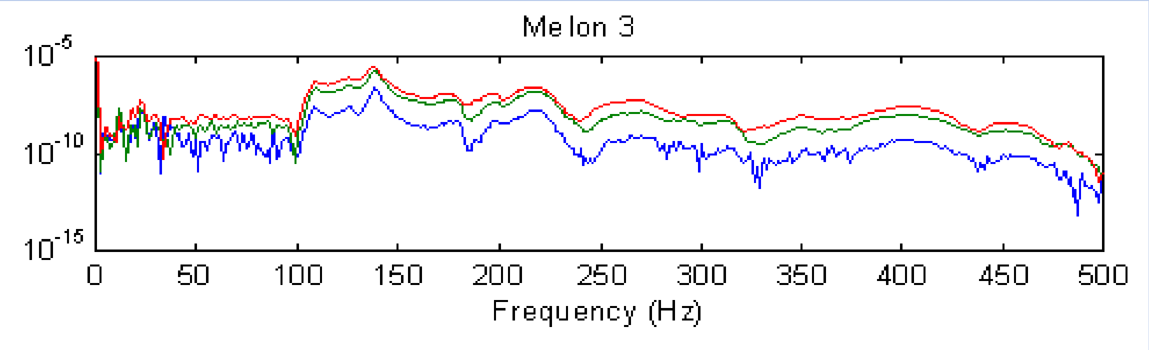

Acoustic Sensing During CA

Field Maturity Measurements

Field Maturity Measurements

Field Maturity Measurements

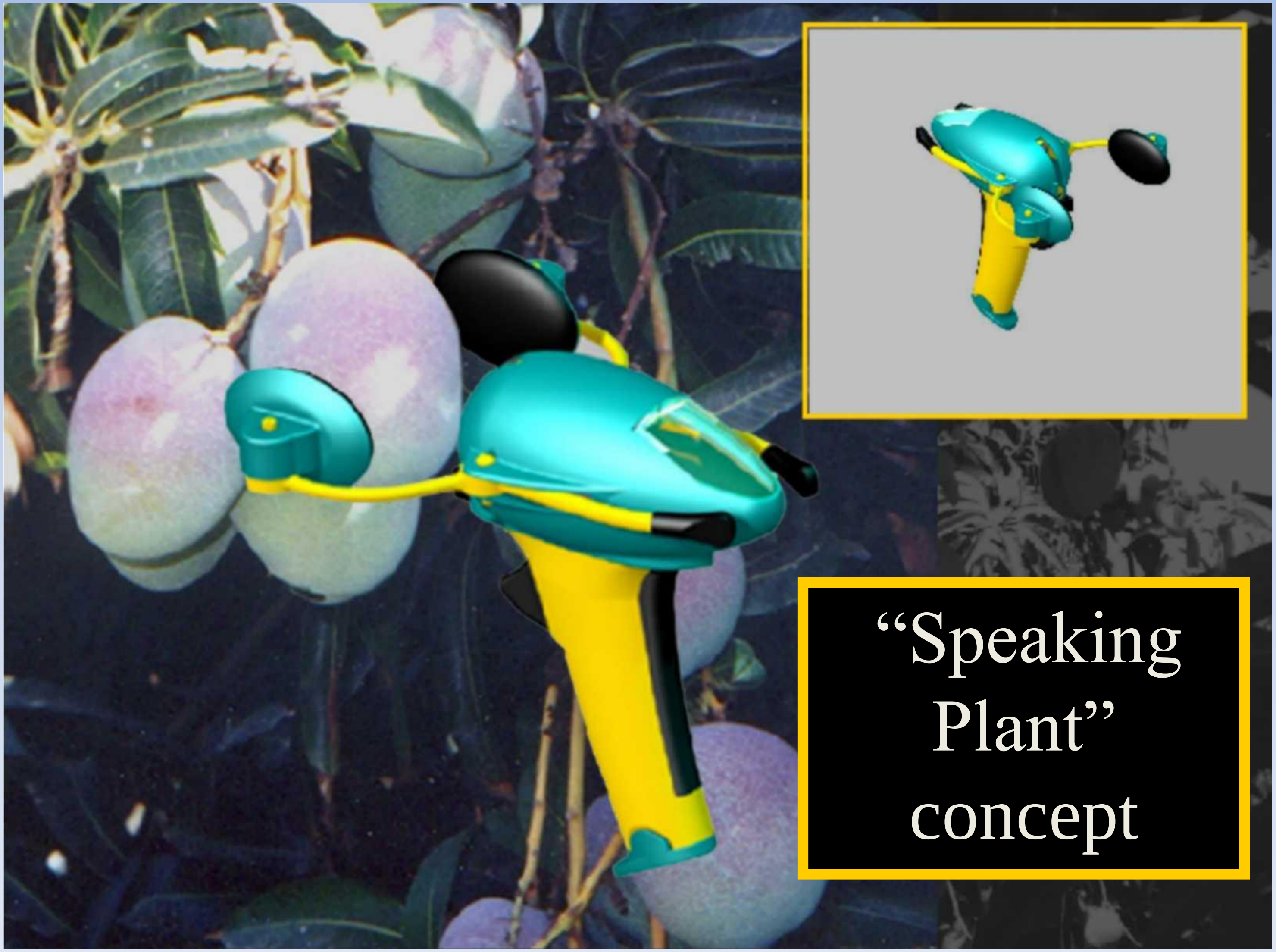

Internal void sorting machine

(Qualitative application)

Each watermelon is placed on a free tray by hand

The tray moves into the detector unit.

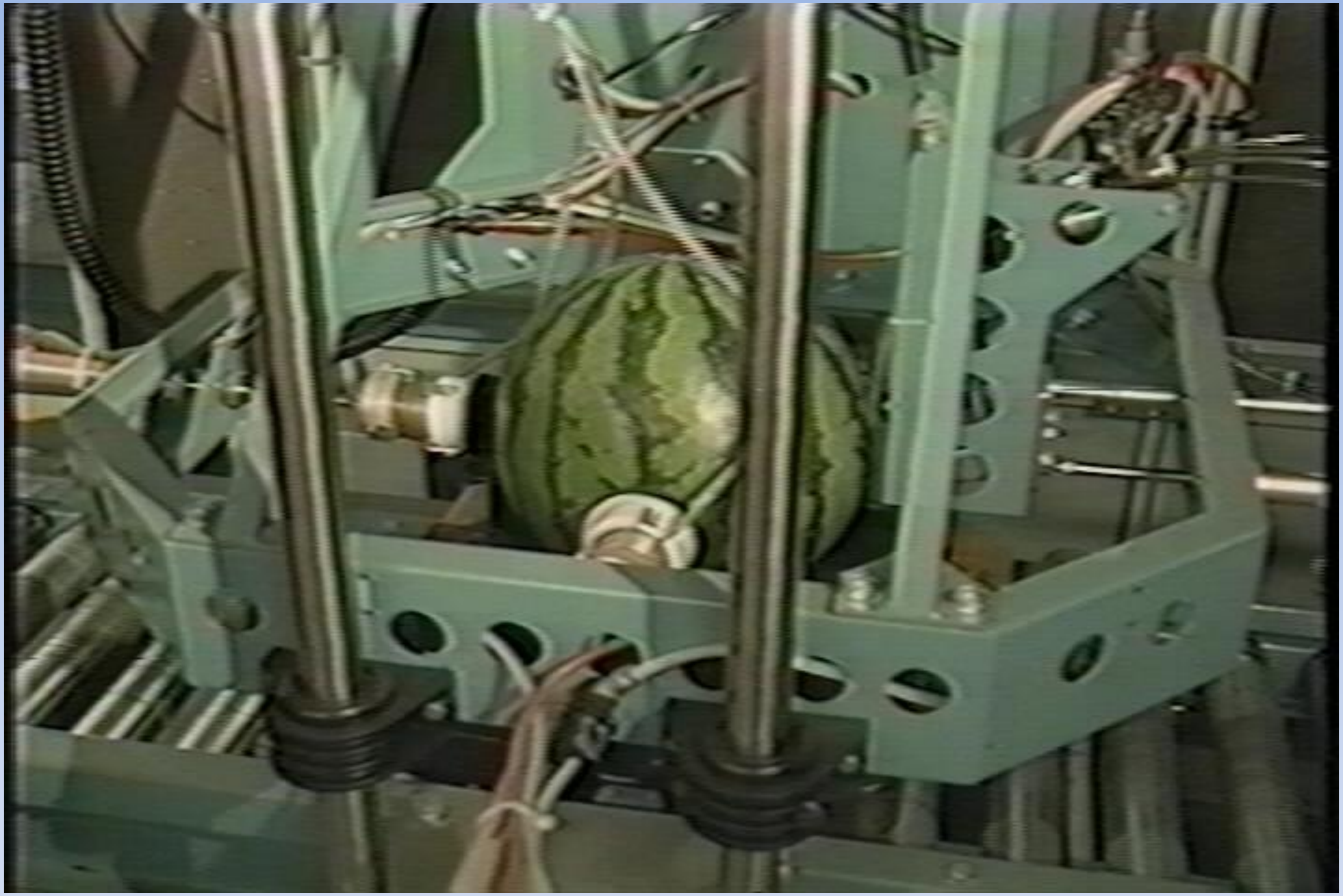

The sorting machine gives an impact to the fruit with a small hammer and then 3 microphones detect the impact sound.

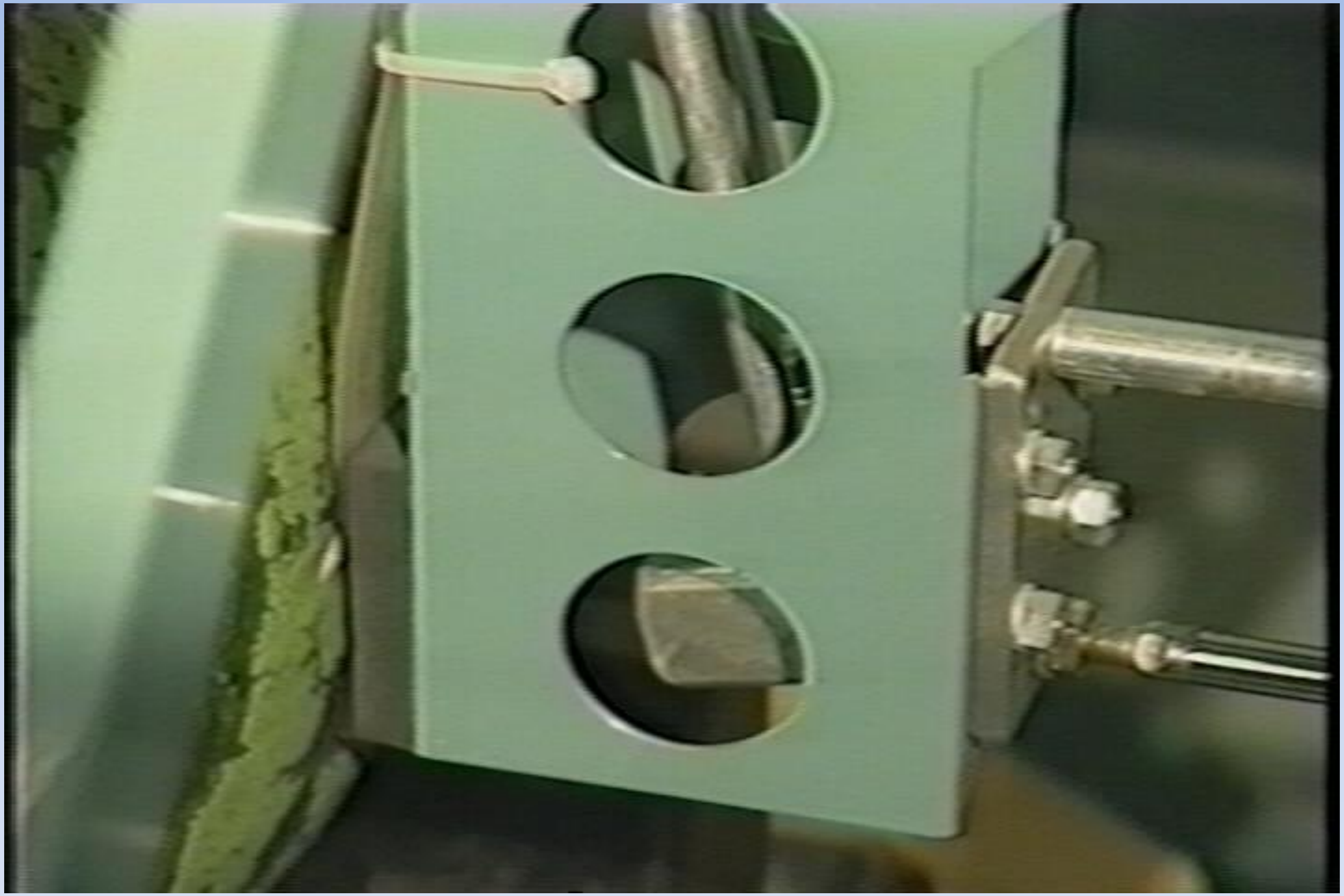

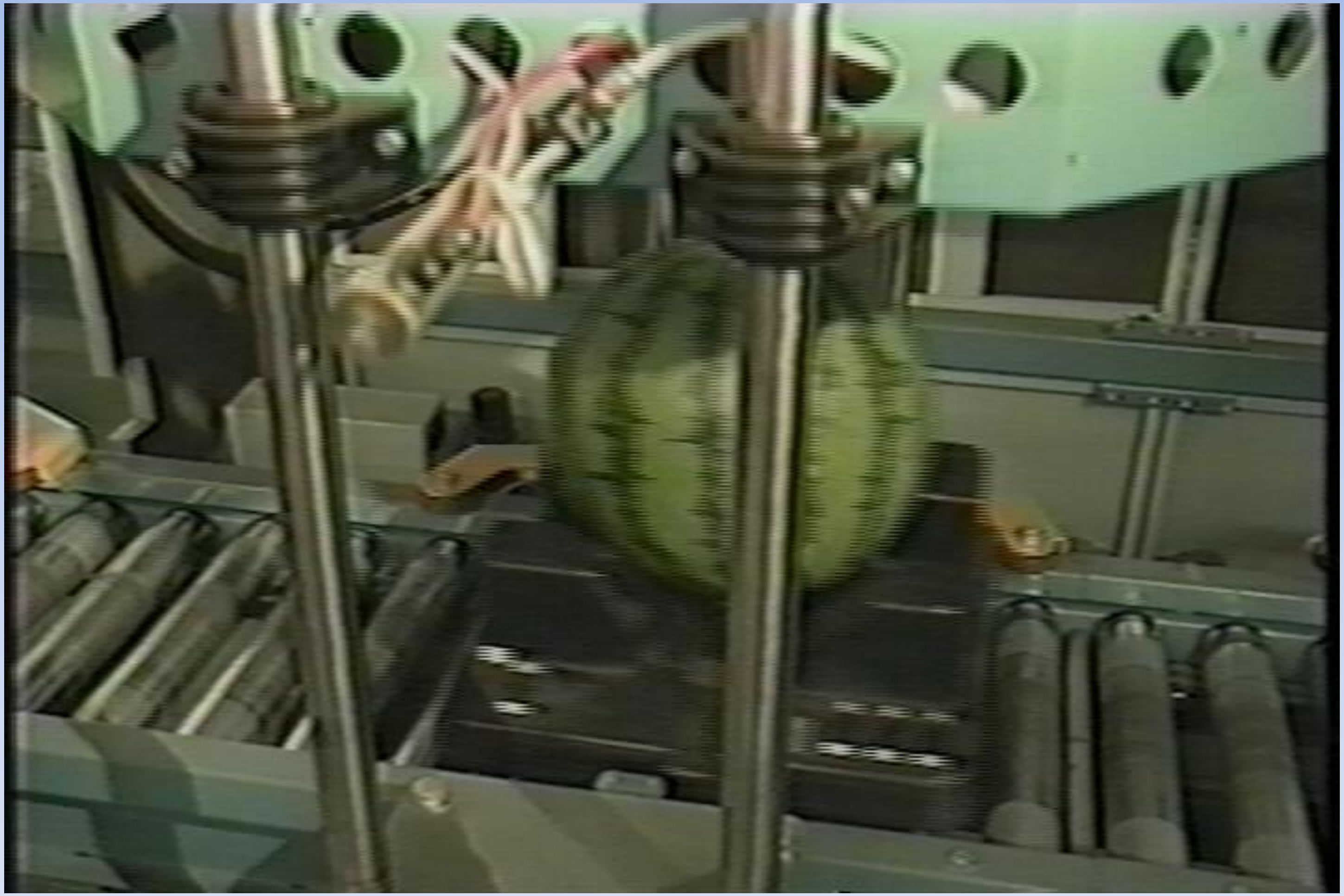

The sound signals from the microphones are compared with each other. If significant differences in shape and phase of the signals exist, the fruit is graded as “ an internal void fruit”.

Free vibration

BIOSYSTEMS ENGINEERING 100 (2008) 206–213

ELSEVIER

Available at www.sciencedirect.com

ScienceDirect

journal homepage: www.elsevier.com/locate/issn/15375110

Biosystems Engineering

Research Paper: PH—Postharvest Technology

An acoustic impact method to detect hollow heart of potato tubers

I.E. Elbatawi

Senior Researcher at Agricultural Engineering Research Institute, Handling and Processing Engineering, P.O. Box 256, Nadi Elsaid Street, Dokki. Giza. Egypt

Fig. 1 – Characteristic hollow heart shown by a star-shaped cavity in the centre of the tuber.

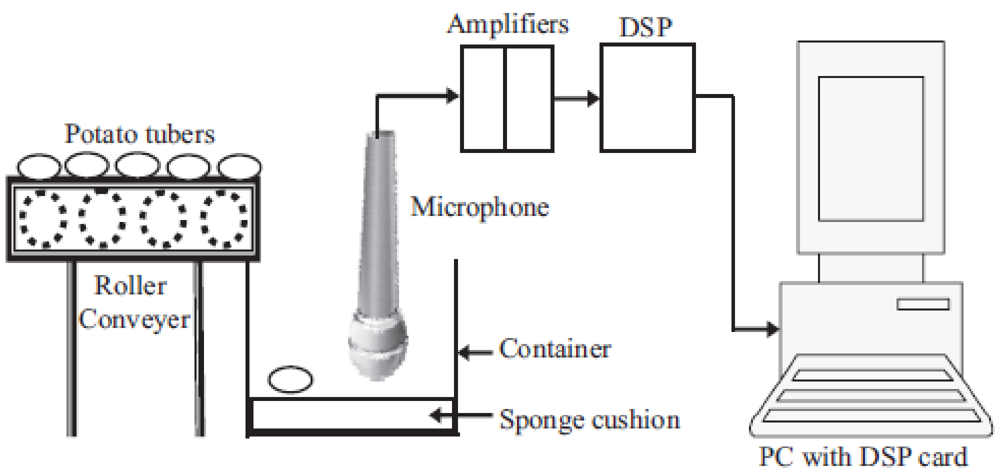

Fig. 2 – Schematic diagram of the experimental and impact sound sorting system.

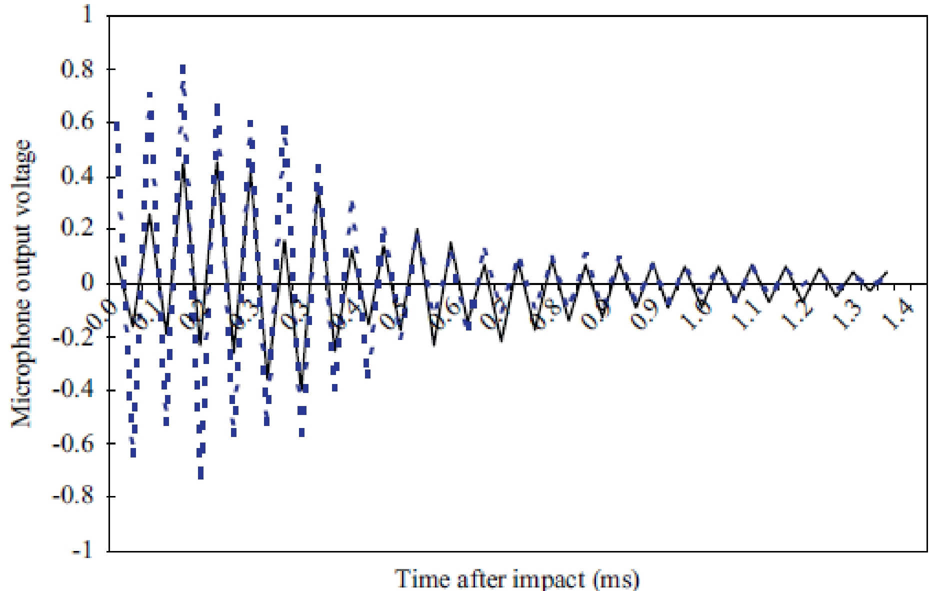

Fig. 3 – Digitised microphone signal of Spunta potato tuber with hollow heart (solid line) and without hollow heart (dashed line).

- Study the effect of impact position on the acoustic response (resonant frequency).
- The effective feature for discrimination between tuber with hollow heart is greater than those without.

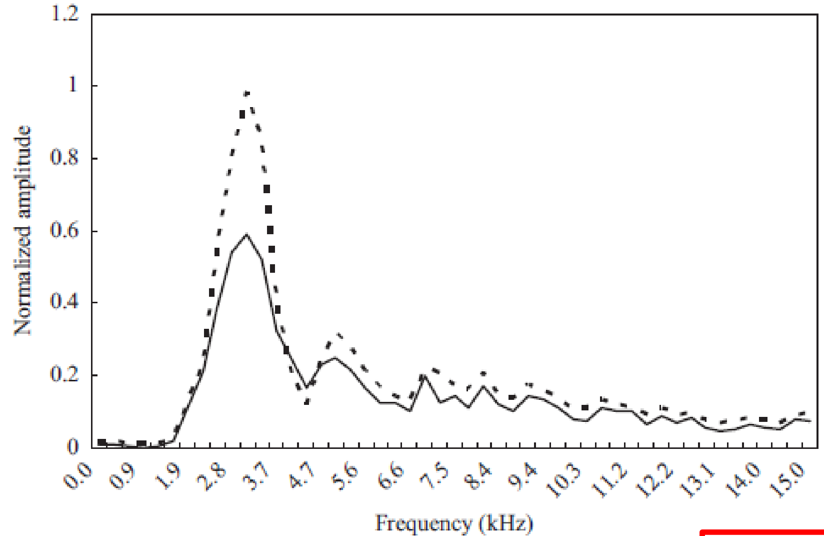

Fig. 4 – Average frequency spectra magnitudes of the impact sound of Spunta potato tuber with hollow heart (solid line) and without hollow heart (dashed line).

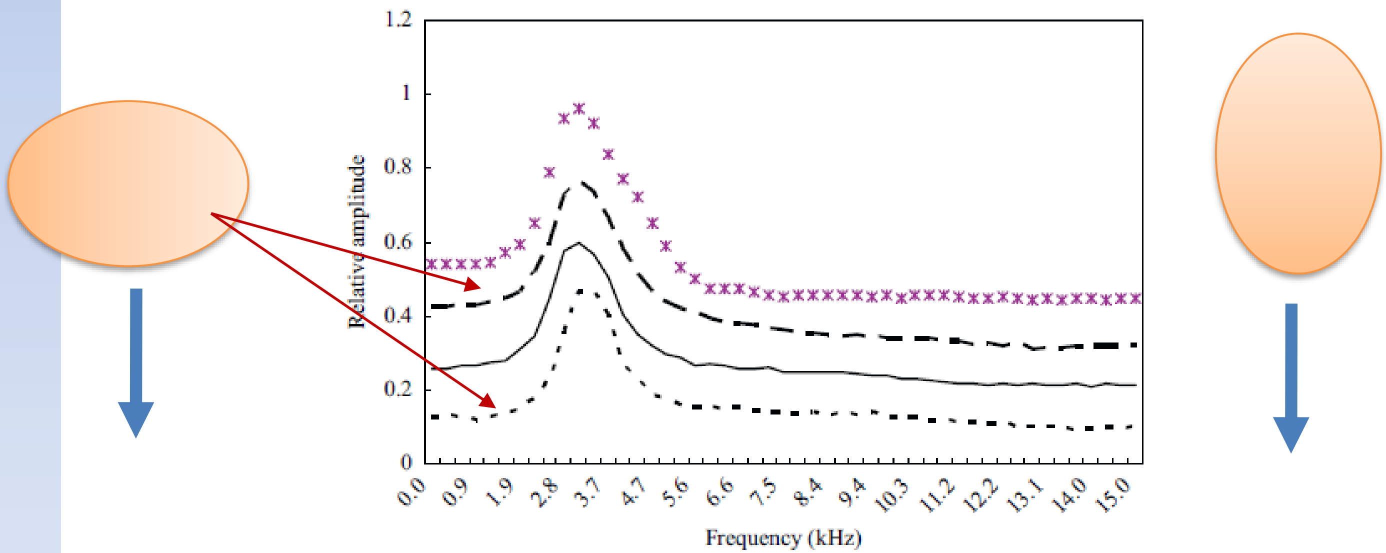

Fig. 5 – Effect of tuber position (twice onto the equators and twice onto the poles) on the acoustic signal and resonant peaks (equator 1 marked by dashed line, equator 2 marked by dotted line, pole 1 marked with x symbol and pole 2 marked by solid line).

- There were different peak frequencies between tubers with hollow heart and those without.
- The magnitude of peak frequency of tuber with hollow heart is lower than those without.
- The criteria to distinguish hollow tubers can be drawn from the average area.

- Only four out of 300 tubers were misclassified in all cases, which represent more than 98% of accuracy.

Application of free vibration to durian industry

Inherent problem of durian export

- Harvest of durian at the beginning of the season:
  - High demand
  - Good price
  - Tendency for immature durian being picked
  - Low quality

Durian maturity indices

- Days after blossom
- Tapping sound
- Stem related characteristics
- Thorn strength
- Color etc.




Acoustic measurement in orchard

Acoustic response

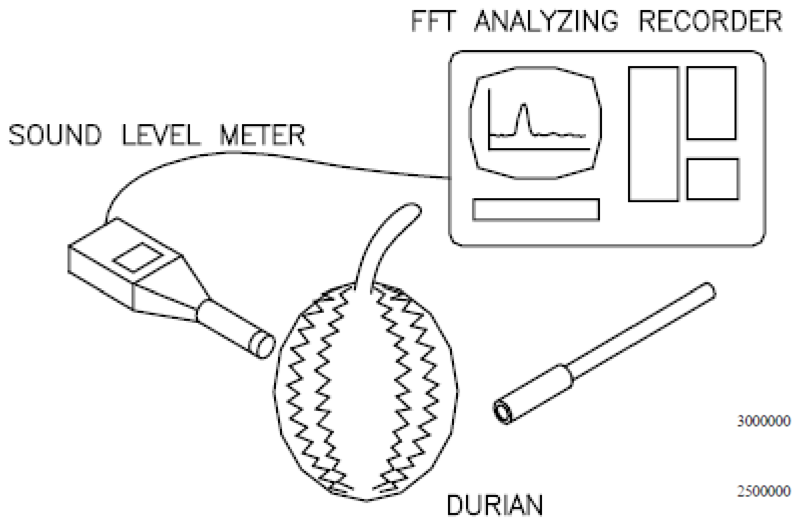

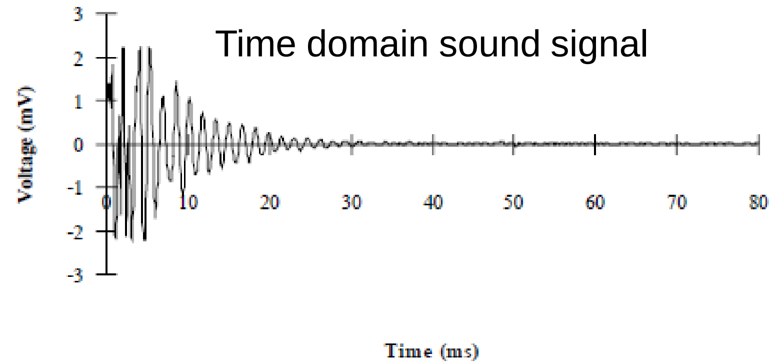

Exponential index = $f^2 \ln(m)$
f = resonant frequency
m = durian weight

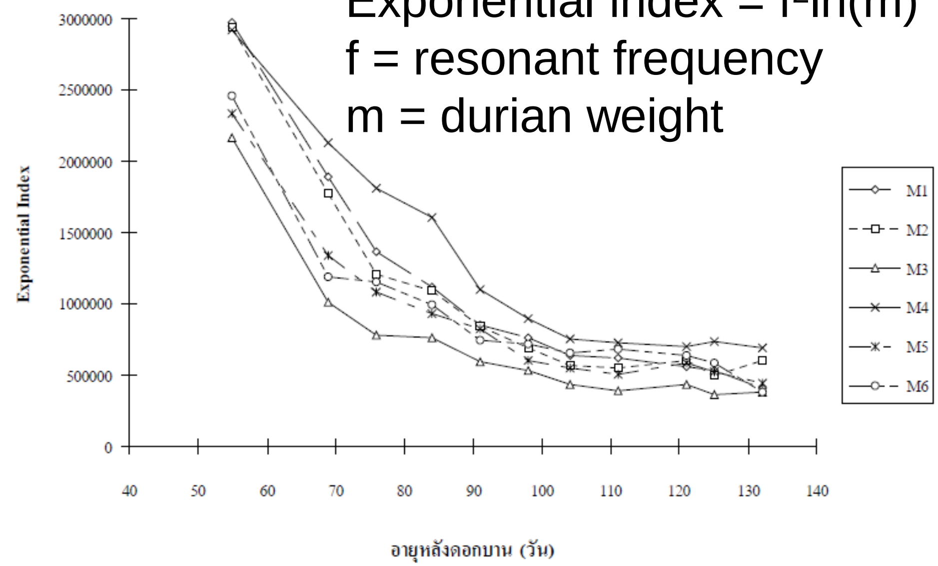

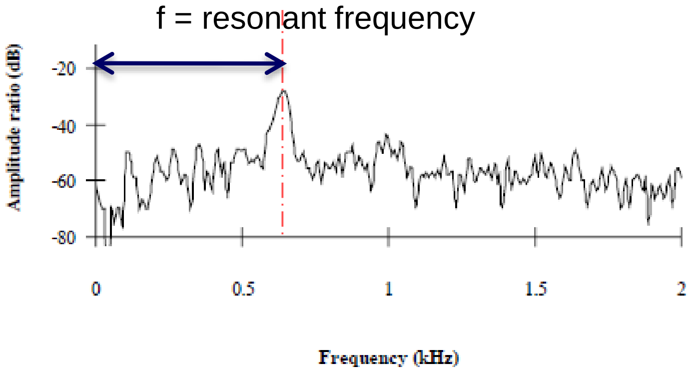

Fast Fourier transformed signal

The more mature the lower the pitch of the tapping sound

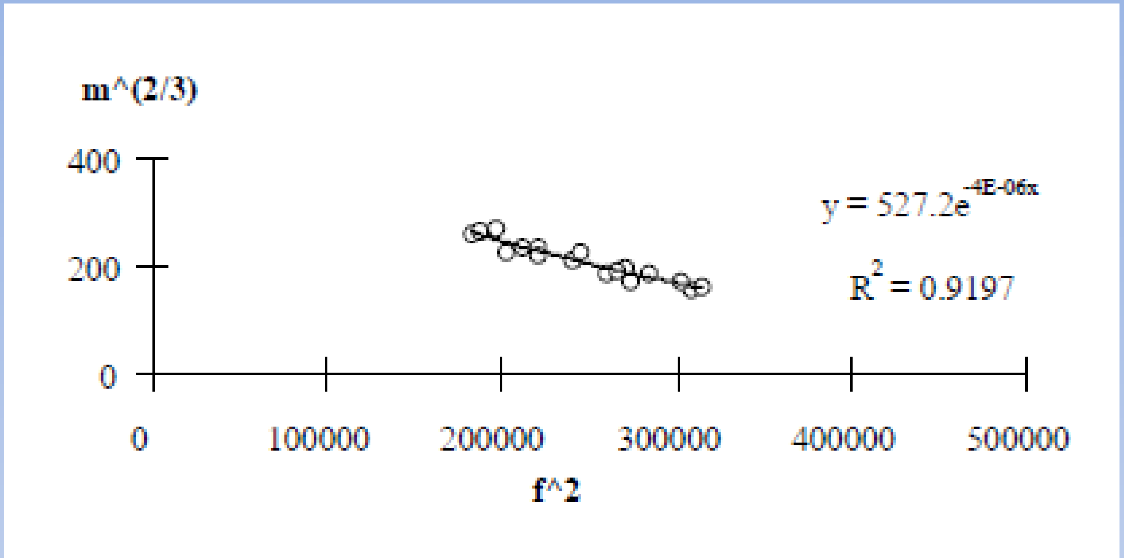

- Firmness index is expressed as follows:

$$\text{Exponential index} = f^2 \ln(m)$$

- where f_R *is the resonant frequency of the first elliptical mode* in Hz and m *is the mass of the durian (g).*

Durian fruit at about 70 days after full blossom

Application to tropical fruit

2. Classification of pineapple maturity

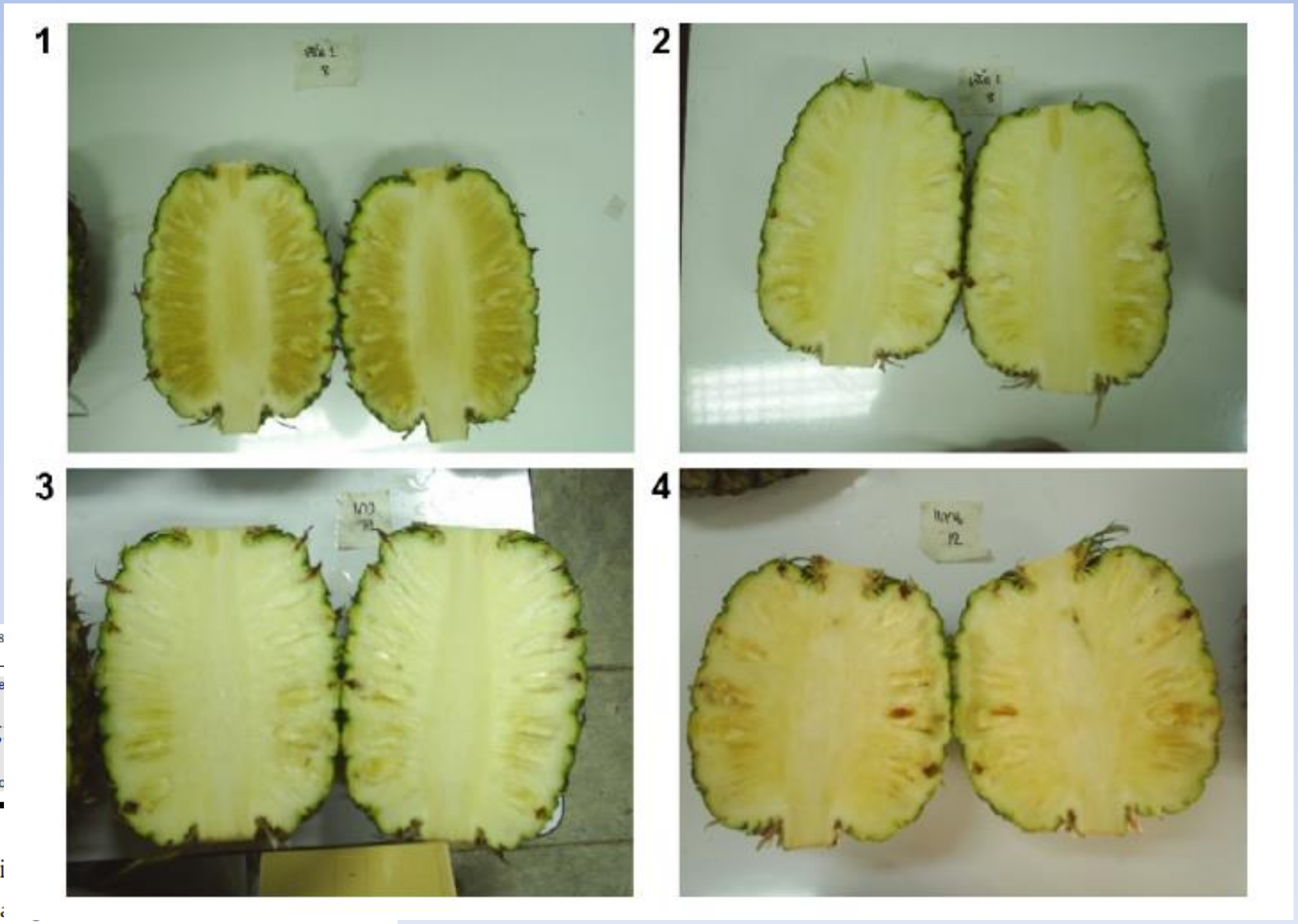

Journal of Food Engineering 89 (2008

Contents lists available at Scie

Journal of Food Eng

journal homepage: www.elsevier.co

ELSEVIER

Multivariate data analysis for classification of pi

Siwalak Pathaveerat[a,*], Anupun Terdwongworakul[b], Artit Pha

[a] Department of Agricultural Engineering, Faculty of Engineering at Kamphaeng Saen, Kamphaeng Saen Campus, Nakhon Pathom 73140, Thailand
[b] Department of Food Engineering, Faculty of Engineering at Kamphaeng Saen, Kamphaeng Saen Campus, Nakhon Pathom 73140, Thailand

Application to tropical fruit

2. Classification of pineapple maturity

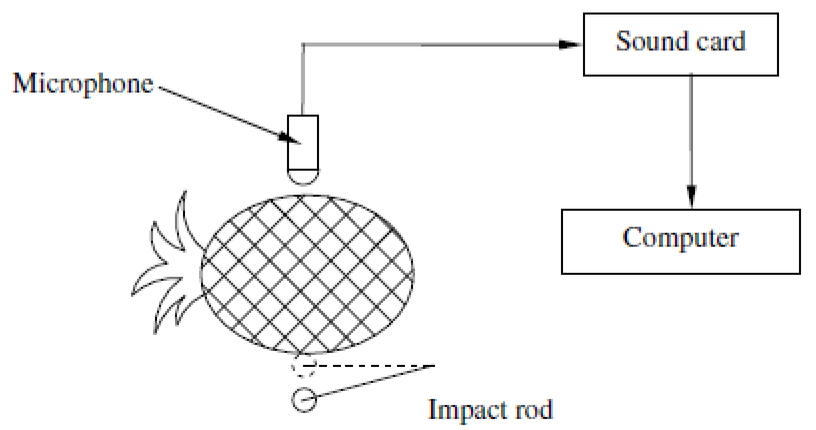

Fig. 1. Arrangement of the acoustic impulse method.

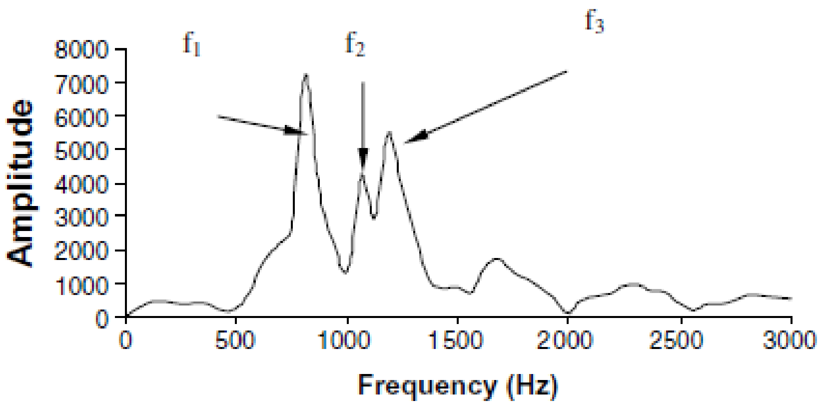

Fig. 3. Acoustic impulse response of a pineapple sample showing three peaks.

Journal of Food Engineering 89 (2008) 112–118

Contents lists available at ScienceDirect

Journal of Food Engineering

journal homepage: www.elsevier.com/locate/jfoodeng

ELSEVIER

Multivariate data analysis for classification of pineapple maturity

Siwalak Pathaveerat [a,*], Anupun Terdwongworakul [b], Artit Phaungsombut [a]

[a] Department of Agricultural Engineering, Faculty of Engineering at Kamphaeng Saen, Kamphaeng Saen Campus, Nakhon Pathom 73140, Thailand
[b] Department of Food Engineering, Faculty of Engineering at Kamphaeng Saen, Kamphaeng Saen Campus, Nakhon Pathom 73140, Thailand

Application to tropical fruit

2. Classification of pineapple maturity

Table 3
Cross-validated classification matrices showing the performance of classification into sets distinguished

Parameters	*Actual group*	Correctly classified fruits (%)
All destructive and nondestructive parameters for all classes	Class A	81.3
	Class B	59.4
	Class C	78.6
	Class M	82.1
Total		**75.7**
All destructive and nondestructive parameters for only maturity classes	Class A	78.1
	Class B	63.0
	Class C	89.3
Total		**77.0**
Nondestructive parameters (SG, SC1, SC2 and SC3) for only maturity classes	Class A	90.6
	Class B	63.0
	Class C	92.9
Total		**82.8**

Numbers in bold represent the correctly classified individual pineapples.
SG = Specific gravity; SC1 = $f_1{}^2m^{2/3}$; SC2 = $f_2{}^2m^{2/3}$; SC3 = $f_3{}^2m^{2/3}$.

ELSEVIER jou

Multivariate data analy

Siwalak Pathaveerat[a,*], Anupun Terdwongworakul[b], Artit Phaungsombut[a]
[a] Department of Agricultural Engineering, Faculty of Engineering at Kamphaeng Saen, Kamphaeng Saen Campus, Nakhon Pathom 73140, Thailand
[b] Department of Food Engineering, Faculty of Engineering at Kamphaeng Saen, Kamphaeng Saen Campus, Nakhon Pathom 73140, Thailand

Application to tropical fruit

3. Maturity sorting of fresh young coconut

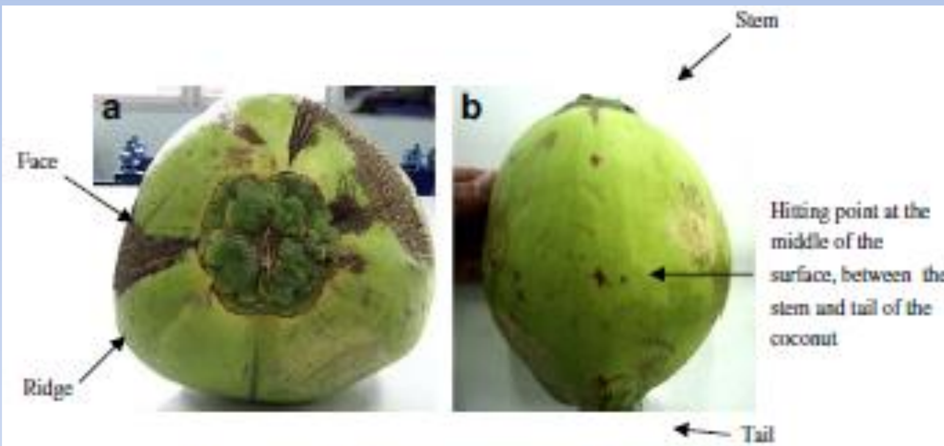

Fig. 2 – (a) Fruit orientation and (b) Hitting point.

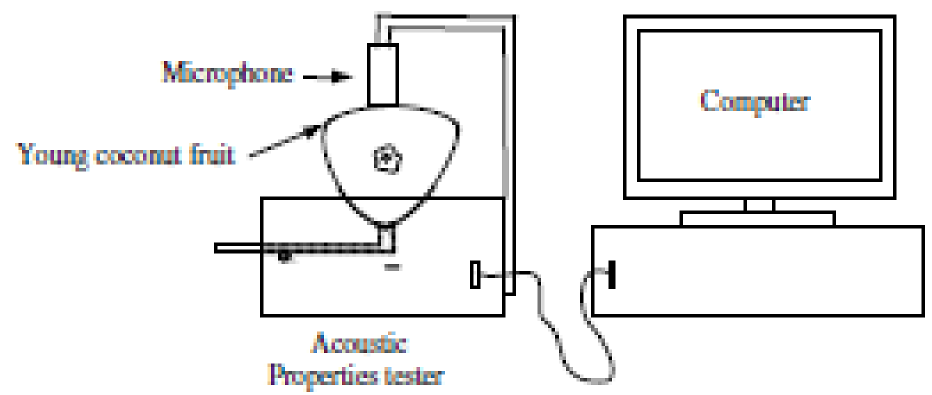

Fig. 1 – Acoustic property tester.

BIOSYSTEMS ENGINEERING 103 (2009) 208–216

ELSEVIER

Available at www.sciencedirect.com

ScienceDirect

journal homepage: www.elsevier.com/locate/issn/15375110

Biosystems Engineering

Research Paper: PH—Postharvast Technology

Physical properties of fresh young Thai coconut for maturity sorting

Anupun Terdwongworakul[a], *Songtham Chaiyapong*[b], *Bundit Jarimopas*[a,*], *Weerakul Meeklangsaen*[c]

Application to tropical fruit

3. Maturity sorting of fresh young coconut

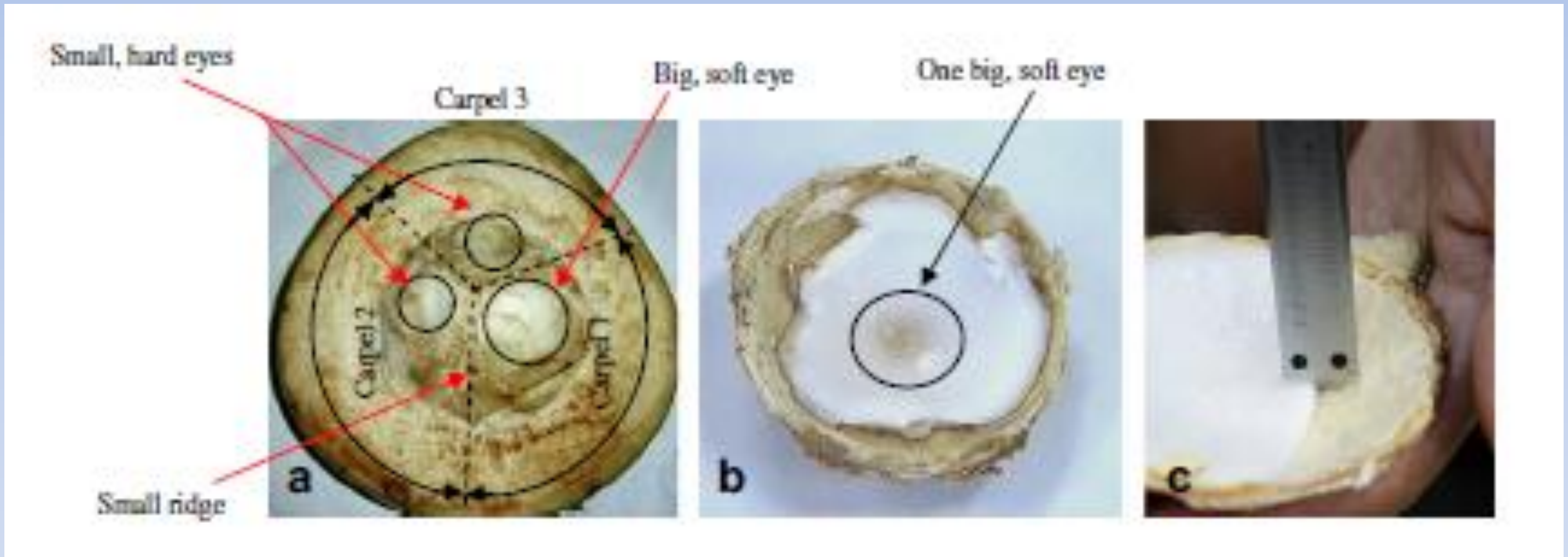

BIOSYSTEMS ENGINEERING 103 (2009) 208–216

Available at www.sciencedirect.com

ScienceDirect

journal homepage: www.elsevier.com/locate/issn/15375110

ELSEVIER

Research Paper: PH—Postharvast Technology

Physical properties of fresh young Thai coconut for maturity sorting

Anupun Terdwongworakul[a], Songtham Chaiyapong[b], Bundit Jarimopas[a,], Weerakul Meeklangsaen[c]*

Application to tropical fruit

3. Maturity sorting of fresh young coconut

Table 2 – Statistics of calibration and validation of FT and the lower and upper limits of a 95% confidence interval for the ratio of the true standard deviations

Properties	R^2_{cal}	RMSECV	No. of PLS factors	R^2_{pre}	RMSEP	SEP	BIAS	$SEP_1/(SEP_2 \times L)^b$	$SEP_1 \times L/SEP_2$
SSL, HF_r, f_n, SF_r, F_W, HSL, D_W, SG, TSS, TSS/TA, TA	0.986	0.168	1	0.980	0.203	0.204	0.009		
HF_r, SSL, SF_r, F_w, HSL	0.991	0.133	1	0.991	0.133	0.133	0.004		
HF_r, SSL, SF_r, F_w	0.991	0.135	1	0.990	0.141	0.142	0.001	0.886	1.113
HF_r, SSL, SF_r	0.986	0.171	1	0.985	0.172	0.173	−0.001	0.697	0.952
HF_r, SSL	0.994	0.155	1	0.986	0.167	0.168	0.004	0.709	0.987
HF_r[a]	0.988	0.155		0.988	0.157	0.158	0.001	0.728	0.998
SSL[a]	0.977	0.218		0.980	0.200	0.201	−0.002	0.594	0.824
SF_r[a]	0.968	0.257		0.967	0.257	0.259	−0.001	0.460	0.645
F_w[a]	0.966	0.264		0.967	0.260	0.261	0.006	0.456	0.637
HF_r, HSL, f_n, SG	0.978	0.212	2	0.980	0.199	0.200	0.005	0.603	0.820
f_n, SG	0.889	0.466	1	0.856	0.541	0.544	0.000	0.214	0.314
f_n[a]	0.937	0.359		0.927	0.385	0.386	0.034	0.300	0.440
SG[a]	0.351	1.149		0.406	1.099	1.104	−0.016	0.105	0.155

R^2_{cal}, coefficient of determination of calibration; R^2_{pre}, coefficient of determination of prediction; RMSECV, Root Mean Square of Standard Error of Cross Validation; RMSEP, Root Mean Square of Error of Prediction; SEP, Standard of Error of Prediction.

a Multiple linear regression model.

b $k = 1 + 2(1 - r^2)t^2_{(N_p-2),0.025}/N_p - 2$ where $t^2_{(N_p-2),0.025}$ is the upper 2.5% percentile of a t-distribution with $N_p - 2$ degrees of freedom $L = \sqrt{[k + \sqrt{(k^2 - 1)}]}$ (Snedecor and Cochran, 1989).

ELSEV

Researc

Physi

sortir

Anupun Terdwongworakul[a], Songtham Chaiyapong[b], Bundit Jarimopas[a,], Weerakul Meeklangsaen[c]*

5. Near infrared spectroscopy

Principle:

- Functional groups C-H, O-H and N-H absorbs light in NIR region (740 – 2500 nm).

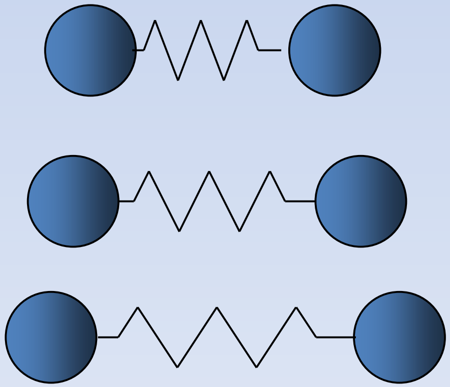

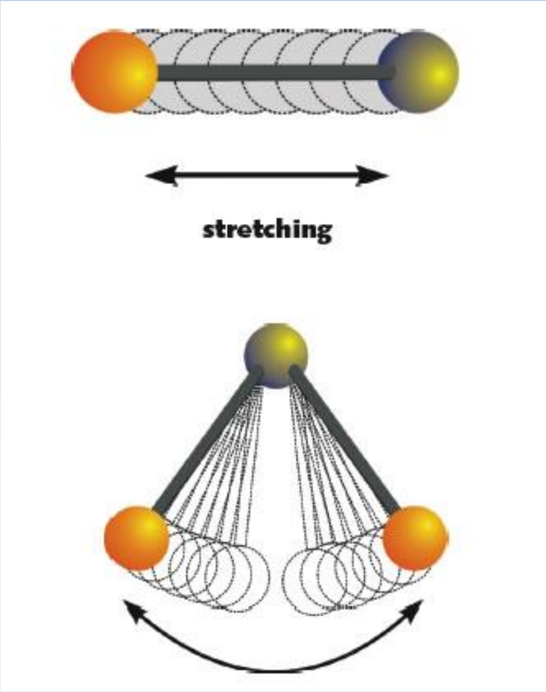

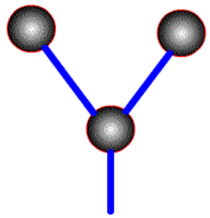

Symmetrical stretching

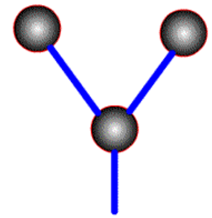

Asymmetrical stretching

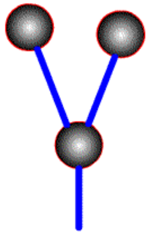

Symmetrical
In-plane deformation
(Scissoring)

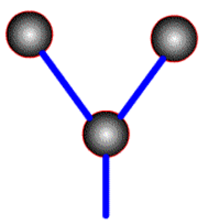

Asymmetrical
In-plane deformation
(Rocking)

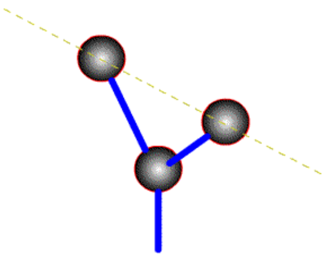

Symmetrical
Out-of-plane deformation
(Wagging)

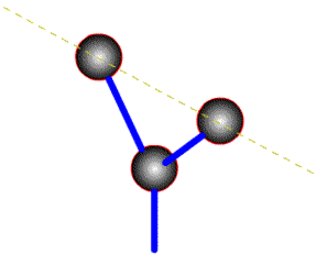

Asymmetrical
Out-of-plane deformation
(Twisting)

Principle of absorbance

http://www.youtube.com/watch?v=pxC6F7bK8CU

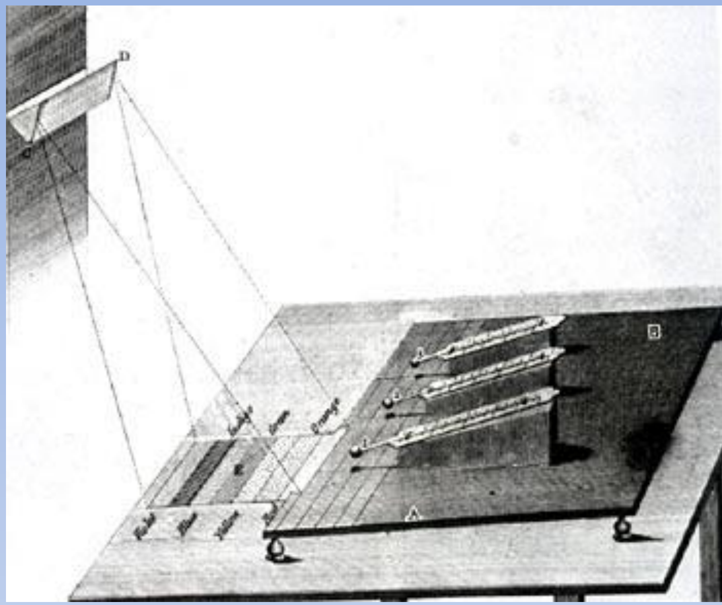

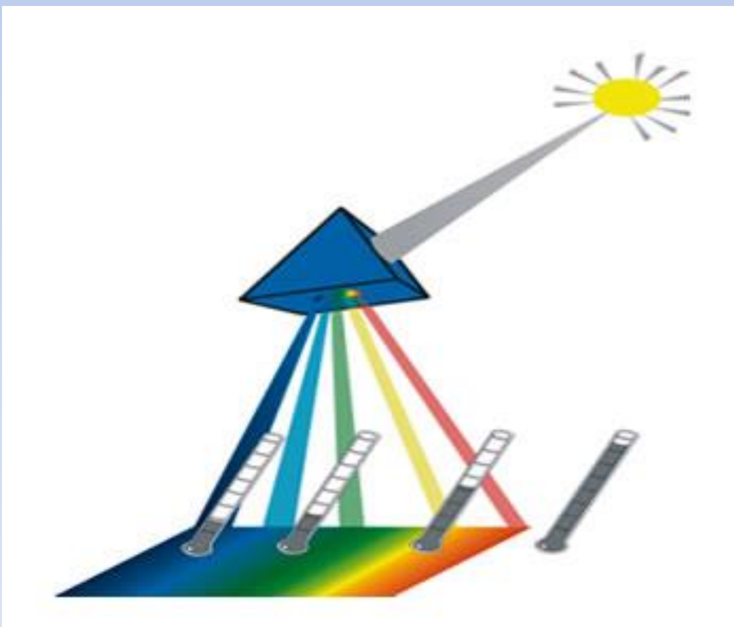

www.cartage.org.lb/.../herschel/herschel.htm

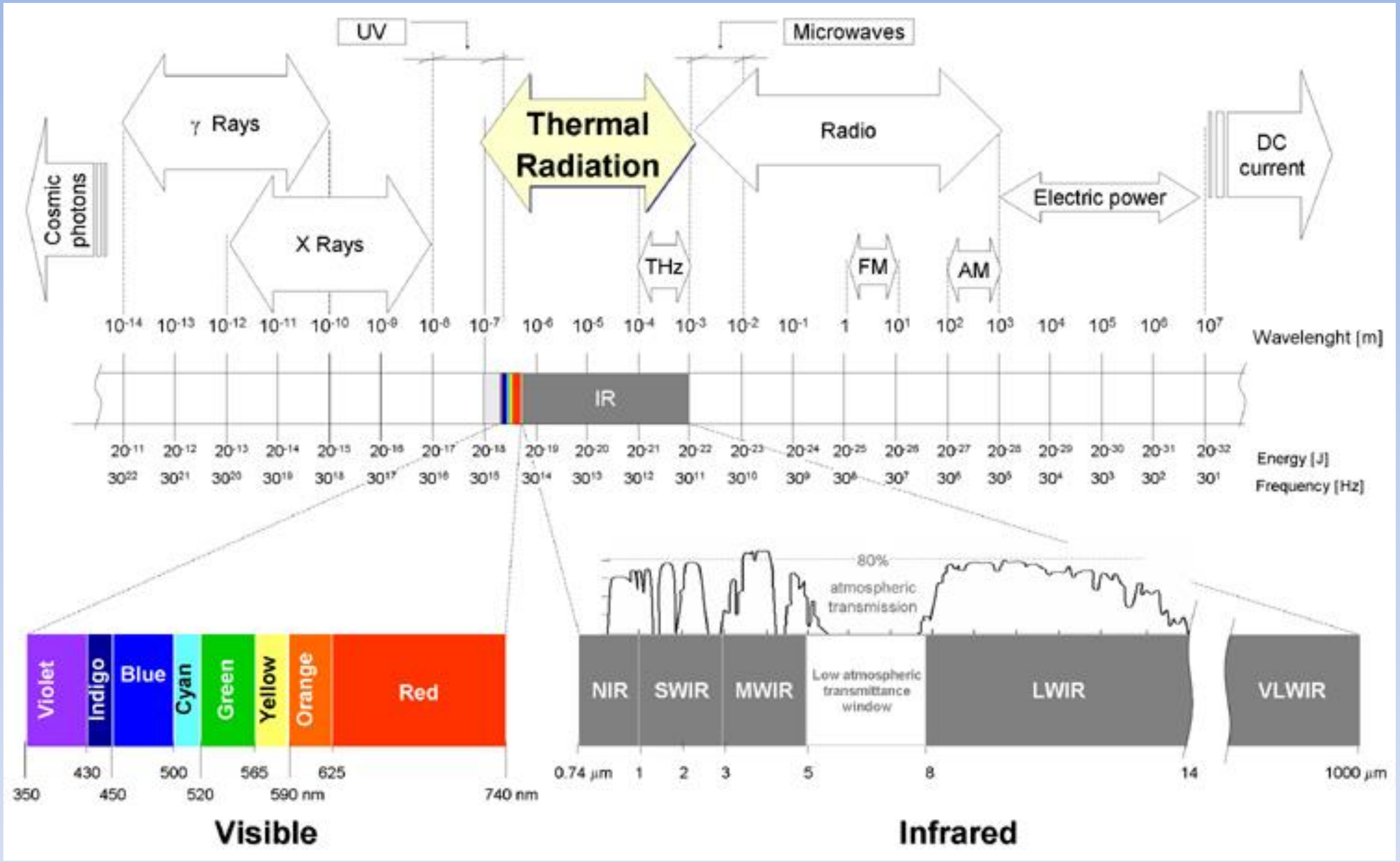

UV
Microwaves
γ Rays
Thermal Radiation
Radio
DC current
Cosmic photons
X Rays
Electric power
THz
FM
AM
Wavelenght [m]
IR
Energy [J]
Frequency [Hz]
80%
atmospheric transmission
Violet
Indigo
Blue
Cyan
Green
Yellow
Orange
Red
NIR
SWIR
MWIR
Low atmospheric transmittance window
LWIR
VLWIR
350
430
450
500
520
565
590 nm
625
740 nm
0.74 μm
1
2
3
5
8
14
1000 μm
Visible
Infrared

Principle of Near Infrared Spectroscopy

- **Beer-Lambert law or Beer's law and absorbance**

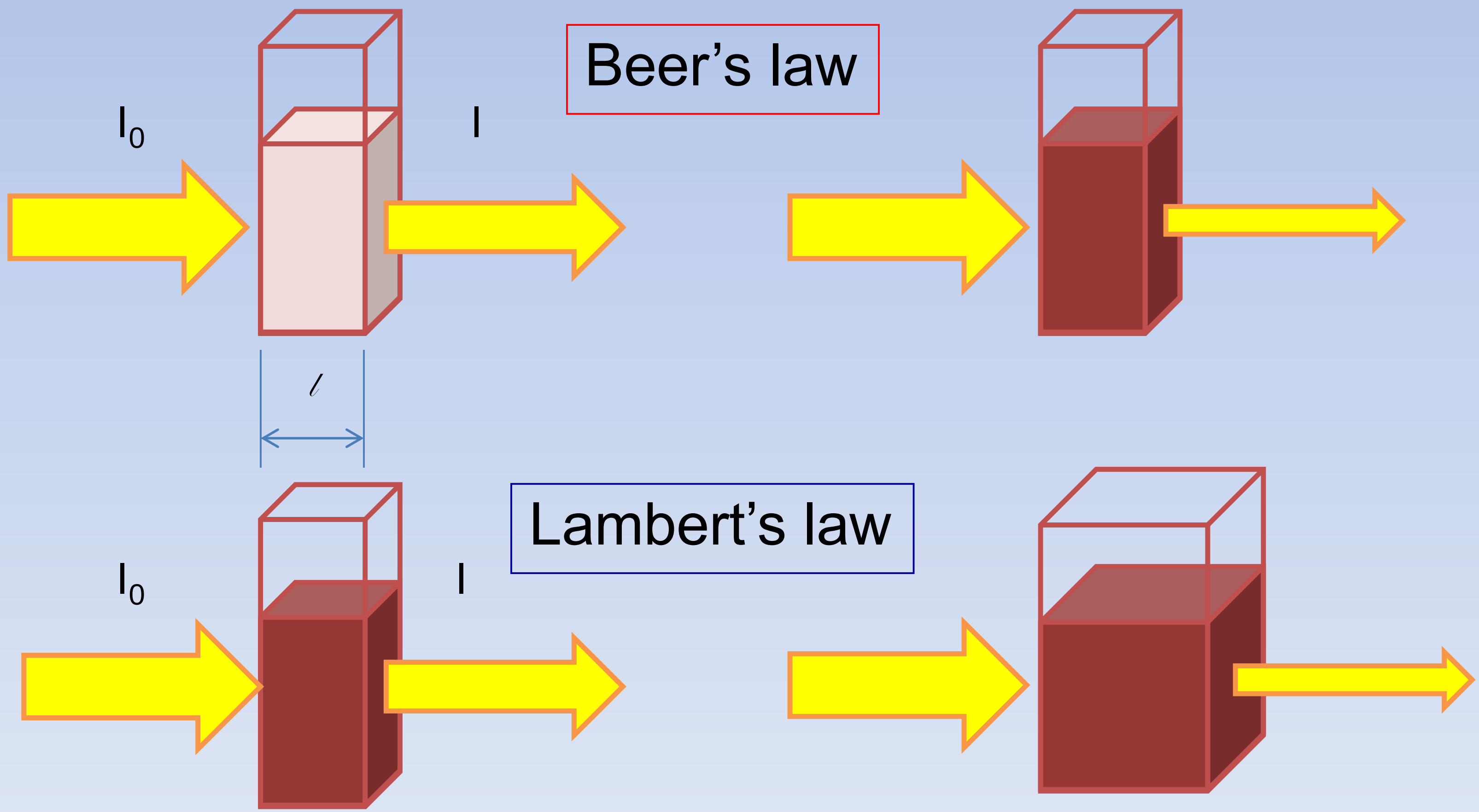

Principle of Near Infrared Spectroscopy

Beer-Lambert law or Beer's law and absorbance

$$\text{Absorbance (optical density)} = -\log\left(\frac{I}{I_0}\right) = \varepsilon\, l\, c$$

Beer's law

Lambert's law

- where ε is molar absorptivity (liter/(mole·cm)

  c is concentration (mole/liter)

  l is light path length or thickness of the sample

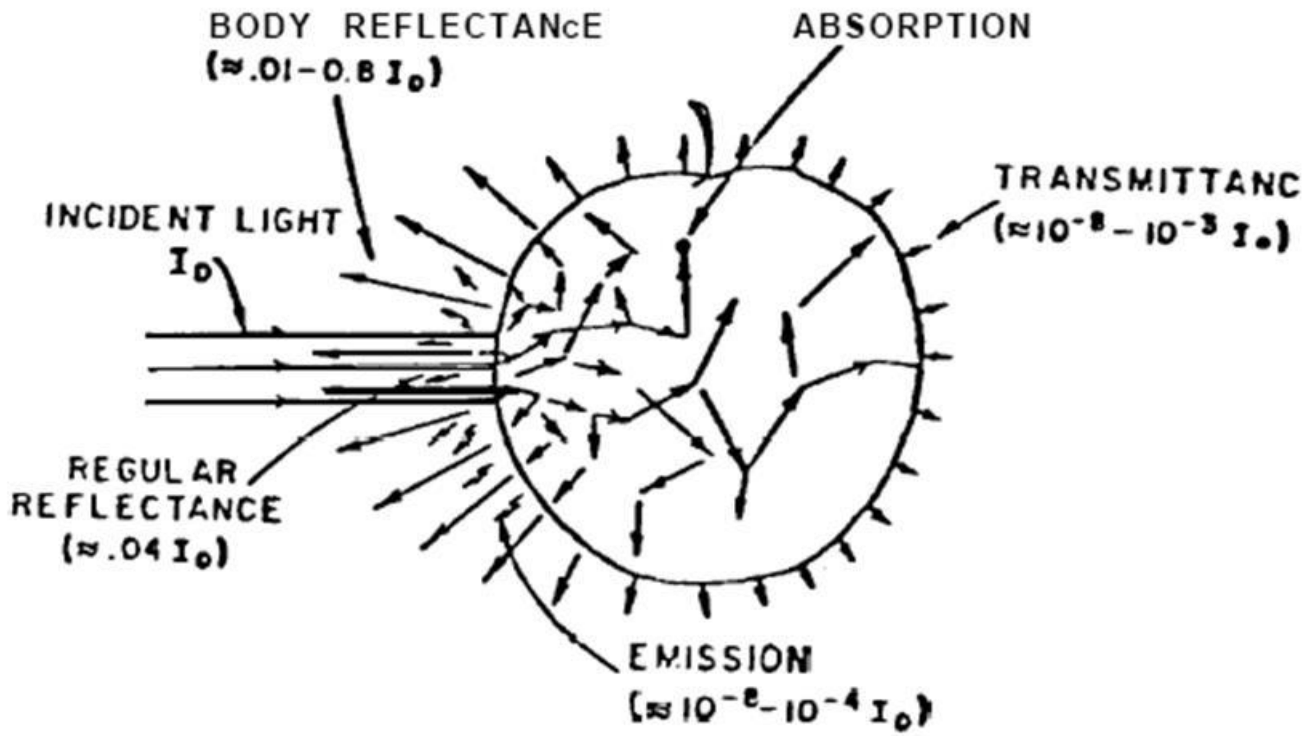

FIGURE 5. A simplified schematic diagram showing the interaction between light and a fruit. (From Chen, P., J. *Food Process Eng.*, 2, 307, 1978. With permission.)

Information inside NIR spectra

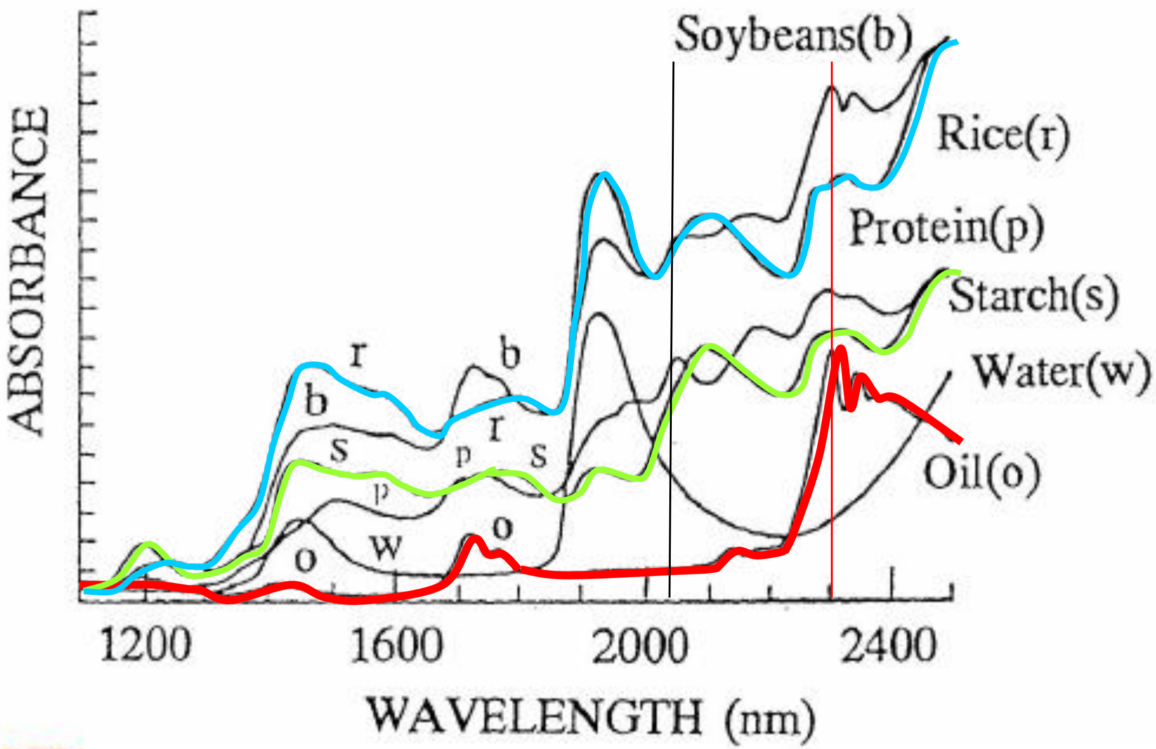

20

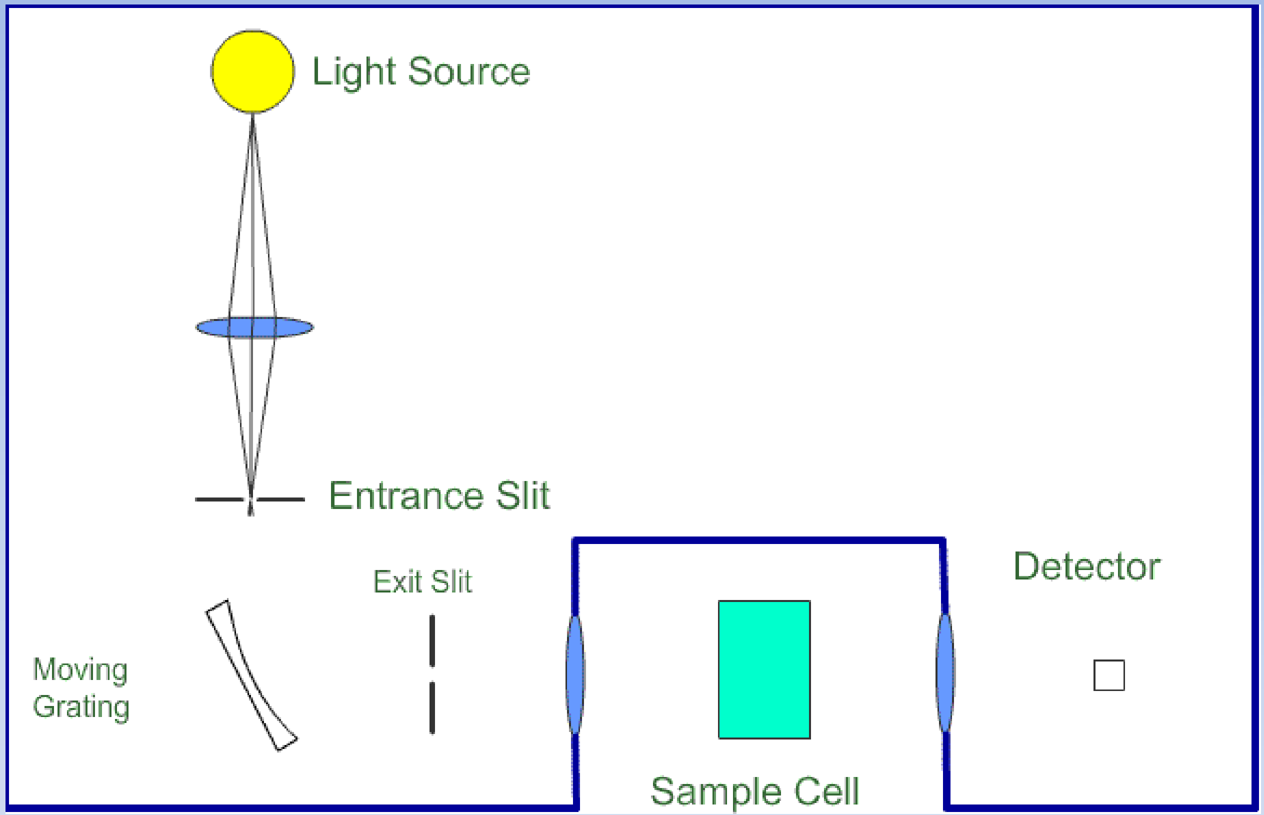
Light Source
Entrance Slit
Exit Slit
Detector
Moving
Grating
Sample Cell

Application

Fast determination of boiling time of yardlong bean using visible and near infrared spectroscopy and chemometrics

- Pengcheng Nie , Di Wu , Yan Yang, Yong He
- College of Biosystems Engineering and Food Science, Zhejiang University 866 Yuhangtang Road, Hangzhou, 310058, China
- College of Electronic and information Engineering, Nanchang Hangkong University Nanchang 330069, China

- Journal of Food Engineering (2011), doi: 10.1016/j.jfoodeng.2011.09.018

- averaged reflectance spectra of yardlong beans at different boiling time.

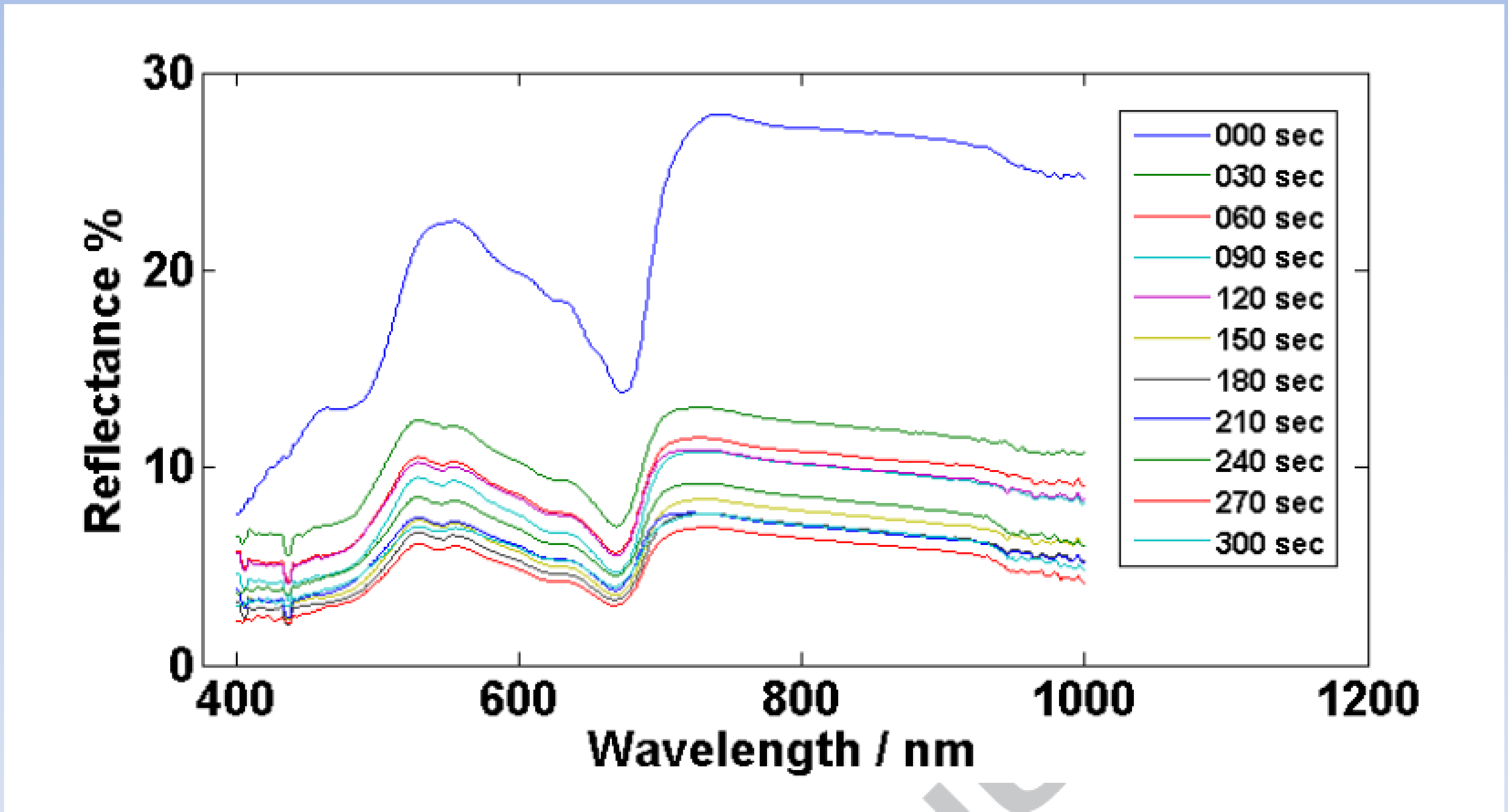

Table 2 Prediction results of boiling time of yardlong beans by different calibration models based on pre-processed spectra

Calibration	r_{cal}^2	RMSEC	r_{pre}^2	RMSEP	RPD
PLS	0.8917	31.3940	0.9043	29.6865	3.2297
PCR	0.8432	37.7769	0.8616	35.5092	2.6873
LS-SVM $_{lin}$	0.9218	26.7133	0.8961	30.9608	3.0998
LS-SVM $_{RBF}$	0.9621	18.6458	0.9306	25.0830	3.7847
R-LS-SVM $_{lin}$	0.9191	27.1815	0.8960	31.1016	3.0997
R-LS-SVM $_{RBF}$	0.9457	22.2614	0.9271	25.8890	3.6887

Pergamon

0097-8485(95)00012-7

Computers Chem. Vol. 19, No. 3, pp. 299–301, 1995

0097-8485/95 $9.50 + 0.00

SOFTWARE NOTE

QUANTITATIVE AND QUALITATIVE ANALYSES IN NEAR INFRARED ANALYSIS OF BASIC COMPOUNDS IN SUGAR BEET LEAF*

W. B. MROCZYK[1]† and K. M. MICHALSKI[2]

[1]Department of Chemistry, University of Agriculture, Woj. Polskiego 75, Poznań 60 625, Poland

[2]Plant Breeding and Acclimatization Institute, Strzeszyńska 36, Poznań 60 449, Poland

- The great advantage of NIR is rapid analyses and its non-destructive character, and possibility of measuring many different components at the same time.
- The NIR method was used to study changes in chemical composition in leaves of sugar-beet under the influence of various fertilizers.
- The results obtained show that this method is an effective tool to predict protein, nitrogen and saccharides.

Table 2. Calibration and validation statistics for the measurement of constituents in leaves using filter instrument

Method	Calibration				Prediction	
	$r2$	F	SEC	r	SEP	Bias
	protein					
MLR	0.911	40.23	0.02	0.942	0.03	1.0
PCR	0.918	39.81	0.02	0.949	0.03	0.7
	nitrogen					
MLR	0.895	34.28	0.10	0.935	0.09	1.18
PCR	0.902	35.52	0.11	0.941	0.09	1.07
	saccharides					
MLR	0.925	54.47	1.2	0.960	1.0	−1.9
PCR	0.940	54.53	1.1	0.965	1.0	−1.5
	potassium					
MLR	0.803	25.52	0.50	0.872	0.61	−2.0
PCR	0.809	25.13	0.46	0.874	0.59	−1.0
	iron					
MRL	0.895	40.11	29.0	0.920	26	−2.73
PCR	0.902	42.20	28.2	0.927	25	−1.80

ELSEVIER

Available online at www.sciencedirect.com

ScienceDirect

Postharvest Biology and Technology 44 (2007) 165–174

Postharvest Biology and Technology

www.elsevier.com/locate/postharvbio

Visible and near-infrared spectroscopy for nondestructive quality assessment of pickling cucumbers

I. Kavdir[a,*], R. Lu[b], D. Ariana[b], M. Ngouajio[c]

[a] *Department of Agricultural Machinery, College of Agriculture, Canakkale Onsekiz Mart University, 17020 Canakkale, Turkey*
[b] *USDA Agricultural Research Service, 224 Farrall Hall, Michigan State University, East Lansing, MI 48824, USA*
[c] *Department of Horticulture, A428 Plant and Soil Sciences Michigan State University, East Lansing, MI 48824, USA*

- This study was aimed at developing a nondestructive method for measuring the firmness, skin and flesh color, and dry matter content of pickling cucumbers by means of visible and near-infrared (Vis/NIR) spectroscopy.

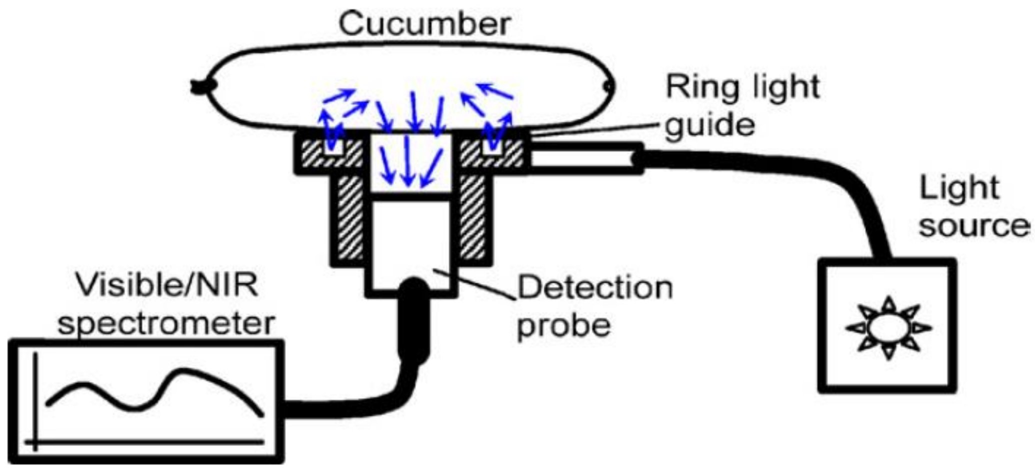

Fig. 1. Spectral measurement of cucumber fruit in interactance mode.

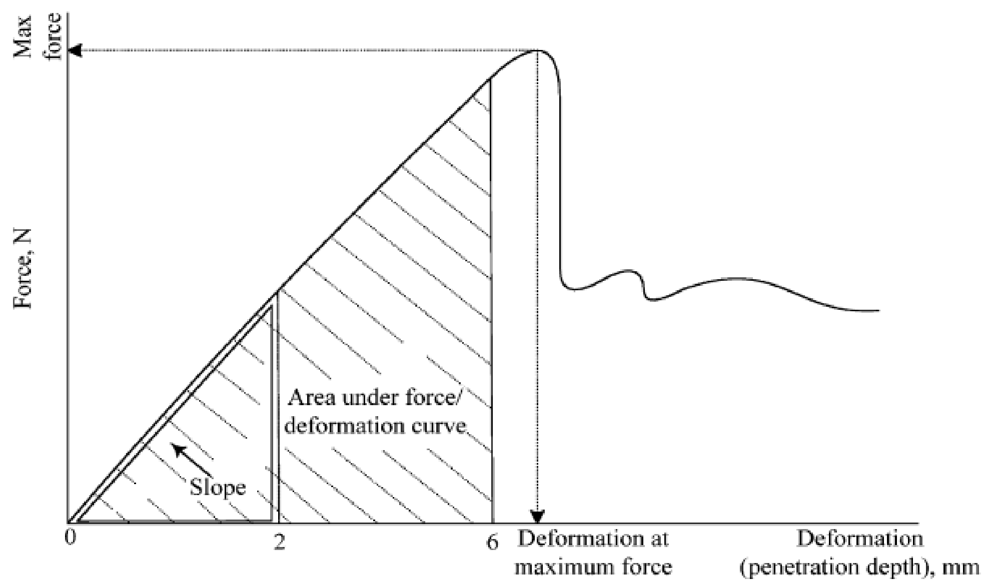

Fig. 2. Extracting maximum force, slope (on the force/deformation curve) and strain energy (area under the force/deformation curve) from the Magness–Taylor force/deformation curve for a cucumber sample.

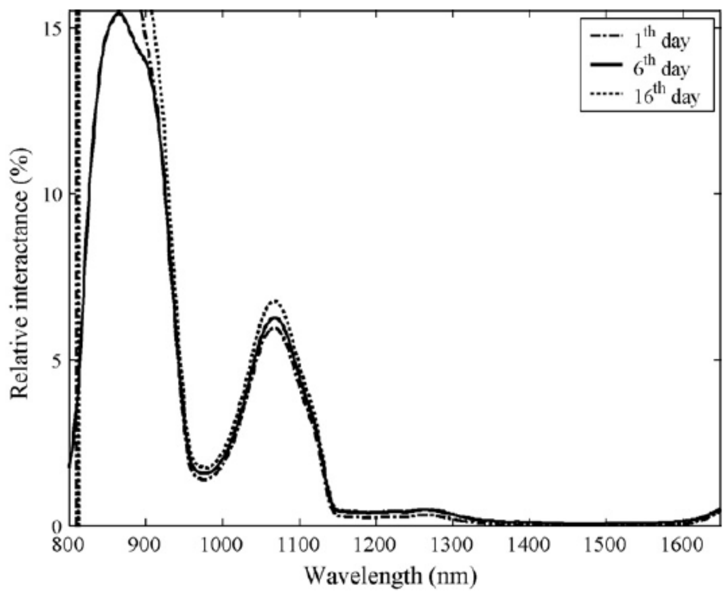

Fig. 4. Average relative interactance spectra of 'Journey' cucumbers at the 1st, 6th and 16th day of the storage period as obtained by the NIR spectrometer.

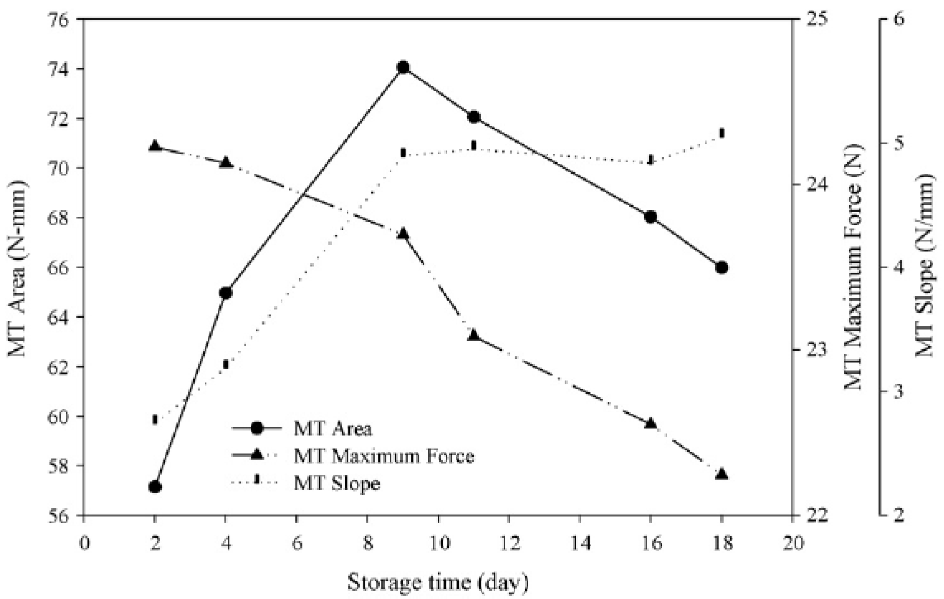

Table 2
Summary of the calibration and validation results for firmness, skin and flesh color and dry matter by using the partial least squares analysis for the pooled spectral data of 'Journey' and 'Vlaspik' cucumbers obtained with the near-infrared spectrometer

Parameter measured	Data type	Factors	Calibration		Validation	
			R^2	SEC	R^2	SEP
Firmness						
Area[a]	Relative	20	0.70	11.90	0.70	12.97
	Logarithm	16	0.67	12.50	0.64	14.08
Slope[b]	Relative	19	0.73	0.90	0.67	1.04
	Logarithm	16	0.69	0.96	0.67	1.02
Maximum force	Relative	18	0.58	4.06	0.52	4.34
	Logarithm	16	0.56	4.13	0.52	4.30
Color						
Skin chroma	Relative	11	0.32	5.09	0.21	5.23
	Logarithm	15	0.48	4.46	0.27	5.14
Skin hue	Relative	11	0.32	0.04	0.22	0.04
	Logarithm	15	0.40	0.04	0.23	0.04
Flesh chroma	Relative	18	0.48	3.52	0.10	4.62
	Logarithm	17	0.49	3.47	0.04	5.04
Flesh hue	Relative	19	0.61	0.02	0.48	0.02
	Logarithm	15	0.51	0.02	0.40	0.02
Dry matter content	Relative	12	0.30	0.28	0.20	0.37
	Logarithm	18	0.50	0.24	0.28	0.35

R^2: coefficient of determination; SEC (or SEP): standard error of calibration (or prediction).
[a] Area (N mm) under the Magness–Taylor force/deformation curve (from 0 to 6 mm of deformation, Fig. 2).
[b] Slope (N/mm) was obtained from the line connecting the two points at 0 and 2 mm on the MT force/deformation curve.

Bioresource Technology 102 (2011) 9542–9549

Contents lists available at SciVerse ScienceDirect

Bioresource Technology

journal homepage: www.elsevier.com/locate/biortech

Direct prediction of bioethanol yield in sugar beet pulp using Near Infrared Spectroscopy

C. Magaña [a], N. Núñez-Sánchez [b,*], V.M. Fernández-Cabanás [b], P. García [a], A. Serrano [b], D. Pérez-Marín [b], J.M. Pemán [a], E. Alcalde [a]

[a] *Syngenta Seeds S.A., Barcelona 08006, Spain*
[b] *NIR Soluciones, S.L., Cordoba 14006, Spain*

- Sugar beets are a raw material for the production of sugar and ethanol.
- A Near Infrared (NIR) Spectroscopy-based approach was tested for the direct prediction of the potential bioethanol production from sugar beets.

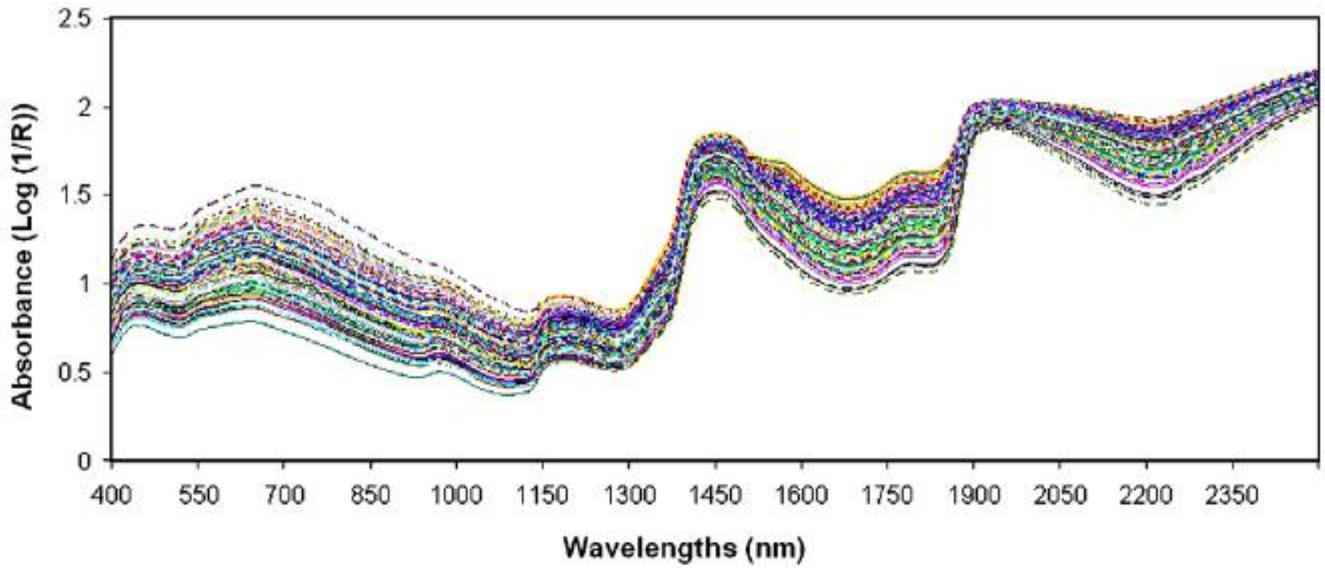

Fig. 3. NIRS absorbance spectra of sugar beet samples used as calibration set.

Table 3b
Calibration and validation statistics for the equations obtained for the prediction of bioethanol yield in sugar beet in the spectral region 1100–2500 nm.

Scatter correction	Derivative	Outliers[a]	Mean ($g\,L^{-1}$)	SD ($g\,L^{-1}$)	SECV[b] ($g\,L^{-1}$)	r^{2c}	Terms[d]	SEP[e] ($g\,L^{-1}$)	RPD[f]
SNV + DT	1,5,5,1	2	26.92	1.71	0.51	0.91	6	0.54	3.18
	1,10,5,1	3	26.92	1.72	0.51	0.91	6	0.49	**3.47**
	1,10,10,1	2	26.92	1.71	0.54	0.90	5	0.58	2.92
	2,5,5,1	2	26.90	1.69	0.52	0.90	5	0.66	2.55
	2,10,5,1	1	26.86	1.76	0.50	0.92	5	0.54	3.28
	2,10,10,1	0	26.87	1.76	0.52	0.91	5	0.52	3.36
MSC	1,5,5,1	1	26.92	1.70	0.52	0.91	6	0.61	2.77
	1,10,5,1	1	26.87	1.77	0.53	0.91	6	0.52	3.41
	1,10,10,1	1	26.87	1.77	0.53	0.91	6	0.51	3.43
	2,5,5,1	1	26.92	1.70	0.57	0.89	4	0.75	2.28
	2,10,5,1	1	26.87	1.77	0.49	0.92	5	0.55	3.23
	2,10,10,1	0	26.87	1.76	0.51	0.92	5	0.53	3.31

[a] Outliers, number of outliers removed in calibration.
[b] SECV, standard error of cross validation.
[c] r^2, coefficient of determination of cross-validation.
[D] Terms, number of PLS terms.
[e] SEP, standard error of prediction from external validation.
[F] RPD, ratio SD/SEP.

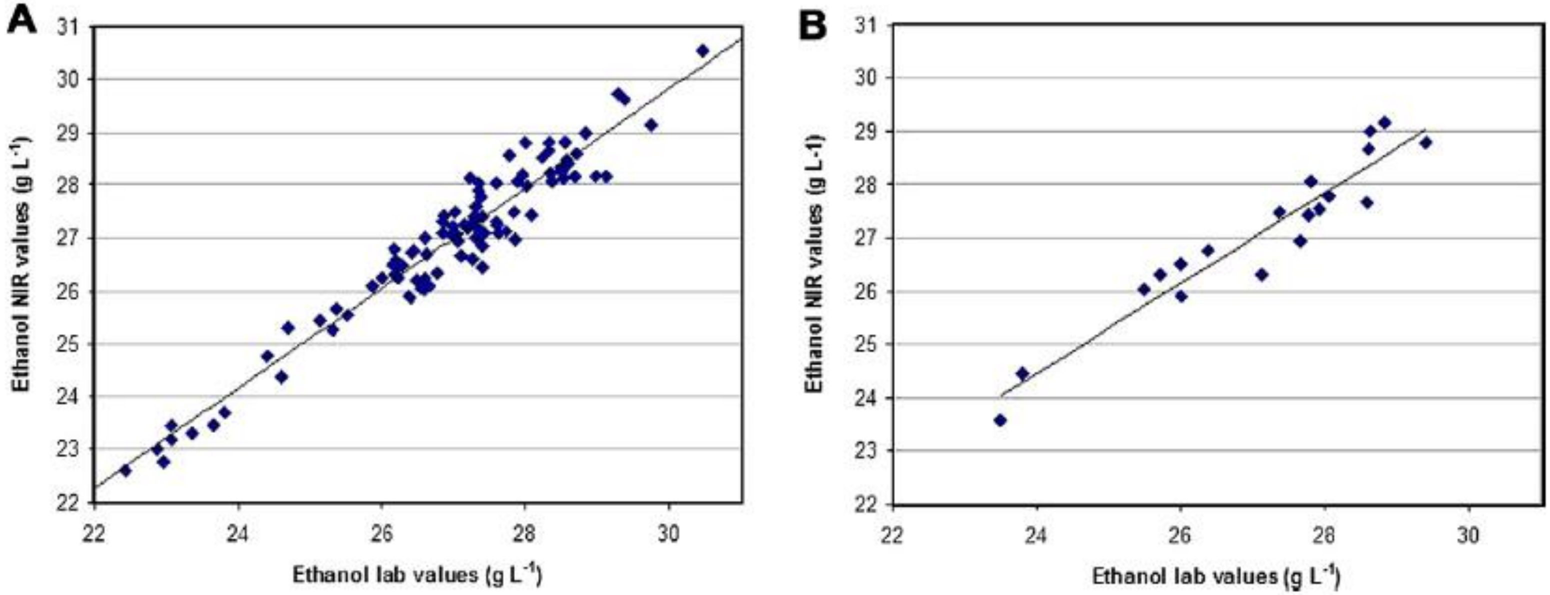

Fig. 4. Plot of predicted versus measured values of bioethanol yield together with regression line for (A) calibration and (B) validation data sets by using SNV + DT and 1,10,5,1 derivative from 1100 to 2500 nm.

Sweetness Sorting Machine

- In 1989, Mitsui Mining and Smelting Co., Ltd. developed and introduced the first sweetness sorting machine for peaches using NIR reflectance method.
- Different type of sweetness sorting machines for other products, say, oranges, melons or water melons, have become possible.

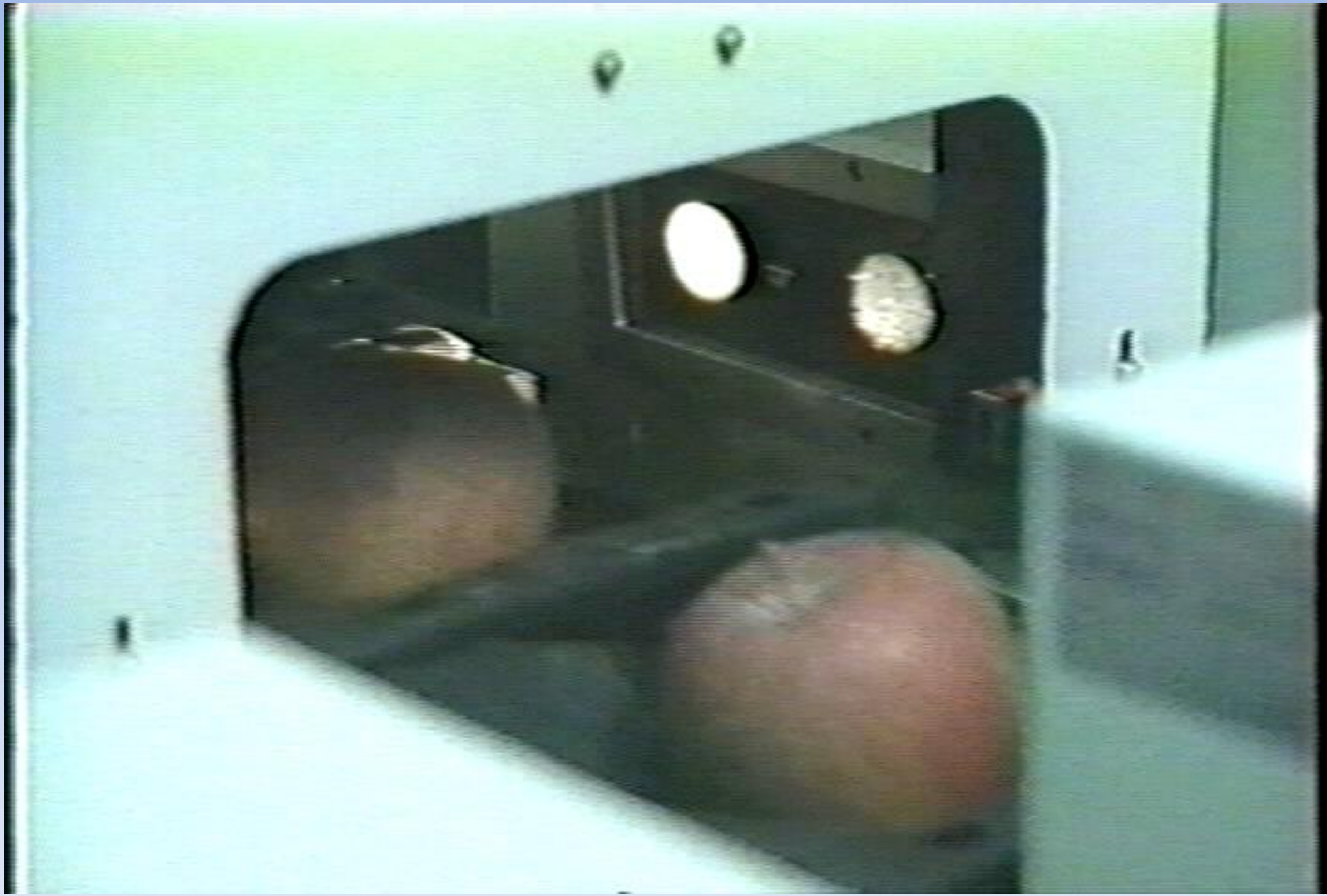

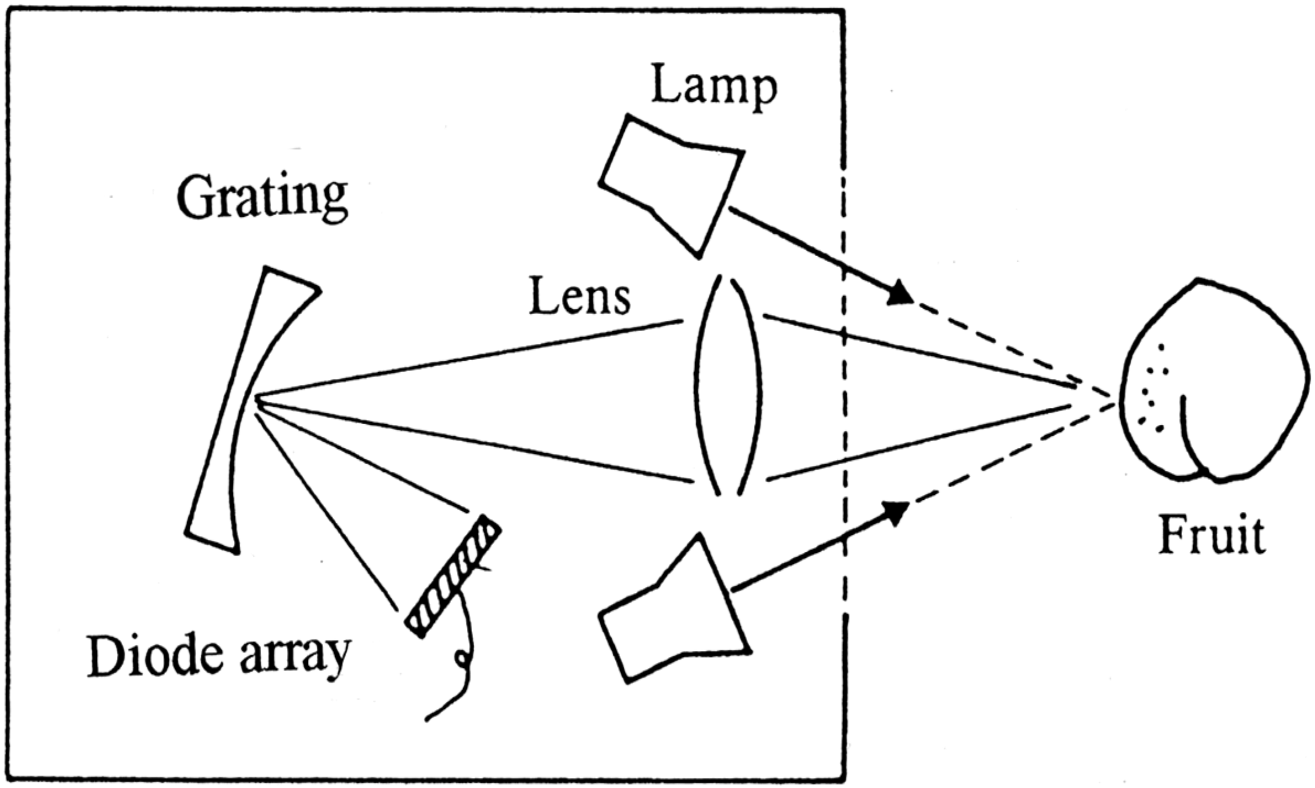
Lamp
Grating
Lens
Fruit
Diode array




フルーツセレクターのつかい方
トマト
1
2
3
100円
100円
800g入 1袋
498円
特産トマトひらとり
OPEN

Application of NIRS to mangosteen

Problems

Mangosteen (Queen of fruits)

- Fruit fly
- Translucency

Handling System for Mangosteen to Japan

Preharvest spray of fungicide and insecticide at the young leaves stage and flowering stage.

↓

Harvest at recommended maturity without damage (cracks, punctures, bruising etc.).

↓

Cleaning, sorting and grading

Bactrocera dorsalis species complex

↓

VHT

Japan:
Heat treatment 46 °C
for 59 min.

↓

Packing in corrugated carton

↓

Export

Fresh Mangosteen

Separation of natural disorder mangosteen fruits (translucent flesh and yellow latex) by immersion in water

Translucent mangosteen fruit is one of internal disorders

The occurrence of flesh browning on translucent mangosteen fruits after heat treatment

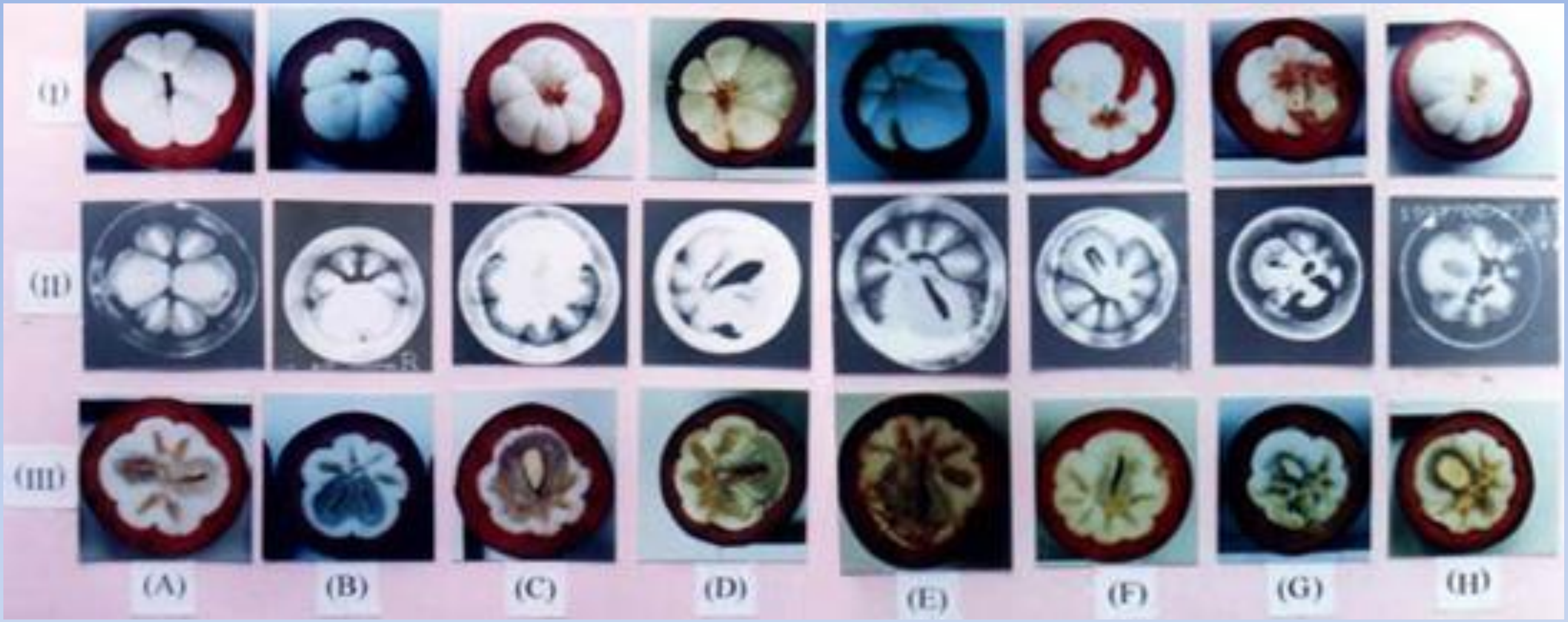

X-ray images of normal and translucent mangosteen

http://www.ist.cmu.ac.th/riseat/nl/2003/04/0201.jpg

Near infrared absorbance of mangosteen

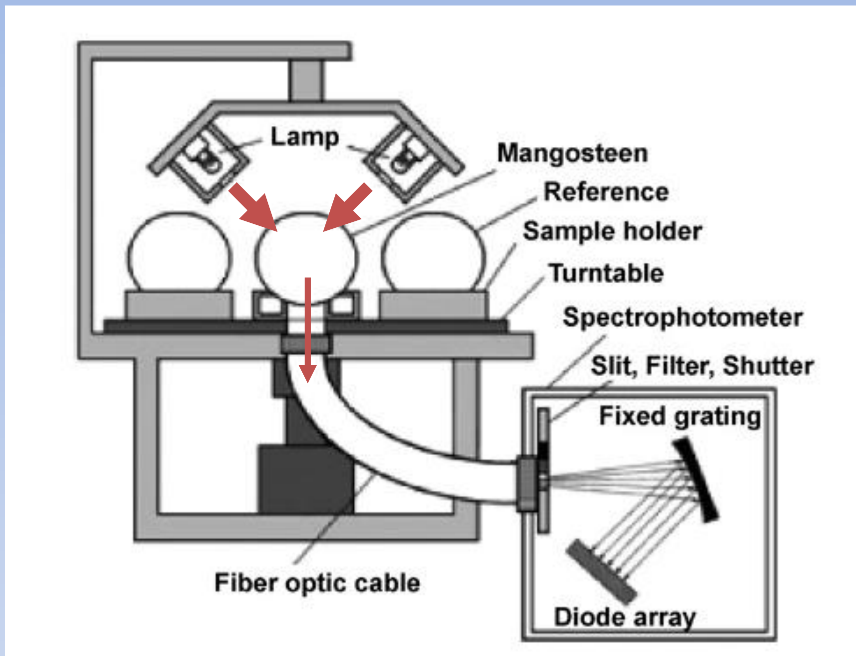

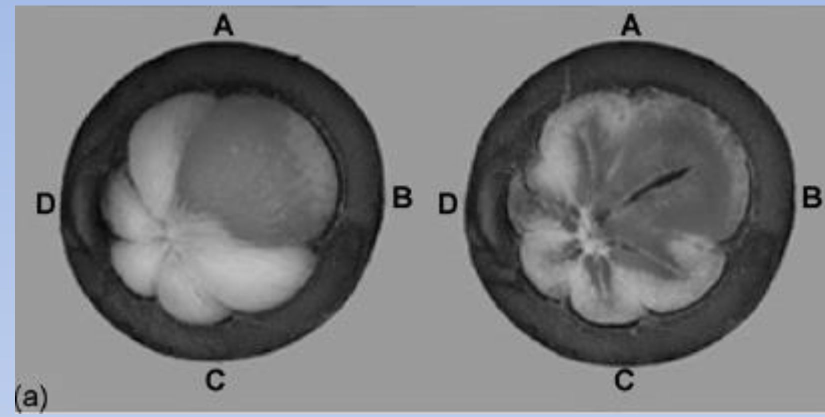

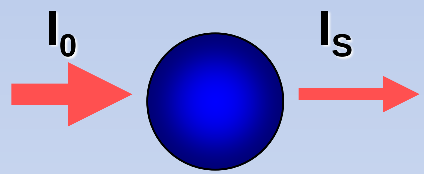

Absorbance = log(1/T)

$\mathbf{T = I_S/I_R}$

The SW-NIR transmittance spectra were obtained at four positions at the equatorial points 90◦ apart.

The samples were kept in a room at a constant temperature of 25 °C prior to the recording of spectral data on the following day by a commercially available SW-NIR instrument (PureSpect, Saika TIF., Japan).

(Teerachaichayut et al., 2007)

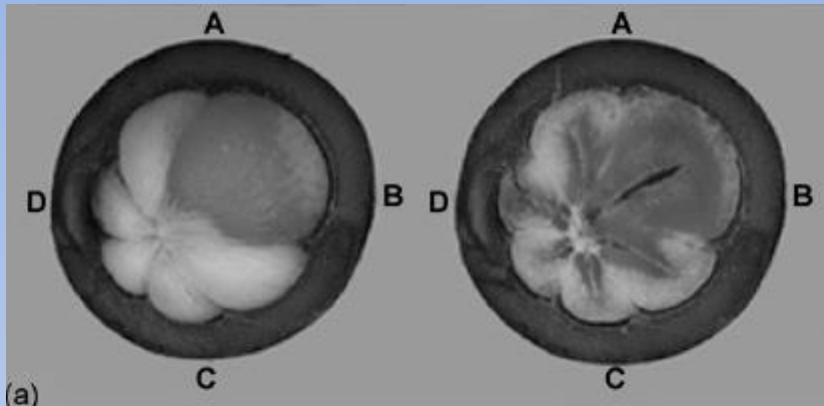

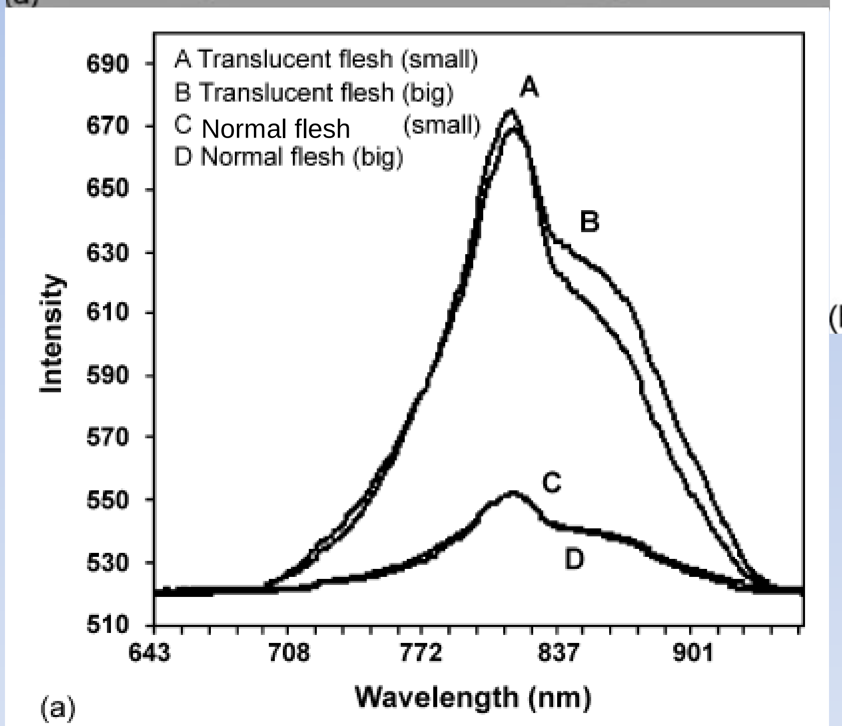

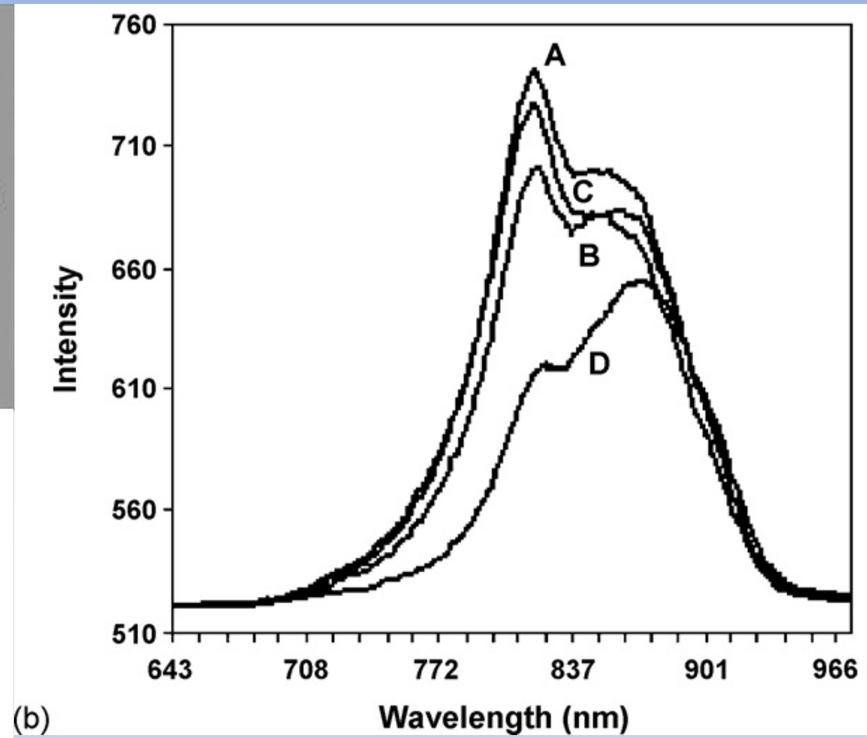

Fruit size had an effect on the SW-NIR intensity spectra, but the difference in the intensity in some regions resulting from the translucent flesh was substantially greater.

SW-NIR classification for normal flesh and translucent flesh mangosteen using discriminant analysis and leave-one-out cross-validation

Acquisition	Number of non-translucent flesh mangosteen	Number of translucent flesh mangosteen	Total number of mangosteen	The most informative wavelength[a] (nm)	NIR classification accuracy (%)
Averaged spectra					
Total	170	23	193	669, 670, 692, 682, 668, 685	89.1
Correct	165	7	172		
Incorrect	5	16	21		
Amended averaged spectra[b]					
Total	168	21	189	669, 677, 700, 694, 668, 692	89.9
Correct	162	8	170		
Incorrect	6	13	19		
Individual spectra[c]					
Total	680	92	772	743, 727, 758, 673, 692, 726	91.2
Correct	672	32	704		
Incorrect	8	60	68		
Amended individual spectra[d]					
Total	607	80	687	743, 727, 723, 762, 692, 673	92.0
Correct	599	33	632		
Incorrect	8	47	55		

[a] The most informative wavelengths suggested by Fisher's linear discriminant function.
[b] Spectra were calculated as average of each sample without hardening pericarp effect with four samples omitted due to completely hardened pericarp.
[c] Spectra were collected from each point of measurement (four points in each sample).
[d] Spectra were collected from each point of measurement without hardening pericarp effect.

Saika Technological Institute Foundation, Japan

Kasetsart University

Collaborators

National Food Research Institute, Japan

Society for Techno-Innovation of Agriculture, Forestry and Fisheries (STAFF)


FRAGILE

DESIGNED SYSTEMS

Type 1

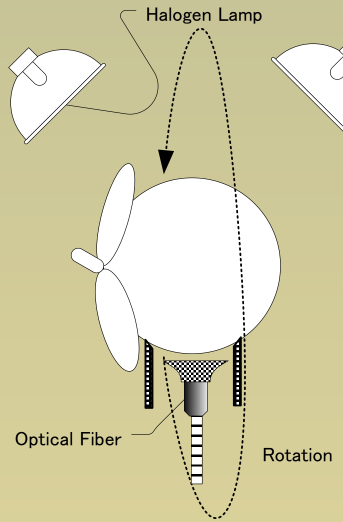

Type 2

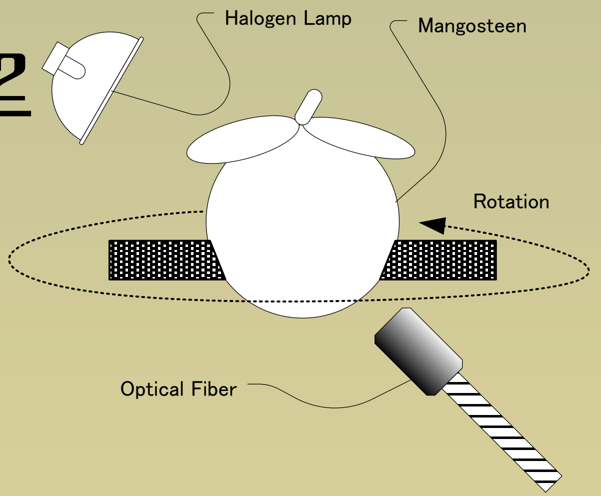

Type 3

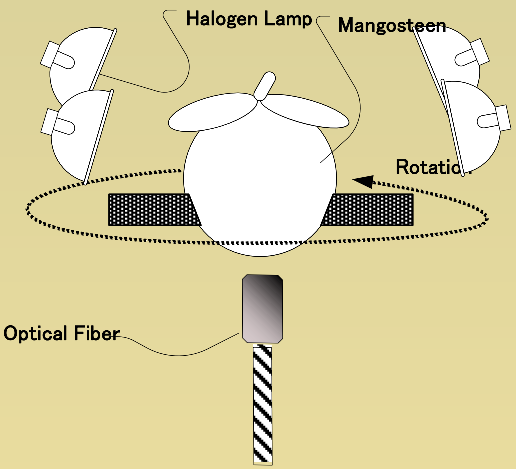

Spectral selecting method - Translucent

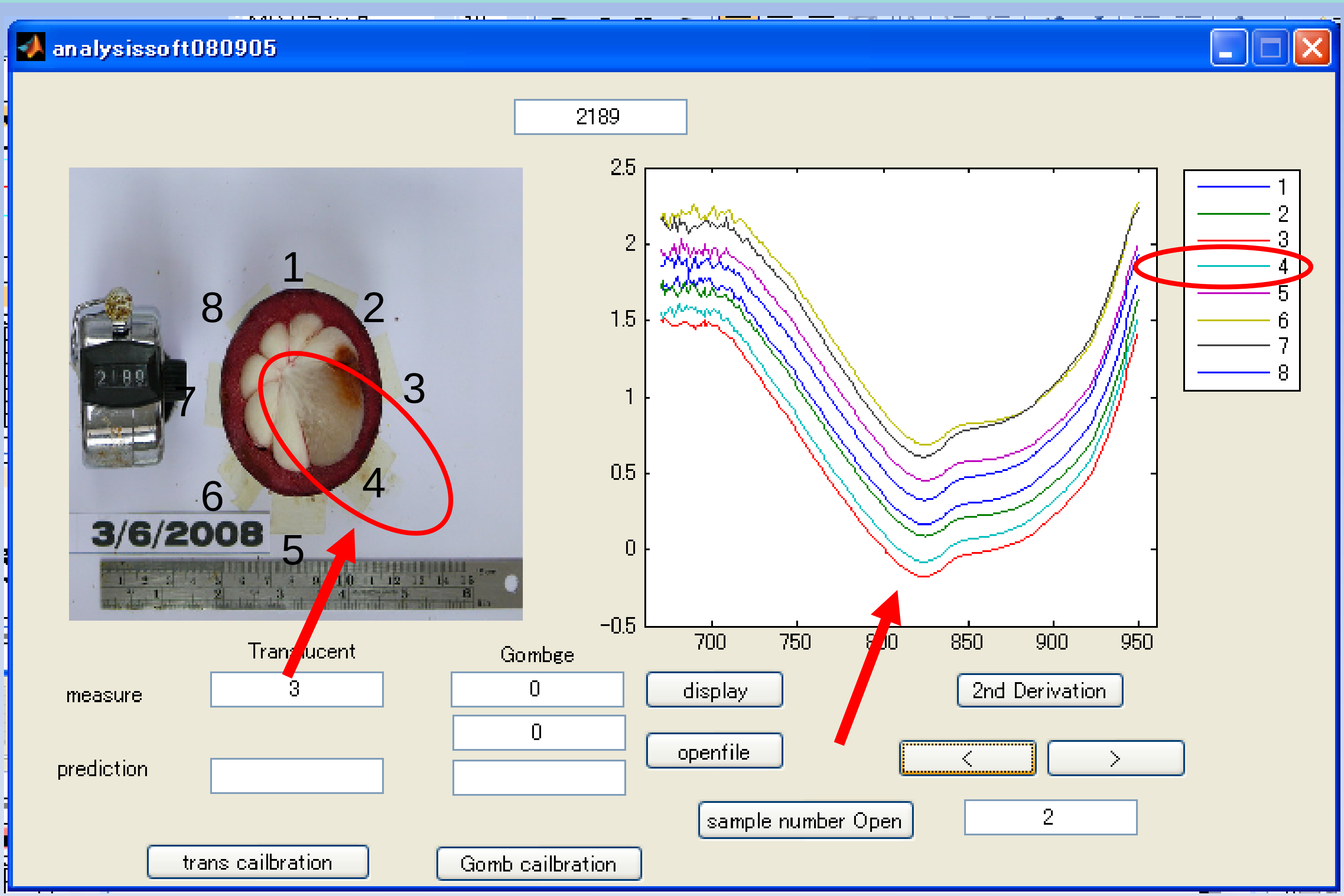

Select a spectrum of No.4 from eight spectra

On-line mangosteen sorting machine using NIRS

6. Nuclear magnetic resonance

- Spinning hydrogen atoms in a biological material act like magnetic dipoles due to the rotation of the electron around the proton.

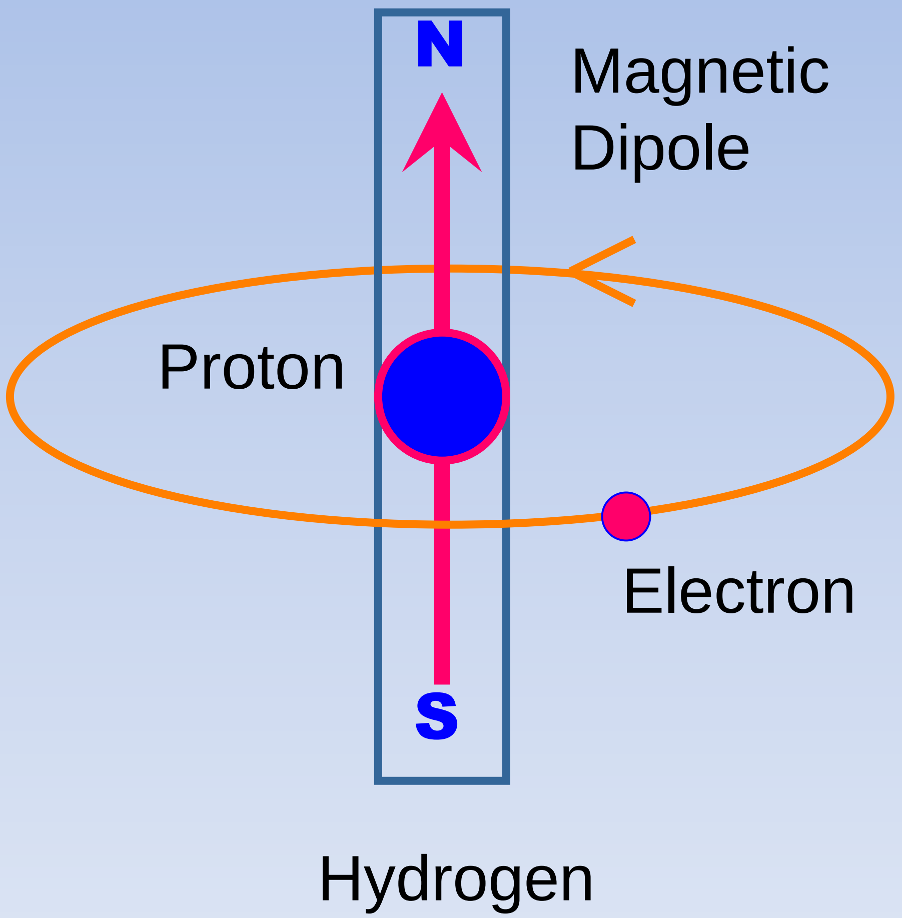

(extracted from Power point of Prof. Slaughter)

Nuclear magnetic resonance

- Under normal conditions the magnetic dipoles point in random directions.

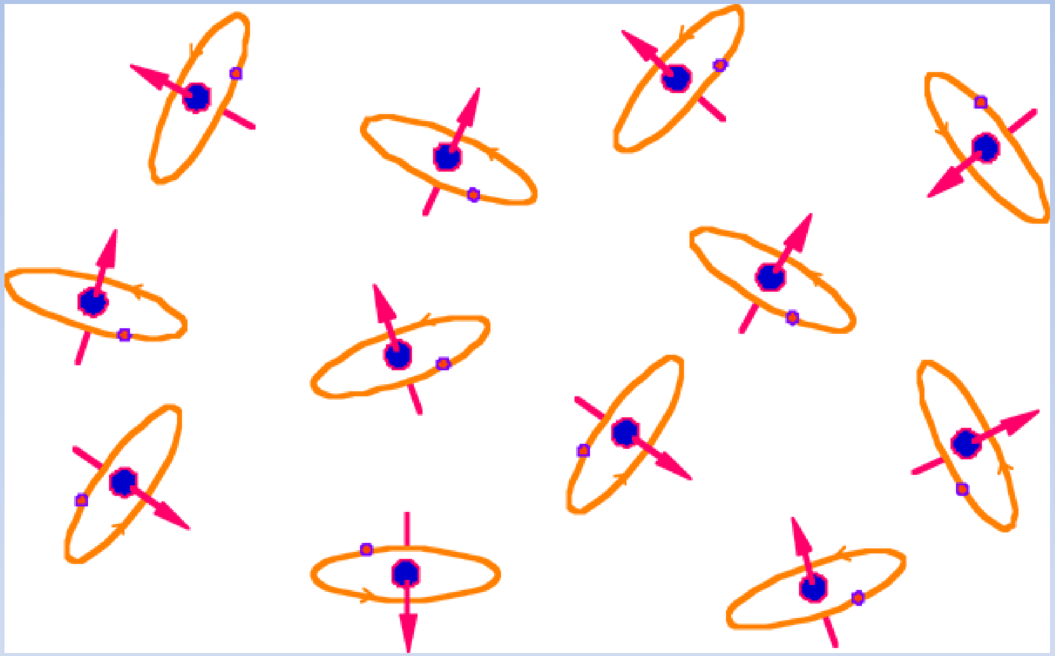

Nuclear magnetic resonance

- The material is placed inside a powerful electro-magnet.
- This causes the dipoles to align with the magnetic field.

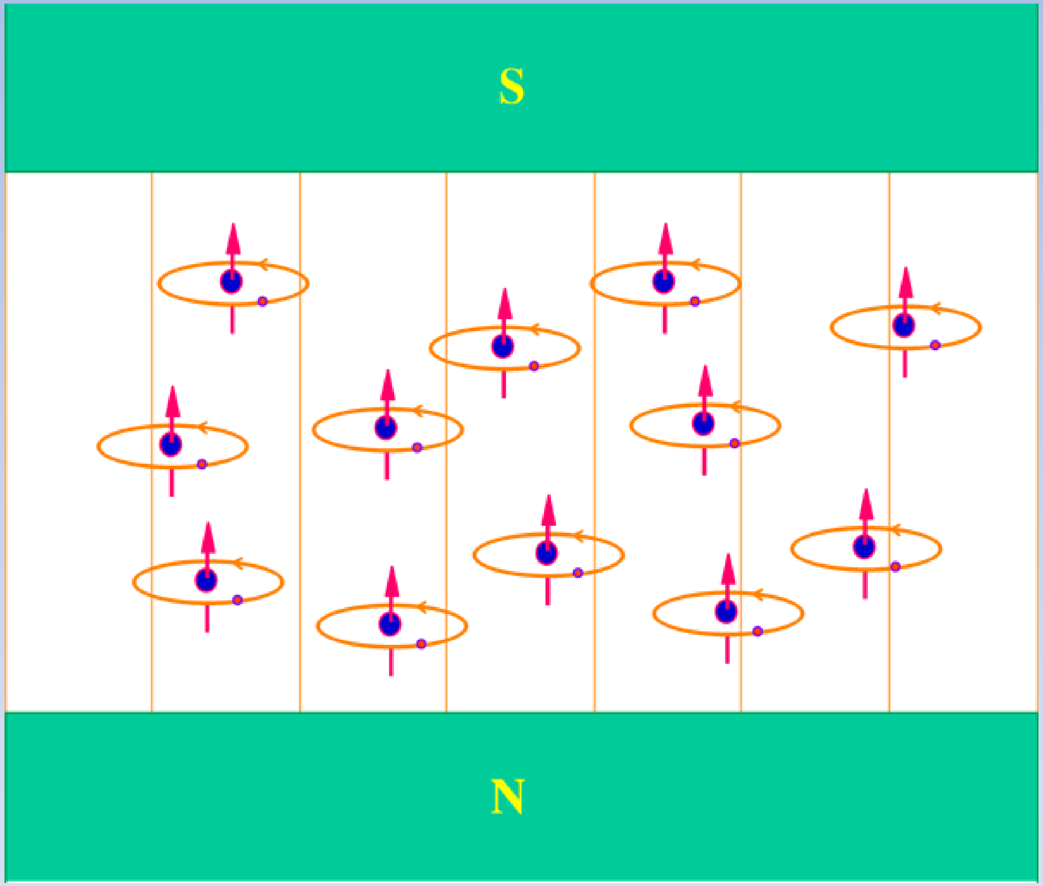

Prof. Slaughter

Nuclear magnetic resonance

- A radio frequency (RF) pulse is then used to “knock” the atoms out of alignment.

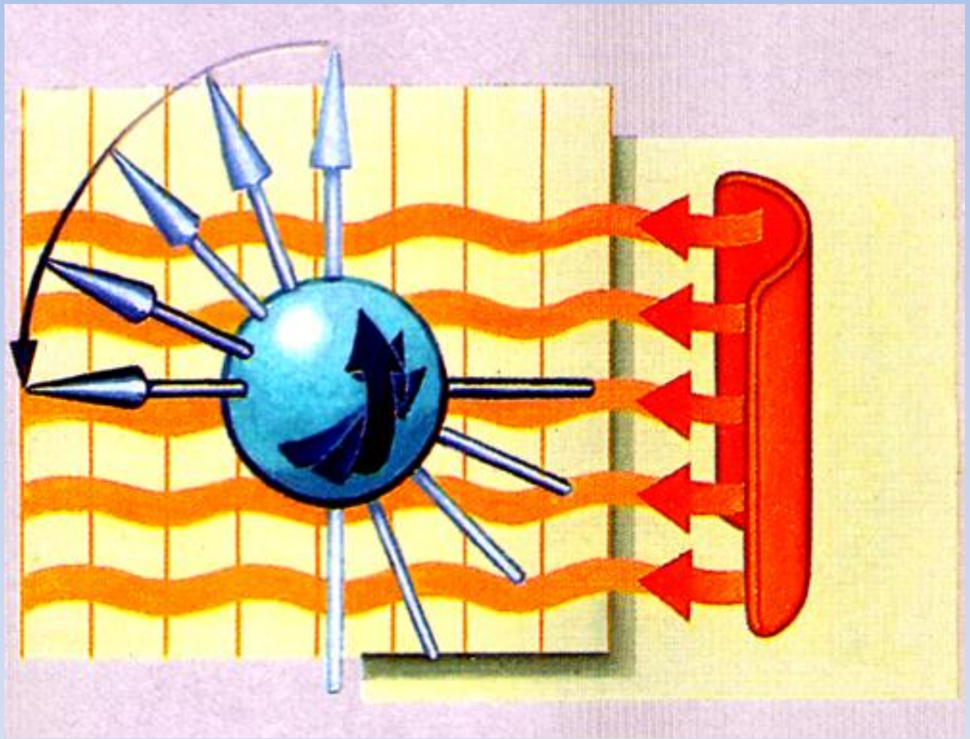

Prof. Slaughter

Nuclear magnetic resonance

- When the RF pulse stops, the atoms spiral back into alignment with the magnetic field.
- The time it takes for realignment is called the relaxation time (usually within milliseconds).
- The realignment process creates its own radio frequency signal that is detected by the system.

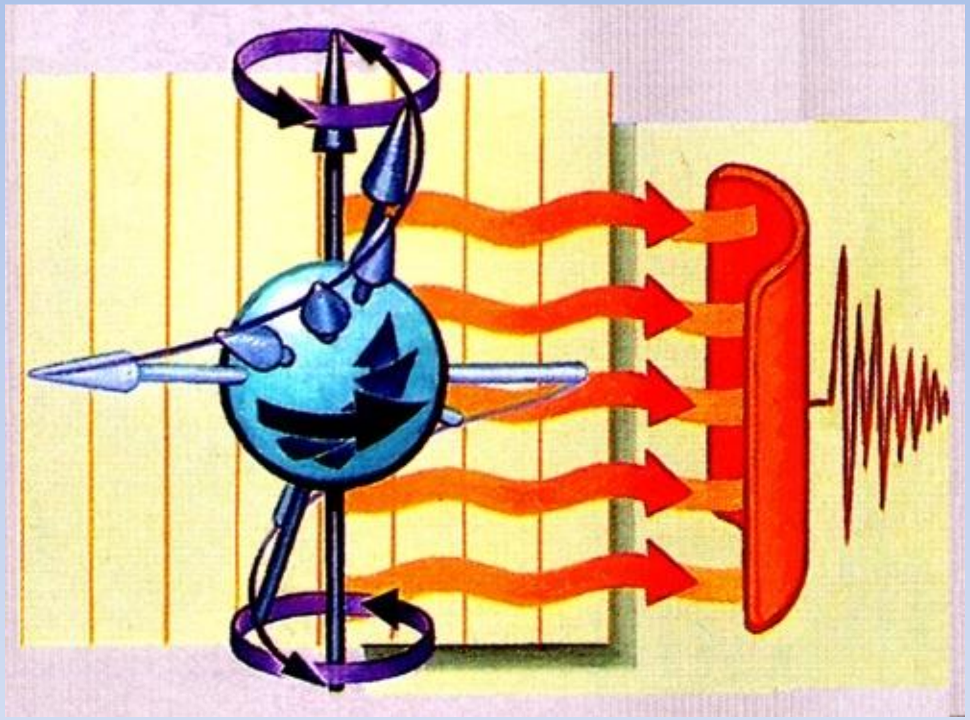

Prof. Slaughter

Precession and tipping

http://www.youtube.com/watch?v=XCrpMwz6Z1g

Output signal of NMR

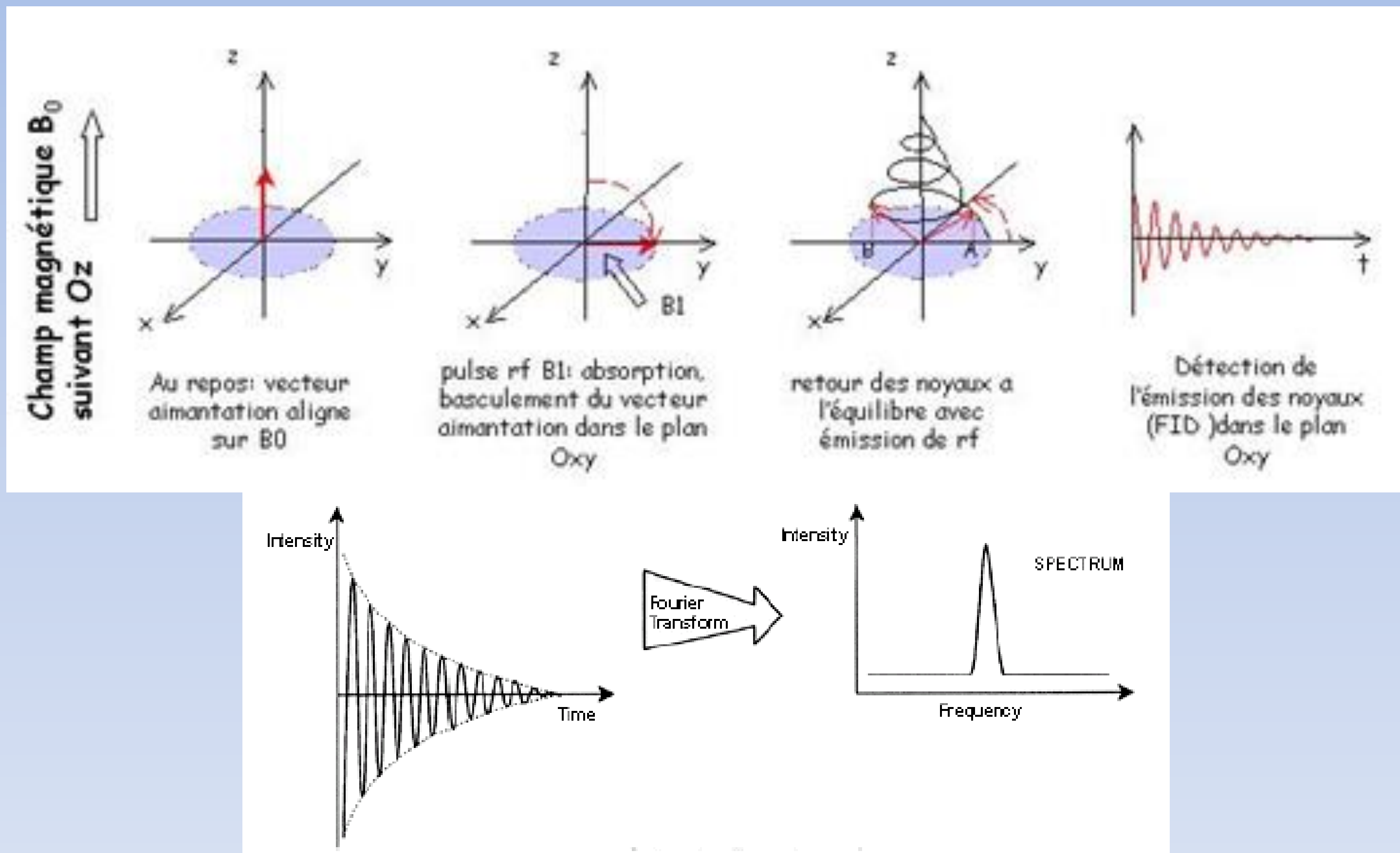

www.jcmr-online.com

http://www.lenaturaliste.net/portail/articles-des-membres/4-sciences-naturelles/68-biologie-structurale-et-spectroscopie-rmn

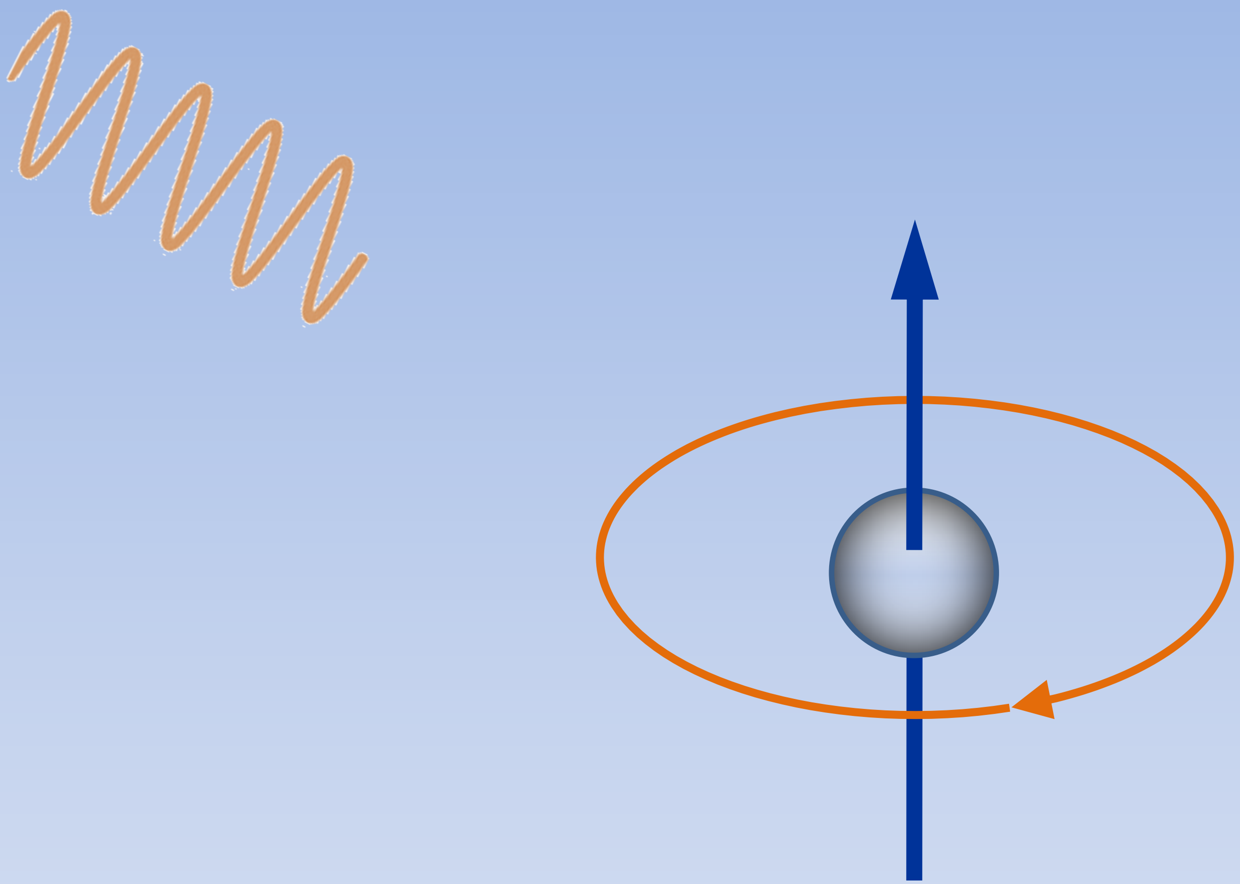

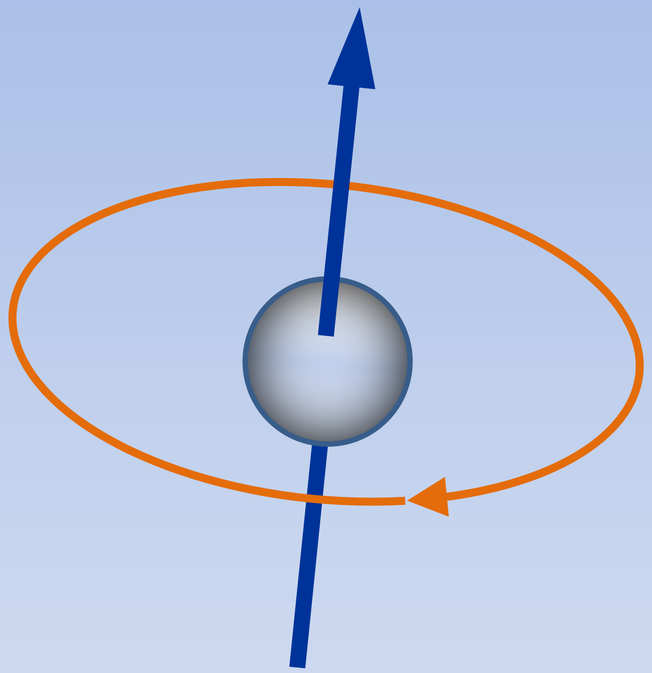

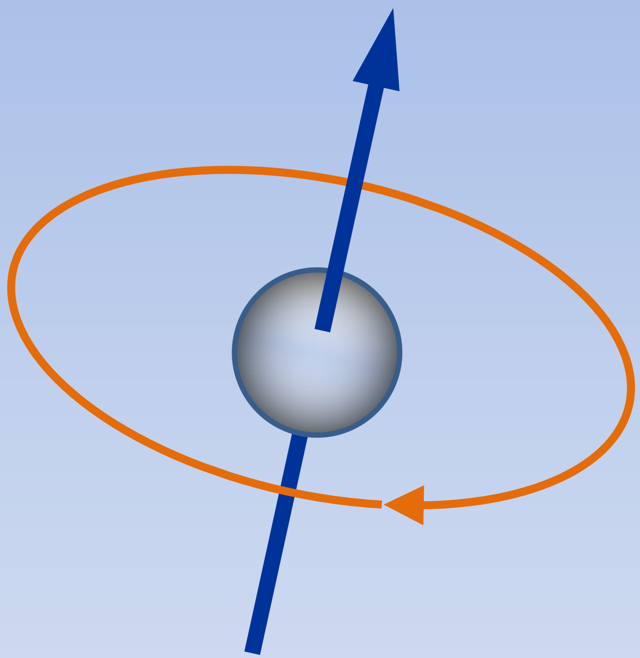

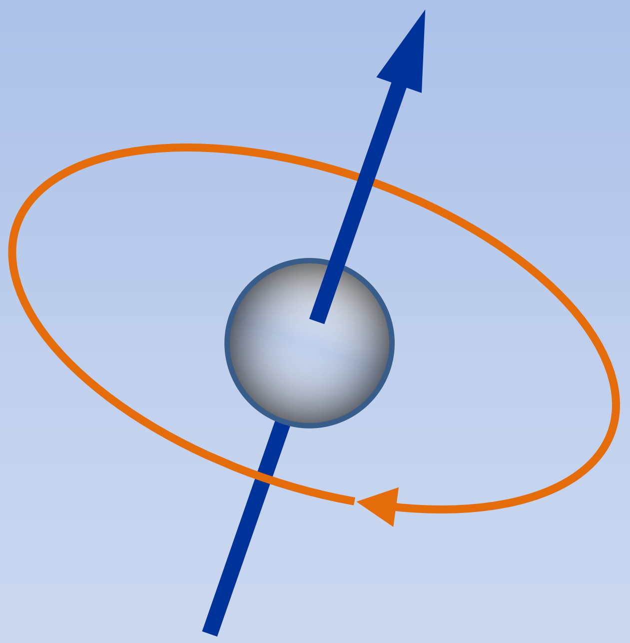

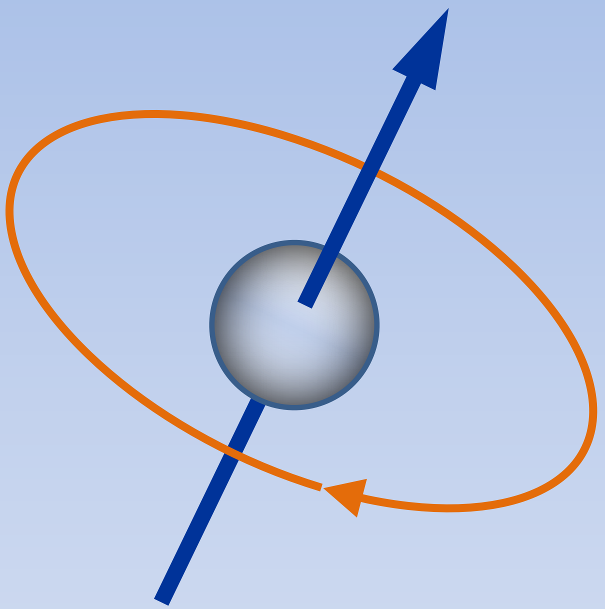

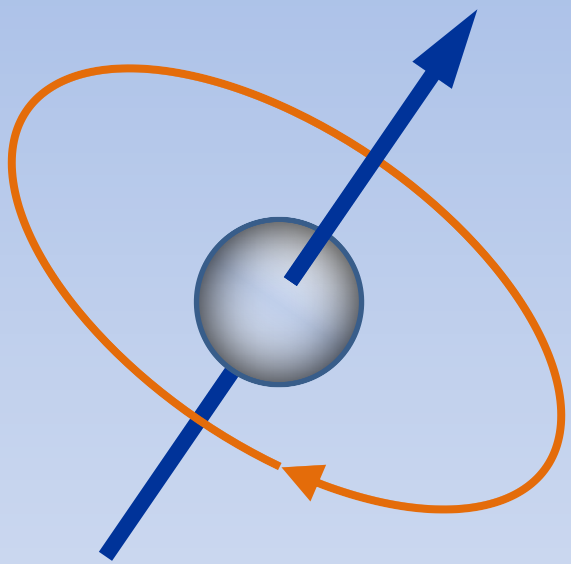

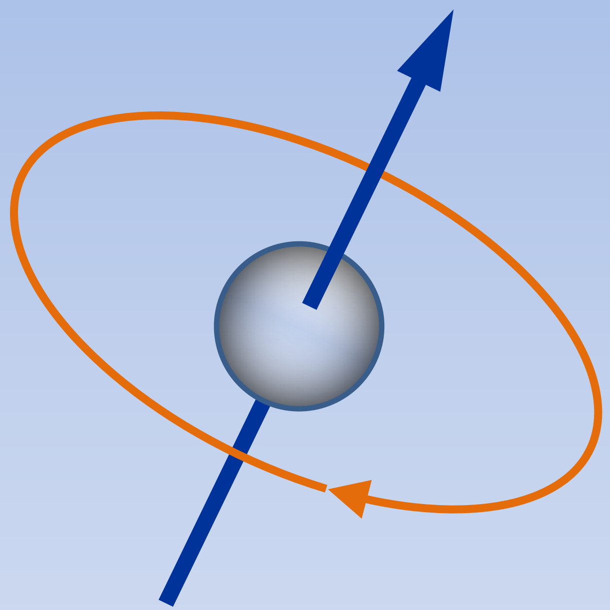

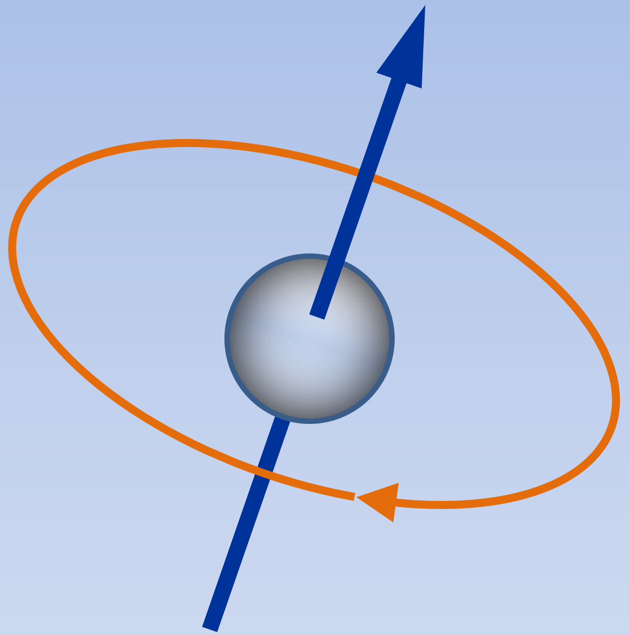

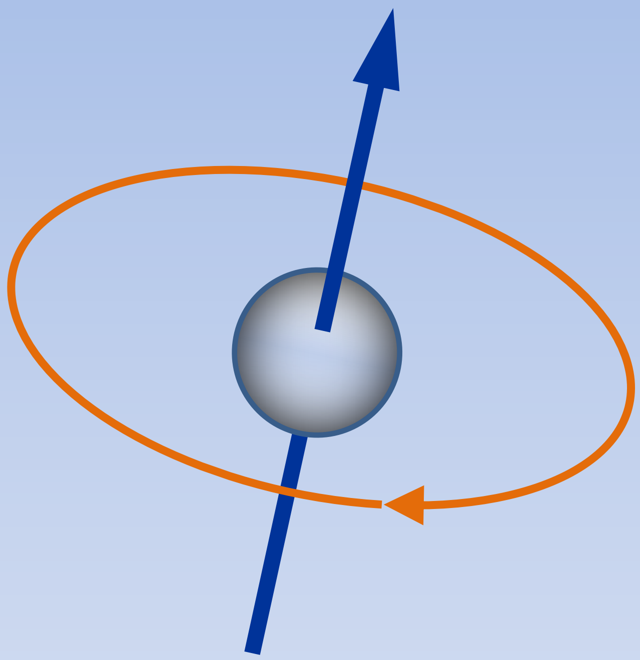

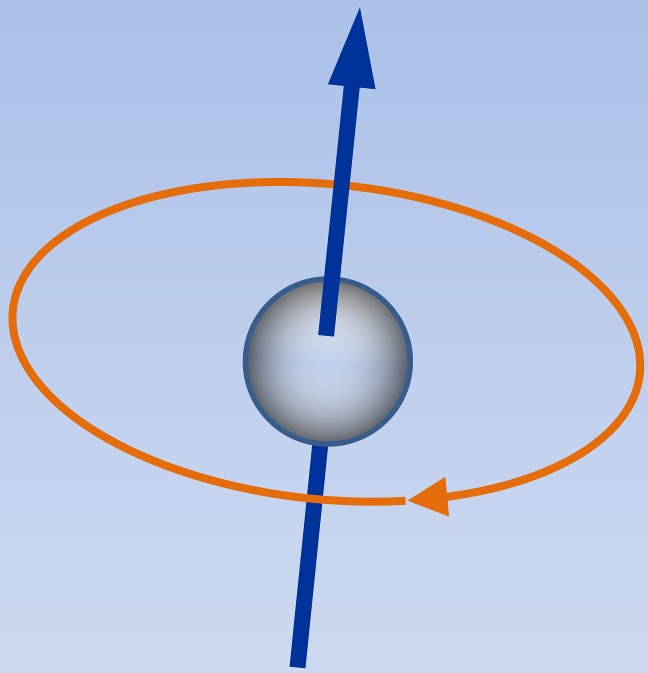

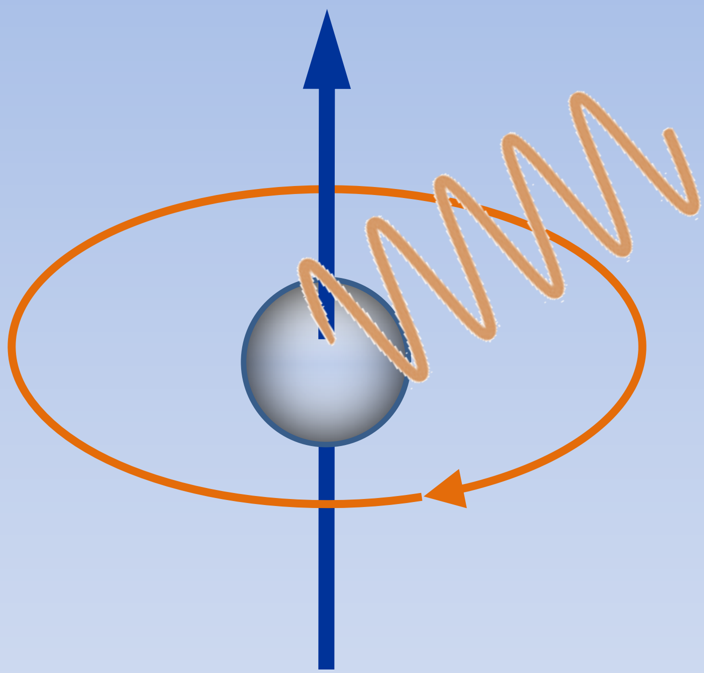

Permanent magnet NMR sensor
(Quantum Magnetics Corporation, San Diego, CA)

Magnet

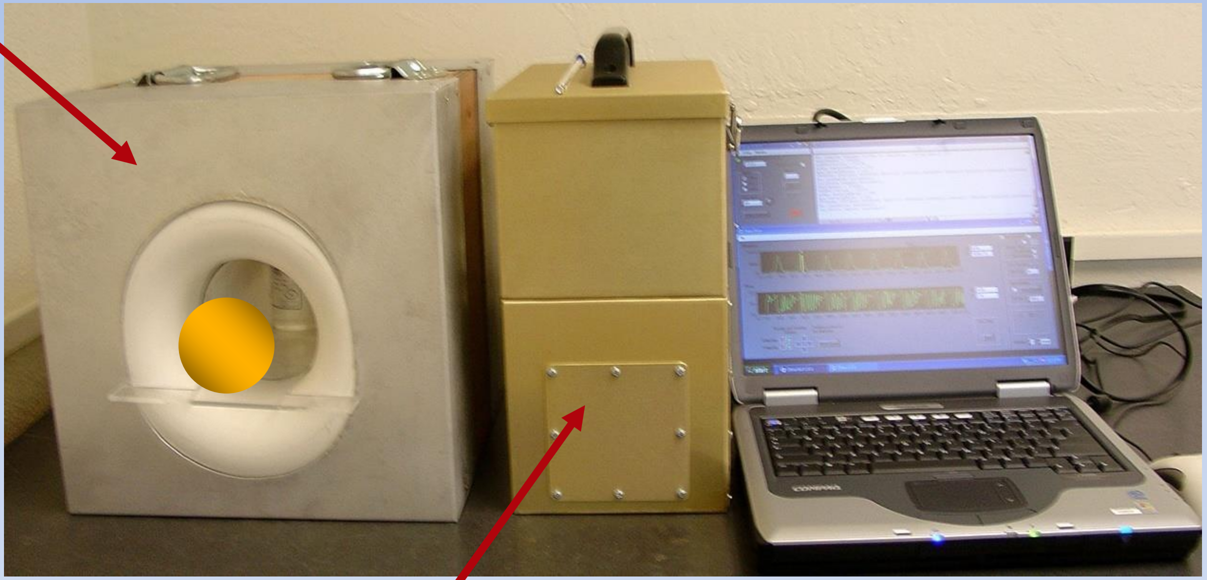

Electronics

Contents lists available at ScienceDirect

Postharvest Biology and Technology

journal homepage: www.elsevier.com/locate/postharvbio

Monitoring the postharvest ripening of tomato fruit using quantitative MRI and NMR relaxometry

Maja Musse[a,b,*], Stéphane Quellec[a,b], Mireille Cambert[a,b], Marie-Françoise Devaux[c], Marc Lahaye[c], François Mariette[a,b]

[a] Cemagref, UR TERE, 17, avenue de Cucillé - CS 64427, F-35044 Rennes Cedex, France
[b] Université européenne de Bretagne, France
[c] INRA, UR1268 Biopolymères, Interactions et Assemblages, BP 71627, F-44316 Nantes, France

- Magnetic Resonance Imaging (MRI)was performed on tomato fruit during two 3-week periods of postharvest ripening.

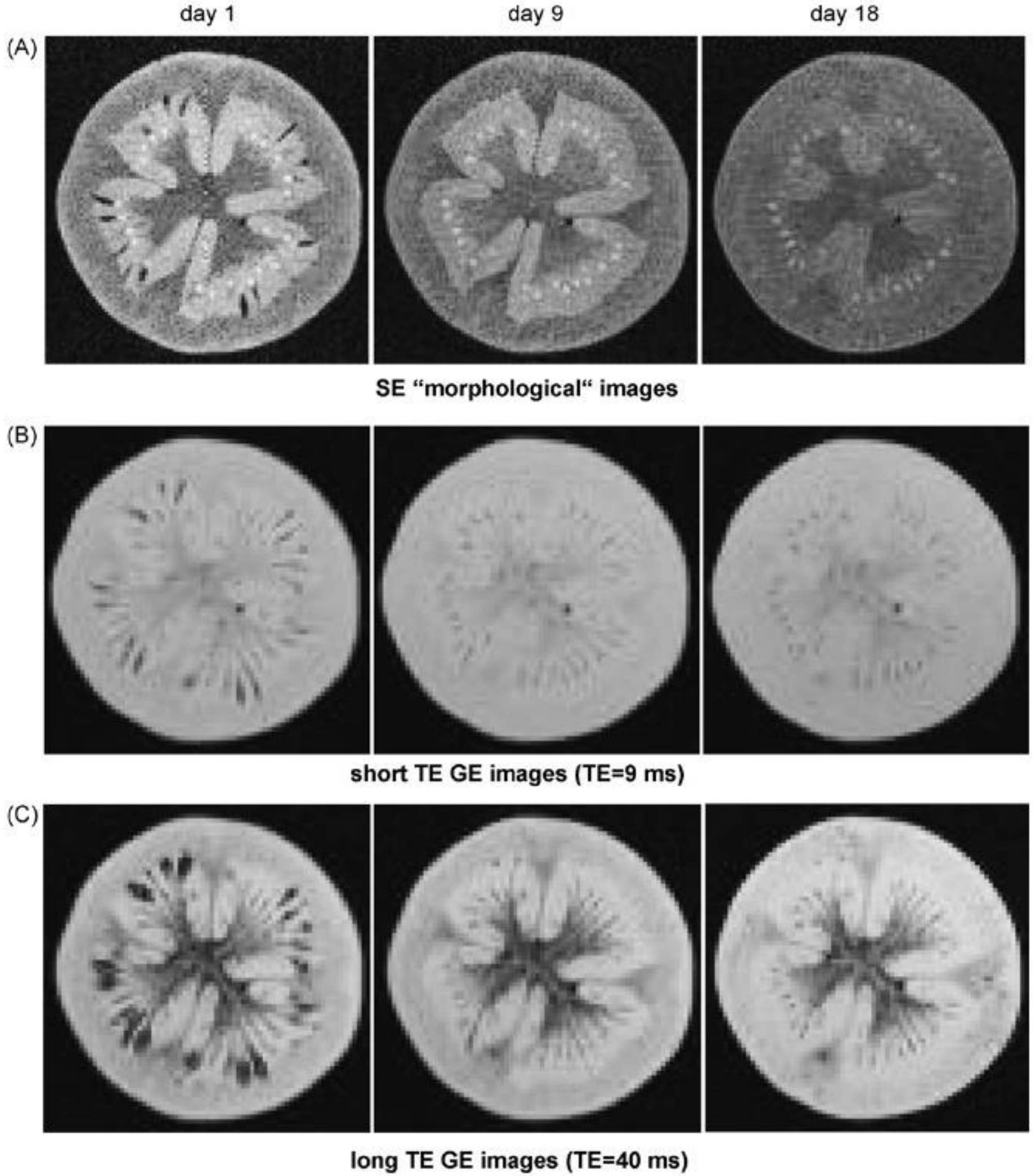

Fig. 1. Typical «morphological» SE image (A) along with short TE (B) and long TE (C) GE images of a tomato fruit at three different ripening stages.

Nuclear Magnetic Resonance Imaging of Fresh and Frozen Courgettes

S. L. Duce, T. A. Carpenter & L. D. Hall
Herchel Smith Laboratory for Medicinal Chemistry, University of Cambridge School of Clinical Medicine, University Forvie Site, Robinson Way, Cambridge CB2 2PZ, U.K.

- The internal structure of courgette and the effect of freezing the courgette was investigated by nuclear magnetic resonance imaging.

- The skin, vascular tissue, cortex, seed-bed and seeds were clearly delineated in the fresh vegetable; however, the image of frozen/thawed courgette showed very little contrast between the different tissues.
- Freezing ruptures the cell walls and alters the tissue morphology; this affects the transverse relaxation of water in the tissue, which in turn changes the image contrast.

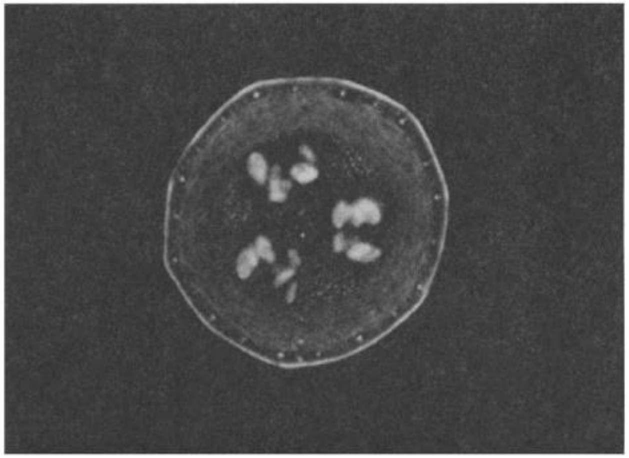

Fig. 1. 256 × 256 NMR spin-echo image of 5-cm diameter fresh courgette. TE = 40 ms; TR = 6 s.

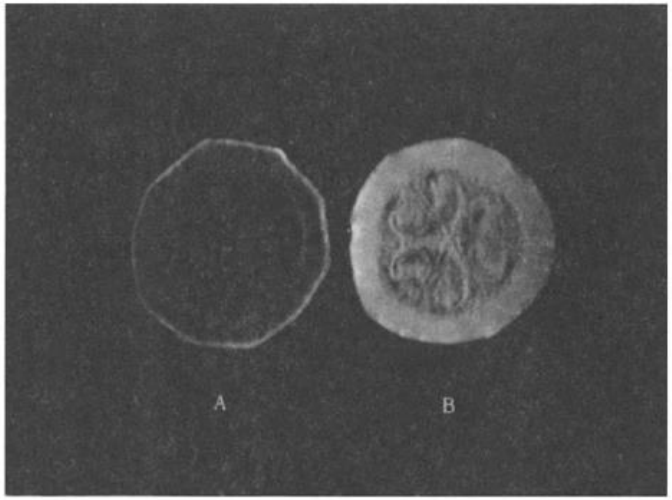

Fig. 2. 256 × 256 NMR spin-echo image of fresh and frozen 3-cm diameter courgette. TE = 40 ms; TR = 6 s. A: fresh sample; B: frozen/thawed sample.

Examples of
MRI images of fruits and vegetable

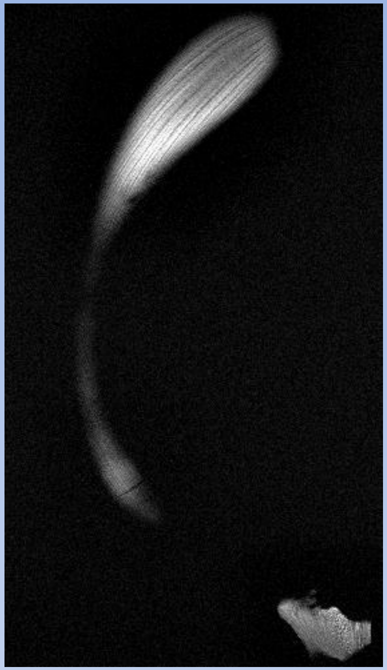

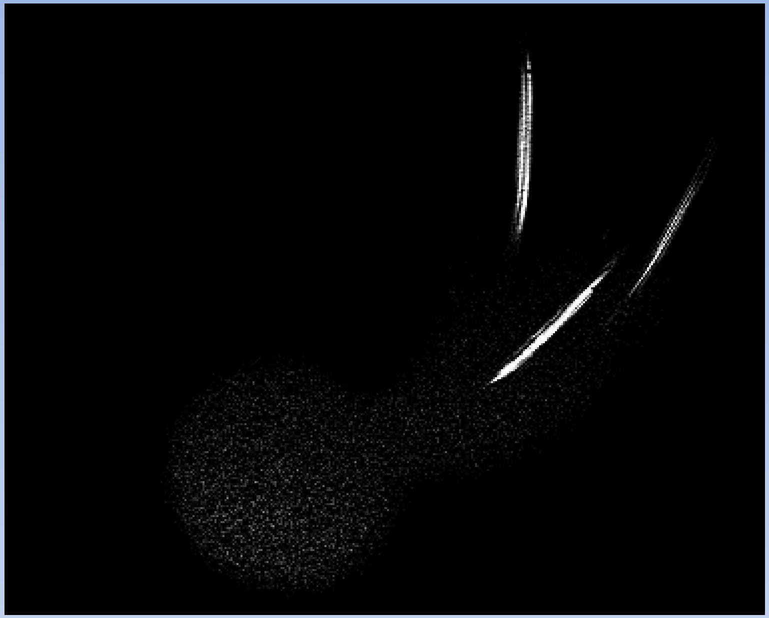

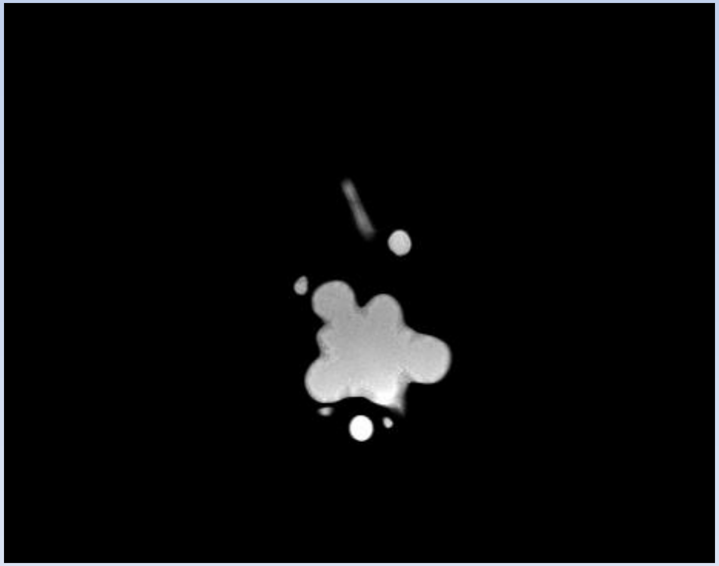

http://mashable.com/2014/04/21/mri-fruits-and-vegetables/

Beet

Bell pepper

Broccoli

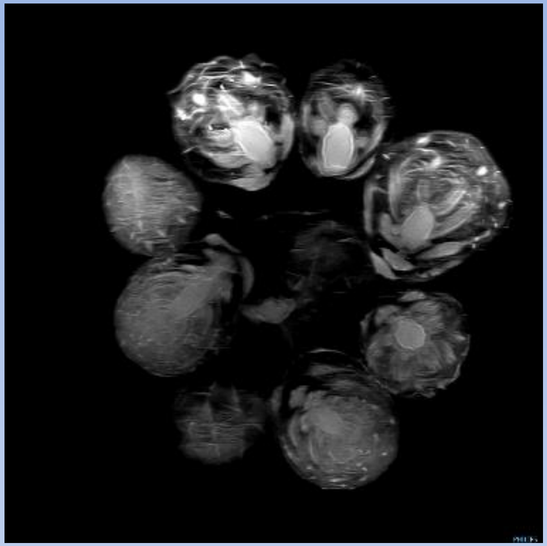

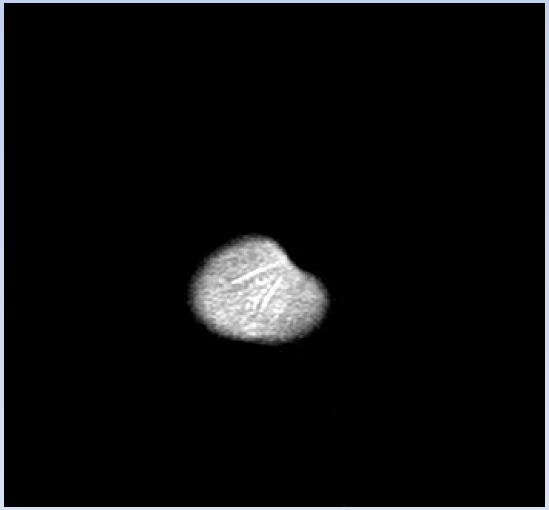

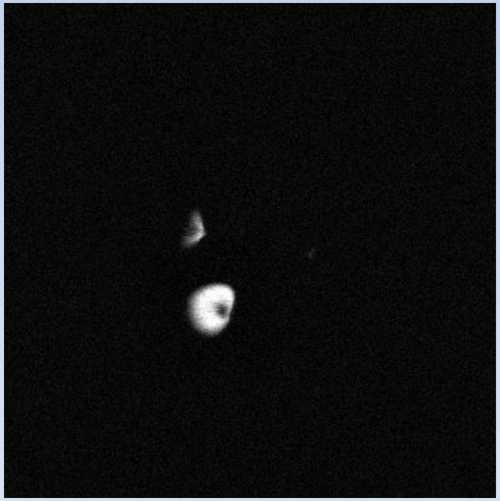

http://mashable.com/2014/04/21/mri-fruits-and-vegetables/

Brussels sprout

Eggplant

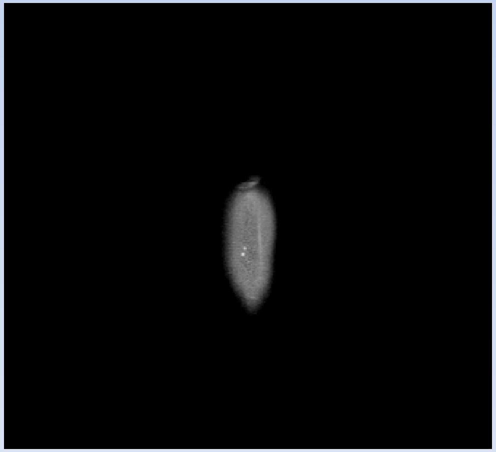

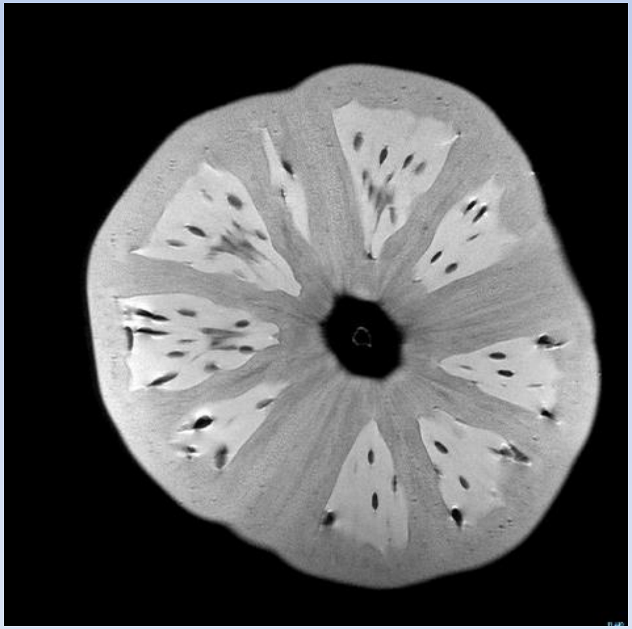

http://mashable.com/2014/04/21/mri-fruits-and-vegetables/

Okra

Spaghetti squash

Thanks for attention.